

Oceans and Coasts Annual Science Report 2024

Report No. 24



forestry, fisheries
& the environment

Department:
Forestry, Fisheries and the Environment
REPUBLIC OF SOUTH AFRICA



G20 SOUTH
AFRICA
2025



Oceans and Coasts

Annual Science Report 2024
Department of Forestry, Fisheries
and the Environment



CONTENTS

INTRODUCTION

MONITORING PROGRAMMES

1. Initial characterisation of the nearshore oceanography in Alexander Bay, Northern Cape	1
2. Chlorophyll variability on the west and south coasts	2
3. Surface chlorophyll <i>a</i> concentrations along the St Helena Bay Monitoring Line	3
4. Macronutrients limiting phytoplankton growth in the Southern Benguela Upwelling System	4
5. Microbial dynamics along the SAMBA Monitoring Line from 2022 to 2024	5
6. Long-term monitoring of microhabitat temperatures in Elands Bay	6
7. Exploring the microhabitats of the Cape sea urchin <i>Parechinus angulosus</i>	7
8. Monitoring meanders in three major western boundary currents	8
9. Long-term variability in bottom temperature on the Prince Edward Islands shelf	9
10. Long-term observations of currents on the Prince Edward Islands shelf	10
11. Patterns of potential Vulnerable Marine Ecosystems in the Southern Ocean	11

RESEARCH HIGHLIGHTS

12. A first look at seasonal variability of currents on the Prince Edward Islands shelf	12
13. Microplankton diversity around the Prince Edward Islands	13
14. Macronutrient distributions around Gough Island	14
15. Distributions of carbonate system parameters around Gough Island	15
16. Chlorophyll <i>a</i> and oxygen concentrations around Gough Island	16
17. Distributions of dissolved trace metals around Gough Island	17
18. Chlorophyll <i>a</i> and phytoplankton abundance along the SAMBA Monitoring Line	18
19. Lagrangian coherent structures and particle transport on the Agulhas Bank	19
20. Agulhas Current meanders redistribute intermediate waters along the southeast coast of South Africa	20
21. A complementary optical-molecular approach to exploring zooplankton communities	21
22. Modelling distributions and drivers of sponge taxa on the west and south coasts of South Africa	22
23. Cross-shelf exchanges around Diepgat submarine canyon in the northern KwaZulu-Natal	23
24. Harvesting impacts on the abundance of rocky shore organisms in the Dwesa-Cwebe MPA	24
25. Mark recapture reveals the longevity of Cape gannets in the Benguela ecosystem	25
26. Unusual predatory behaviour by mole snakes on African penguins at Robben Island	26
27. Overlap in feeding areas of Cape fur seals and African penguins	27

SCIENCE TO POLICY

28. Evaluating the enhanced bathtub model for coastal flood risk assessment in Table Bay, South Africa	28
29. South African (macro-, meso-, micro-) plastics programme (SAMP)	29
30. Initiating a global database on microplastics	30
31. A biodiversity sector plan for Marine Spatial Planning	31

PLATFORMS, TECHNOLOGY & INNOVATION

32. Filling in the blanks – improved bathymetry observations at the Prince Edward Islands	32
32. Tracking current cores and edges (TRACCE) of major Western Boundary Currents	33
34. Picture Perfect: rapid classification of plankton – mesozooplankton	34
35. MIMS master data management plan guide: a framework for fair and trustworthy marine and coastal data for DFFE	35

TRAINING & OUTREACH

36. Flow cytometry training for marine microbial analysis	36
37. Harmonising collection of microplastics in beach sand and surface water in Africa under the UN IAEA initiative	37

OUTPUTS FOR 2024

38. Peer-reviewed publications	38
39. Presentations at symposia, conferences and workshops	39
40. Published datasets	40
41. Published reports	57
42. Theses	57
43. Unpublished reports	57

ACKNOWLEDGEMENTS

Most staff members of the Chief Directorate: Oceans & Coastal Research contributed in one way or another to the contents and production of the Oceans and Coasts Annual Science Report, 2024. The Department wishes to express its appreciation to the many other agencies that have contributed to the work presented in this report. The at-sea, ship-based work and many coastal field trips for data collection and community engagements undertaken by the Branch: Oceans and Coasts are facilitated by the Chief Directorate's science managers and made possible by the various units within the Branch's Corporate Management Services and Financial Management Services.

EDITORS

JA Huggett, T Lamont, T Haupt, I Halo, M Krug, SP Kirkman

AUTHORS, CONTRIBUTORS AND AFFILIATIONS

DFFE Oceans and Coasts: Oceans and Coastal Research (OC Research)

Anders DA, Baliwe N, Britz K, Cebekhulu T, Filander Z, Gebe Z, Halo I, Hansraj Y, Haupt T, Huggett JA, Jacobs LM, Janson L, Kakora H, Khoza I, Kirkman SP, Kiviets G, Kotze D, Krug M, Lamont T, Lentswana S, Louw GS, Maduray S, Makhado AB, Mahanjana A, Maseti T, Masiko O, Masotla MJ, McCue S, Mdazuka Y, Mdokwana BW, Mooi G, Mtshali T, Mushanganyisi K, Ngwenze Z, Pillay K, Qhu T, Rasehlomi T, Rasmeni B, Russo CS, Samaai T, Samuels K, Seakamela M, Setati S, Soeker MS, Tsanwani M, Tutt GCO, van den Berg MA, van der Poel J, Vena K, Visagie L, Williams LL, Williamson R, Worship MM

DFFE Oceans and Coasts: Specialist Monitoring Services (SMS)

Coetzee T, Langa Z, Ramakulukusha M

DFFE Fisheries Management: Fisheries Research and Development (Fisheries R&D)

Auerswald L, Snyders L, Somhlaba S, Yemane D

Aix-Marseille University, France

Thibault D

BD Biosciences

Adams R

Benguela Current Marine Spatial Management and Governance Project (MARISMA)

Holness A, Sorgenfrei R

Council for Scientific and Industrial Research (CSIR)

Lück-Vogel M

Institute of Marine Research (IMR), Norway

Isari S

Institut de Recherche pour le Développement (IRD), France

Penven P

Nelson Mandela University (NMU)

Carpenter-Kling T, Rautenbach G

Oceanographic Research Institute (ORI)

Govender A, Groeneveld J

South African National Biodiversity Institute (SANBI)

Majiedt P, Sink K

South African Environmental Observation Network (SAEON)

Rautenbach G

Steenberg Vets

du Plessis D

Stellenbosch University (SU)

Roychoudhury R, Valk A, van Coller FJ

UK Polar Data Centre (UK PDC), British Antarctic Survey (BAS), UK

Frémand A

University of Cape Town (UCT)

Dakwa F, Underhill L

University of Fort Hare (UFH)

Nel W

University of South Africa (UNISA)

Hedding D

University of the Western Cape (UWC)

Gibbons MJ

Unaffiliated (ex-OC Research)

Bawuli A, Dyer B

CONTACT INFORMATION

Branch: Oceans and Coasts Physical Address:

2 East Pier Shed, East Pier Road,
Victoria & Alfred Waterfront, Cape Town, Western Cape, South Africa
Tel: 021 819 2410

Website:

www.dffe.gov.za

Chief Director, Oceans and Coastal Research – Ashley S Johnson (Acting)
Director, Oceans Research – Ashley S Johnson (ajohnson@dffe.gov.za)
Director, Biodiversity and Coastal Research – Gerhard J Cilliers (gcilliers@dffe.gov.za)

Editors

Jenny A Huggett (jhuggett@dffe.gov.za), Tarron Lamont (tlamont@dffe.gov.za),
Tanya Haupt (thaupt@dffe.gov.za), Issufo Halo (ihalo@dffe.gov.za), Marjolaine Krug (mkrug@dffe.gov.za),
Stephen P Kirkman (skirkman@dffe.gov.za)

Images

Kelp forests of False Bay, Cape Peninsula. Images by Ken Findlay <https://www.kenfinphoto.com>
Two Oceans Aquarium, V&A Waterfront, Cape Town. Image by Paul Bruins <https://www.flickr.com>

RP321/2025

ISBN: 978-1-83491-218-9

doi: 10.5281/zenodo.15769586

INTRODUCTION

As we approach the halfway mark of the UN Decade of Ocean Science for Sustainable Development (the Ocean Decade, 2021–2030), the Ocean remains in crisis due to cumulative pressures including resource overexploitation, pollution, climate change and biodiversity loss. Although global multilateral agreements such as the Kunming-Montreal Global Biodiversity Framework (GBF) and Agenda 2030 exist to combat these issues, their implementation has generally been characterised by major gaps between commitments and concrete actions at scale. However, 2024 can be seen as a milestone year for ocean governance, marked by several important achievements and policy advances. Key landmarks include, amongst others, (1) progress made towards an imminent Global Plastics Treaty to address plastic pollution across its lifecycle, at a fifth round of negotiations, and (2) the Barcelona Statement, produced at the Ocean Decade Conference in Barcelona. The latter serves as a crucial roadmap identifying priority areas of action for the remainder of the Ocean Decade, highlighting the launch of programmes focused on sustainable ocean planning and sustainable ocean governance and management.

These include specific initiatives for Africa and the blue economy, and emphasise the need for co-design and co-delivery of ocean science and knowledge.

South Africa's role in ocean governance, sustainability and conservation, both in Africa and globally, became more important than ever in late 2024, when it took over the presidency of the G20 from Brazil. Under South Africa's leadership, oceans and coasts have been identified as one of five main priority areas of the G20 Environment and Climate Sustainability Working Group (ECSWG), which serves as the primary forum within the G20 to enhance coordination and cooperation among member countries on environmental and climate challenges. In this regard, a core ambition of the G20 South African Presidency is to enable a lasting and impactful sustainable blue economy transition that delivers on global and national policy goals related to *inter alia* biodiversity protection, climate resilience, equity, sustainable consumption and production, and applying a circular economy approach. This requires integrated, holistic approaches that conserve and regenerate ocean ecosystems while facilitating sustainable use of resources for human wellbeing.



As the primary government body responsible for the strategic leadership, management and promotion of oceans and coastal conservation in South Africa, work done by DFFE Branch Oceans and Coasts (OC) is very much in line with objectives and focus areas of G20's ocean agenda, including Oceans20 (O20)



Towards this end, key focus areas of the ECSWG include Marine Spatial Planning (MSP), ocean governance and combating marine plastic pollution, with a strategic focus on leveraging the G20 platform to advance ocean sustainability globally, but especially for Africa and the Global South. In particular, the South African presidency wishes to promote the practical utility of MSP and other area-based management concepts and tools, and to support more effective delivery of policy and strategies for ocean sustainability.

As the primary government body responsible for the strategic leadership, management and promotion of oceans and coastal conservation in South Africa, work done by DFFE Branch Oceans and Coasts (OC) is very much in line with objectives and focus areas of G20's ocean agenda, including Oceans20 (O20). Some of the relevant programmes led by OC include, amongst others, MSP that is under development to zone ocean space for sustainable use and conservation; Marine Protected Area (MPA) management and expansion to conserve biodiversity, protect critical habitats, and support sustainable fisheries; the Ocean Economy Master Plan to unlock, stabilise, revive, and grow key sub-sectors of South Africa's ocean economy; and the National Coastal Management Programme which includes climate adaptation and management of pollution among its priorities. In the year of its G20 presidency, it will be key for South Africa to demonstrate leadership and innovation in its set priorities—experiences in the above areas can provide the basis for good practice examples, evidence-based guidance and recommendations to inform high-level reporting and advance progress on the priorities.

The development of MSP in South Africa and the application of other tools for achieving conservation and sustainable development is supported by knowledge and information management that is provided by the Oceans and Coasts Information Management System (OCIMS). This is a platform that makes information and decision support for management of South Africa's oceans and coasts accessible to users. The models and analytics provided through the OCIMS user-facing decision support tools are fed by vast quantities of ocean data from various contributors or custodians.

Oceans and Coasts continues to be a primary access point for the collection of ocean data, including in the deep sea, through its at-sea platforms including its research vessels the SA *Agulhas II* and the RS *Algoa* and diverse autonomous instruments. The at-sea platforms are complemented by top predator, coastal, shallow water and estuarine science programmes employing diverse methods including seabird counts, animal telemetry, biodiversity transects, visual imagery and sediment sampling. These activities, which are often carried out in partnership with marine research nodes of other departments and universities in South Africa, and from

other countries and organisations, contribute to South Africa being rich in ocean data, especially in comparison to most other maritime African countries.

With its ocean data resources, advancements in knowledge and information management, and world-renowned capabilities with biodiversity assessment and systematic biodiversity planning, South Africa has developed a good evidence base to support MSP zoning that can secure appropriate biodiversity management and conservation for biodiversity priorities. As such, promoting integration of biodiversity considerations in MSP based on South Africa's perspectives has been identified as a key theme for G20 ECSWG deliverables under South Africa's leadership. This addresses an important element of GBF's Target 1 for reducing biodiversity loss, namely that planning and management of all areas are integrated and biodiversity-inclusive. It also demonstrates one of the desired endpoints of OC science activities; however, the range of OC's science activities have diverse other potential outcomes in policy, decision-making and day-to-day management of South Africa's oceans and coasts.

The science activities are guided by a dedicated science plan that was developed to support OC in fulfilling their mandate of managing and conserving South Africa's coastal and marine environment, as well as addressing the country's regional and international commitments to the conservation and sustainable use of the ocean and its biodiversity. The science plan promotes the development and maintenance of programmes that provide continuous or sustained monitoring and descriptions of key aspects of the marine environment, with a very specific emphasis on the establishment of long-term datasets (monitoring). Shorter-term research projects are also conducted, in search of a deeper, more fundamental understanding of specific areas or ecosystem processes (research), or to support evidence-based recommendations for ocean policy and management (science to policy). The science plan also emphasises the need to continually develop new and innovative platforms and technologies in order to sustain and enhance ocean monitoring, prediction and management (platforms, technology and innovation). The development of human capacity in marine research is integral to the science plan, and the training and development of staff, interns, students and outside researchers is embedded into all programmes and projects (training and outreach).

The different aspects of the OC science and science-related activities, headlined according to the bracketed terms above, represent the different sections of this report, each containing one or more articles reporting on relevant activities. As in previous reports, a list of scientific outputs for the calendar year is provided at the end, including peer-reviewed publications and other products that reflect both the volume and quality of work accomplished by OC Research in 2024.



MONITORING PROGRAMMES

1. INITIAL CHARACTERISATION OF THE NEARSHORE CIRCULATION IN ALEXANDER BAY, NORTHERN CAPE

The Northern Cape province is mineral-rich, with abundant deposits of zinc, iron ore, manganese, copper and diamonds. Mining in alluvial deposits of diamonds in the province began in Alexander Bay, then expanded south to Port Nolloth, Kleinsee and Koingnaas (Fig. 1). Land-, beach- and seabed mining operations provide much needed employment for local people. However, the impact of extensive mining activities on the marine environment of Alexander Bay is not well understood, due to a lack of baseline observational data. Hence the DFFE initiated environmental monitoring at five sites in Alexander Bay (Fig. 1).

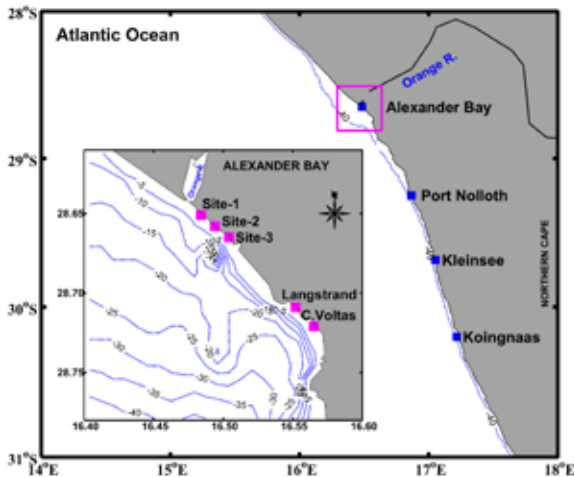


Figure 1. Location of Alexander Bay, showing (bottom left) the locations of the DFFE nearshore monitoring sites impacted by the bay-scale circulation. Contours on the maps are isobaths.

This study aims to characterise the seasonal nearshore circulation in the bay and infer its potential impact at the monitoring sites. Due to a lack of oceanographic data, we used a hydrodynamic model simulation developed by the French Institute for Research and Development. The simulation was run using the Coastal Regional Ocean Community model (CROCO), with a 3 km grid. Boundary conditions for the CROCO model were prescribed using the European Reanalysis winds (ERA5) and the Global Ocean Physics Reanalysis.

Figure 2 shows the monthly means of the wind stress (red arrows) and coastal currents formed by the balance of the main oceanic forces. In summer, the winds were predominantly from the south (Fig. 2A), while in autumn they were southeasterly (Fig. 2B). In winter, the winds

reversed completely to northeasterly (Fig. 2C) and thereafter reversed again in spring to southerly (Fig. 2D). The wind regime off the monitoring sites was similar to the prevailing winds across the bay. Overall, winds were stronger in the mid-shelf than in the nearshore, and more intense off Sites 1–3 than at Langstrand and Cape Voltas, except in winter (Fig. 2C). Geostrophic currents arise from the equilibrium between the Coriolis force and the pressure gradient force. The intensification of these currents (blue arrows, Fig. 2), off Sites 1–3 near the Orange River, could be caused by a strong cross-shore pressure gradient due to the freshening of coastal waters. Ageostrophic currents (green arrows, Fig. 2) occur when the flow is not solely determined by the pressure gradient and Coriolis forces but also influenced by factors such as friction. On some occasions, ageostrophic currents veered to the left of the wind direction, in agreement with the Ekman theory, thus highlighting the impact of the wind. At other times however, winds were not the main driver, emphasising the importance of other forces (e.g. bottom friction, buoyancy, waves) in controlling the currents. Note that ageostrophic currents were also stronger off Sites 1–3 than in Langstrand and Cape Voltas.

Depth-averaged ocean currents (black arrows, Fig. 2) show the overall lateral movement of the water-mass. The deviation of depth-averaged currents to the left of the wind direction (Fig. 2A–B, D) suggests that the wind stress controlled the seasonal nearshore circulation in summer, autumn, and spring. Year-around (Fig. 2A–D) circulation off Langstrand and Cape Voltas was north-westward, while off Sites 1–3 it was westward. This indicates an overall seaward net-transport. This result is crucial for environmental impact assessment studies in this region, as it can help to mitigate risks of coastal pollution.

Authors: Halo I, Lamont T (OC Research), Penven P (IRD)
Contributors: Mtshali T, Vena K (OC Research)

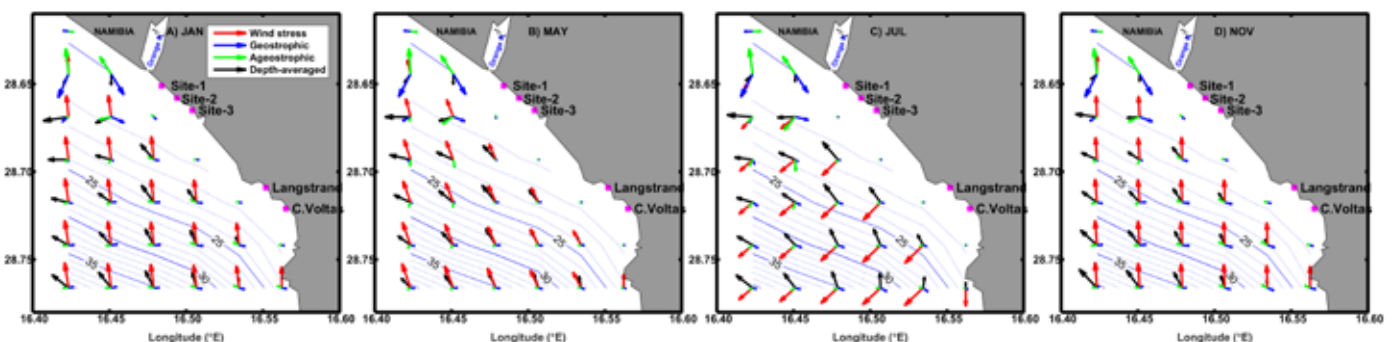


Figure 2. Simulated monthly mean winds and nearshore currents surrounding the DFFE monitoring sites in Alexander Bay in (A) January, (B) May, (C) July and (D) November. Arrows of different colour (see legend) indicate wind stress, ocean currents from geostrophic, ageostrophic, and depth-averaged relations. Vector length indicates flow strength and the blue contours represent simulated isobaths.

MONITORING PROGRAMMES

2. CHLOROPHYLL A VARIABILITY ON THE WEST AND SOUTH COASTS

Phytoplankton are crucial for a number of key marine processes, such as food web modulation and the cycling of carbon and other nutrients. The Benguela upwelling system and the Agulhas Bank, which are found on the west and south coasts of southern Africa, respectively, host productive ecosystems with complex trophic structures that support numerous commercially harvested resources. Both are therefore ecologically and economically significant. To monitor productivity levels of these systems, an index of chlorophyll *a* is computed by integrating satellite-derived surface values from the coast to the 1 mg m⁻³ contour level further offshore (Fig. 1).

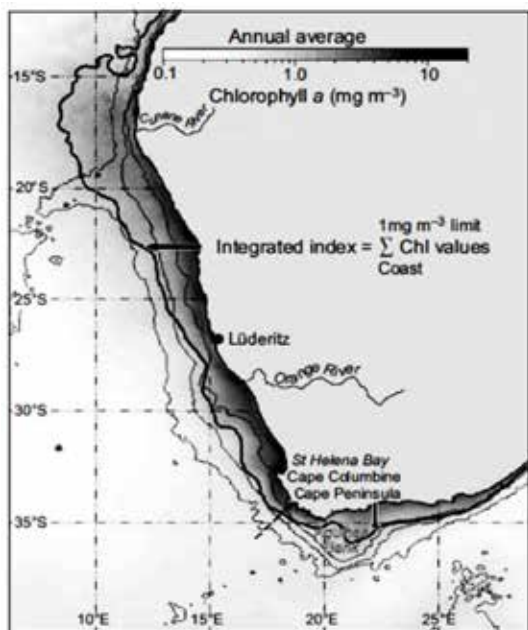


Figure 1. Annual average chlorophyll *a* concentration and location of the 1 mg m⁻³ contour (thick line). Thin black lines indicate bathymetry contours for 200, 1000, and 3000 m.

Higher values are associated with greater phytoplankton biomass and a more productive ecosystem, while lower values indicate lower biomass and a less productive ecosystem.

Highest index values are usually found off Namibia (16–26°S; Fig. 2). Biomass here in 2018 was the lowest since 2013. While elevated in 2019 and 2020, values since 2021 have been lower and more variable. Values were higher between 21–26°S during April–June 2024 but subsequently were more elevated north of 21°S.

Persistent uplift and offshore transport of surface waters at Lüderitz (ca. 27°S) are typically associated with very low index values. Elevated values at Lüderitz during the summers of 2020, 2021 and 2024 suggested decreased upwelling, with lower values implying stronger upwelling in 2022 and 2023. Along South Africa’s west coast (SAWC, 28–34°S), index values are elevated around the Namaqualand, Cape Columbine and Cape Peninsula upwelling cells. Off Namaqualand (28.5–30°S), values in 2018 were the highest since 2013. Elevated values in 2022 and 2024 suggested improved productivity, but lower values during 2021 and 2023 reflected less productivity.

Along South Africa’s south coast (SASC, 18.5–29°E), index values are generally lower than on the SAWC. During 2013–2024, the highest values occurred at 22–23°E in March–May 2024 and at 20–21°E in September–October 2024. Low values in 2016 suggested it was the least productive year for the SASC during 2013–2024. The varying productivity trends across the region, i.e. small but significant long-term increase in chlorophyll *a* off Namibia, and a decrease off the SAWC, appear to have continued over the past year. The SASC trend changed from declining to increasing over the past year.

Author: Lamont T (OC Research)

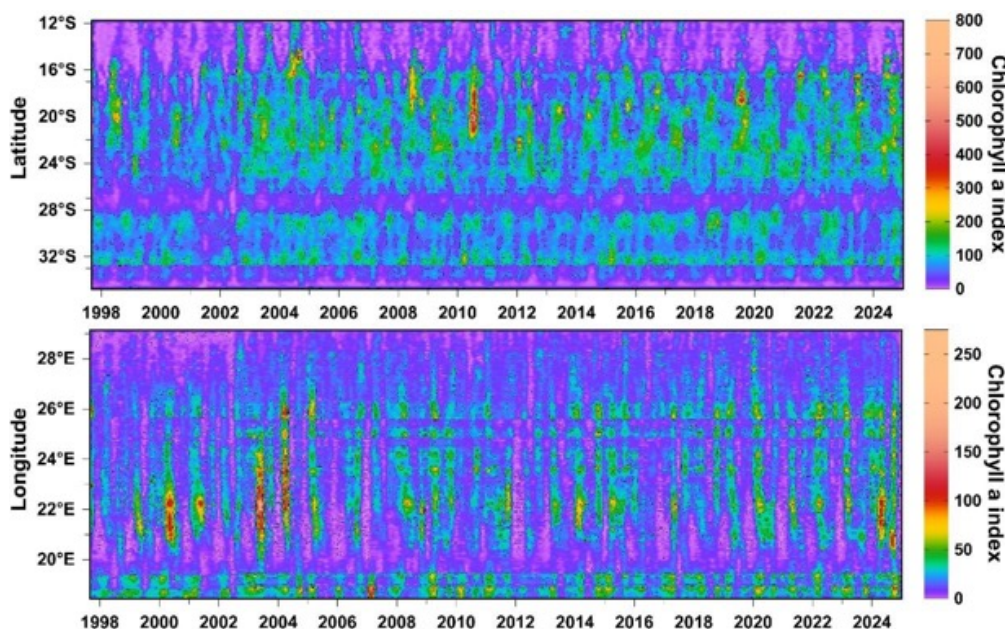


Figure 2. Monthly chlorophyll *a* indices (1997–2024) for the west coasts of Namibia and South Africa (top panel) and for South Africa’s south coast (bottom panel).

MONITORING PROGRAMMES

3. SURFACE CHLOROPHYLL A CONCENTRATIONS ALONG THE ST HELENA BAY MONITORING LINE

St Helena Bay on the west coast of South Africa (Fig. 1) is one of the most productive areas of the Benguela ecosystem and has been the focus of environmental research and monitoring for several decades. It is a retention area, with significantly elevated plankton biomass compared to other areas off South Africa, and is an important region for many species such as small pelagic fish, hake, whales, and rock lobster.

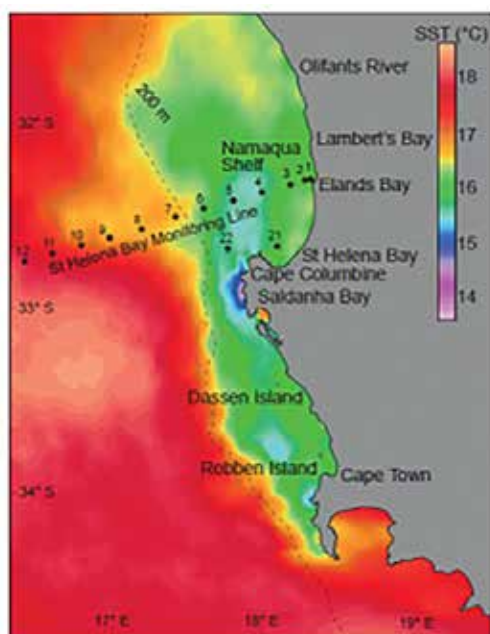


Figure 1. Map of satellite-derived sea surface temperature, illustrating cooler waters typically found inshore and warmer waters offshore. The location of the St Helena Bay Monitoring Line is shown.

Along the west coast, southeasterly winds transfer surface waters offshore, resulting in cool, nutrient-rich waters being uplifted to the surface from deeper depths (i.e. upwelling). On a seasonal scale, higher chlorophyll a (chl a) coincides with larger amounts of upwelling that occur during October–March each year (the upwelling season). Satellite-derived surface chl a illustrates this seasonality, with maxima in spring/early summer (usually October) and during the late summer/autumn months of February and March (Fig. 2). Higher chl a is usually associated with greater phytoplankton biomass and a more productive ecosystem, which largely results from the higher nutrient availability in the upper ocean during upwelling. In contrast, lower chl a indicates lower phytoplankton biomass and a less productive ecosystem, usually associated with less upwelling and nutrient availability in the upper ocean during late autumn to early spring (April–September) each year. Generally, higher chl a occurs close to the coast due to higher nutrient availability in the surface layers and decreases with distance offshore as nutrient availability decreases (Fig. 2). During 2015, high values ($>20 \text{ mg m}^{-3}$) extended ca. 20 km offshore in autumn (March) and late spring/early summer (September–November). Values $>20 \text{ mg m}^{-3}$ were observed much closer to the coast during 2016–2019, in 2021 and in 2024. Such high values extended ca. 10 km offshore in February–March 2020 and October 2022, but in December 2023 they extended $>30 \text{ km}$ offshore. Elevated chl a ($>5 \text{ mg m}^{-3}$) extended ca. 110

km offshore in March 2015 – the farthest offshore extent for such elevated values since March 2010. Since then, the farthest offshore extent (ca. 95 km) of values above 5 mg m^{-3} was observed in October–November 2024. In February–March 2016 and in April 2022, such values extended ca. 80 km offshore, but did not extend beyond 70 km offshore during 2017–2021 and in 2023. Chl a in 2017 was lower overall than in 2016 but remained elevated throughout the year. Generally lower values in 2018 and 2021 suggested a less productive ecosystem during these years. In contrast, higher values during 2019, 2020 and 2022 suggested increased productivity. During 2023 and 2024, chl a was higher in January–February and in December, with much lower values during March–November suggesting a much less productive autumn-to-spring period compared to the previous decade.

Author: Lamont T (OC Research)

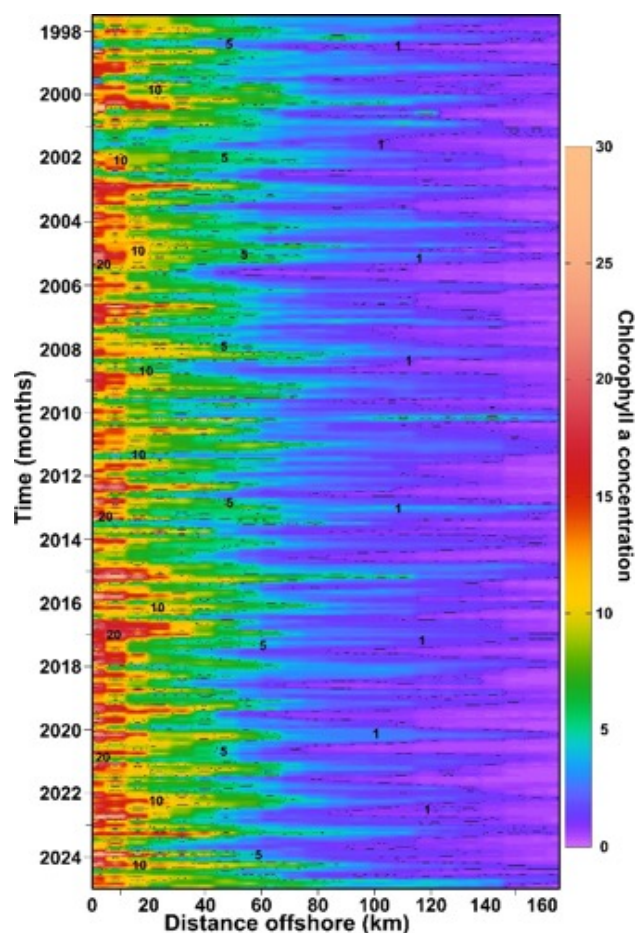


Figure 2. Time series of satellite-derived monthly chlorophyll a (mg m^{-3}) along the St Helena Bay Monitoring Line between September 1997 and December 2024.

MONITORING PROGRAMMES

4. MACRONUTRIENTSLIMITING PHYTOPLANKTON GROWTH IN THE SOUTHERN BENGUELA UPWELLING SYSTEM

Macronutrients (nitrate (NO_3^-), silicate ($\text{Si}(\text{OH})_4$), and phosphate (PO_4^{3-}) play a key role in phytoplankton growth. They are taken up by phytoplankton in a certain stoichiometric ratio known as the "Redfield ratio" (typically expressed as N:C:P = 16:16:1). Changes in this ratio can influence both the composition of the phytoplankton community and their abundance, and in turn, the entire food web. Deviations from the Redfield ratio can highlight which nutrient is most limiting for phytoplankton growth. Here, we present spatial and interannual differences in N:P ratios during summer (February) for the Southern Benguela Upwelling System (SBUS) from 2014 to 2023 (Fig. 1).

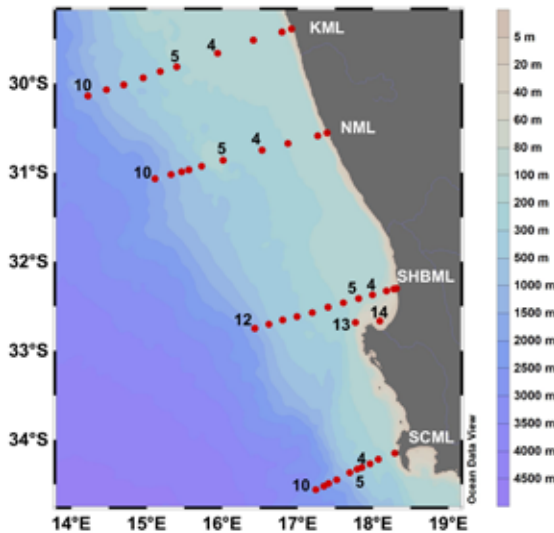


Figure 1. Map showing sampling stations (red dots) along four monitoring lines: Kleinsee (KML), Namaqua (NML), St Helena Bay (SHBML) and Scarborough (SCML), in the SBUS. Numbers indicate inshore stations (1–4, 13 and 14) and offshore stations (5–12). Colour shading indicates ocean bathymetry.

Seawater samples for macronutrient analysis were collected during the Integrated Ecosystem Programme (IEP) cruises, measured using a Flow Injection Autoanalyzer, and quantified using reference standards. Dissolved Inorganic Nitrogen ($\text{DIN} = \text{NO}_3^- + \text{NO}_2^-$) was used to represent all the Nitrogen species. We used data in the upper ocean, from the surface to the base of the Modified Upwelling Waters, at depth of ca. 100 m. DIN:P molar ratios were obtained by linear regression.

DIN:P molar ratios were highly variable along each monitoring line, as well as interannually (Table 1), ranging from 1.3–35.8 overall (Fig. 2). The ratios were lower than the elemental molar ratio of 16:1 at most inshore stations (Stations 1–4 with bottom depth <100 m) than further offshore (Stations 5–12).

Table 1. The annual mean DIN:P ratios (\pm standard deviation), averaged across each monitoring line. ND = No data. Grey shading indicates DIN:P ratios >16:1.

Year	KML	NML	SHBML	SCML
2014	10.0 \pm 3.8	10.8 \pm 3.7	12.0 \pm 2.0	9.3 \pm 5.3
2015	14.6 \pm 4.0	14.5 \pm 2.2	19.5 \pm 8.3	ND
2017	12.8 \pm 8.3	13.7 \pm 4.4	14.8 \pm 2.8	13.6 \pm 5.2
2020	17.5 \pm 2.3	17.4 \pm 5.8	16.0 \pm 5.3	18.0 \pm 2.1
2022	18.5 \pm 3.6	19.6 \pm 4.6	16.3 \pm 4.8	15.9 \pm 4.2
2023	16.9 \pm 1.4	16.3 \pm 5.3	15.4 \pm 6.4	15.0 \pm 2.0

Prior to 2020, except for a few peaks at some stations during 2015 and 2017, most stations along each monitoring line showed DIN:P ratios below 16:1 (Fig. 2). In contrast, during 2020–2023, the DIN:P ratios were generally higher than 16:1 at the offshore stations (Fig. 2). On average, the DIN:P ratios showed an increase, with the values rising from <12.0 in 2014 to >13.0 in 2015–2017, and to >16.0 during 2020–2023 (Table 1).

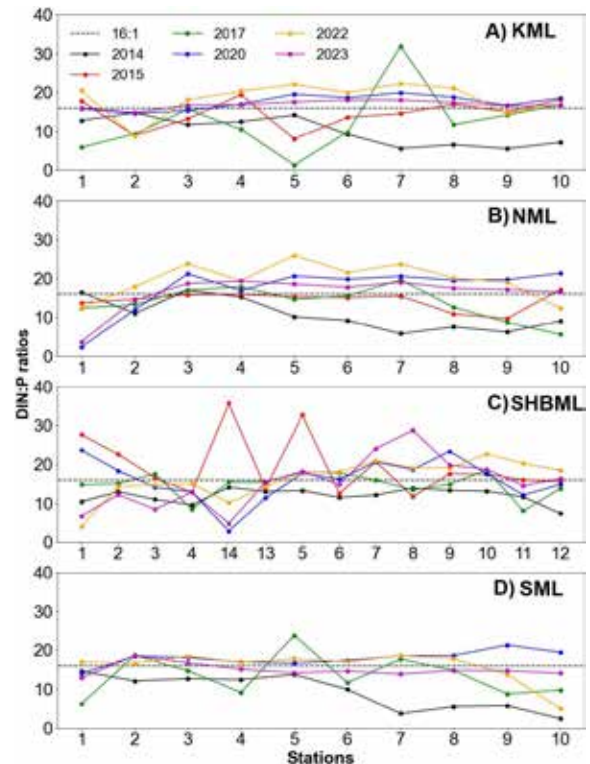


Figure 2. Spatial and interannual variability in DIN:P molar ratios along (A) KML, (B) NML, (C) SHBML and (D) SCML for six years during February. Station numbers are shown on the x-axes. The horizontal black dotted lines represent the Redfield ratio of 16:1 for N:P required for phytoplankton growth.

These results suggest that phytoplankton production during summer blooms in the SBUS was potentially DIN-limited during 2014–2017, but was P-limited during 2020–2023. Both DIN and P are essential nutrients, and examining their ratios of occurrence can inform on whether management measures should be implemented for N-loading, P-loading, or both, in coastal waters.

Authors: Mtshali TN, Tsanwani M (OC Research)

Contributors: Vena K, Kiviets G, Mdokwana B, Britz K (OC Research)

MONITORING PROGRAMMES

5. MICROBIAL DYNAMICS ALONG THE SAMBA MONITORING LINE FROM 2022 TO 2024

The South Atlantic Meridional Overturning Circulation Basin-wide Array (SAMBA) Monitoring Line extends southwest from the west coast of South Africa across the continental shelf, and then along 34.5°S from the edge of the continental shelf across the Cape Basin to 0°E (Fig. 1). Physical, chemical and biological properties are sampled annually during September–October to assess changes in the physical and chemical conditions and monitor the response of biological organisms to such changes.

Monitoring of microbial groups (tiny living organisms) along the SAMBA Monitoring Line commenced in 2022 in order to supplement fluorescence measurements (an index of phytoplankton biomass) routinely obtained from Conductivity–Temperature–Depth (CTD) profiles. This monitoring focusses on photosynthetic microbes that use the sun for growth and includes organisms ranging in size from 0.5 µm (typically cyanobacteria) to 10 µm (typically small flagellates and diatoms). Monitoring of microbes is essential, as they are good indicators of change in ocean health and play an important role in global nutrient cycles and marine food webs.

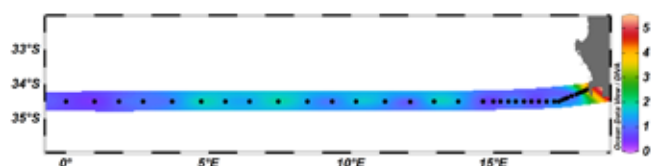


Figure 1. Surface plot of fluorescence (mg m^{-3}) at the CTD stations along the SAMBA Monitoring Line during September–October 2024.

Water samples were collected from the CTD Niskin bottles, filtered, preserved and frozen for later analysis with a flow cytometer, an instrument that rapidly counts cells within a liquid and identifies them by size, shape and light. Microbial (phytoplankton) groups were identified based on their pigment, size and shape. Their average abundance showed variability over the three sampled years (Table 1).

Table 1. Mean abundances (cells mL^{-1}) \pm standard errors of the four phytoplankton groups sampled during 2022, 2023 and 2024.

Microbes	Mean Abundance \pm STD		
	(cells mL^{-1})		
Group	2022	2023	2024
Nanoplankton	176 \pm 24		571 \pm 111
Picoeukaryotes	465 \pm 165		2372 \pm 323
<i>Synechococcus</i>	2733 \pm 463	15418 \pm 8013	6571 \pm 1187
<i>Prochlorococcus</i>	4493 \pm 490	17345 \pm 5604	7788 \pm 800
No. of samples	25	65	38

Larger microbes (nanoplankton (2–10 µm) and picoeukaryotes (1–3 µm)) were not present in 2023, but they increased in mean abundance from 2022 to 2024. Their absence in the 2023 samples may indicate that they were not present in the ecosystem at the time, or that there was deterioration of the samples during freezing. For picoeukaryotes, the increase was significant ($F = 63.86$, $p < 0.001$) with the 2024 abundance being more than five times larger than in 2022. Smaller microbes (*Synechococcus*, 0.8–2 µm; and *Prochlorococcus*, 0.5–0.7 µm) were more abundant than the larger microbial

groups. They also increased in abundance from 2022 to 2024 (Table 1), but not significantly (*Synechococcus*: $F = 2.12$, $p = 0.06$ and *Prochlorococcus*: $F = 2.09$, $p = 0.013$). The vertical distribution of these phytoplankton groups showed high abundances in the upper 40 m of the water column at the nearshore stations during the three years (Fig. 2). At ca. 40 m depth between 0–5°E longitude, the mean distribution of *Synechococcus* and *Prochlorococcus* was skewed to higher values due to much higher abundances during 2024 than in previous years (Fig. 2c and d).

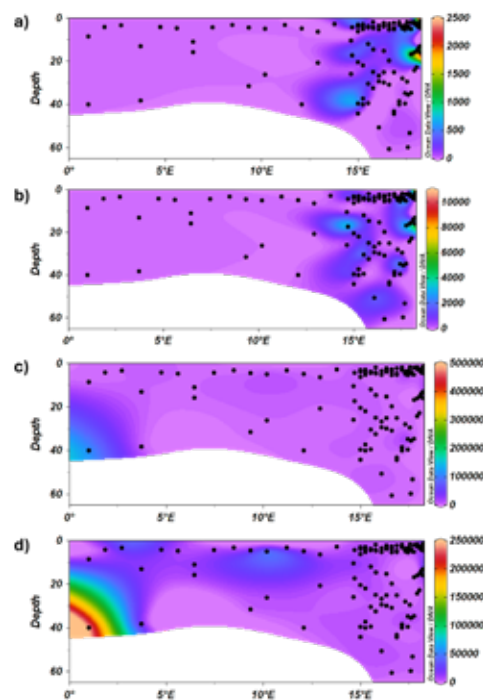


Figure 2. Vertical distribution of average abundance (cells mL^{-1}) during 2022–2024 for (a) nanoplankton, (b) picoeukaryotes, (c) *Synechococcus*, and (d) *Prochlorococcus*. The black dots are sampling positions through the water column. White shading indicates areas of no data.

The nanoplankton abundance increase from 2022 to 2024 was related to increases in both salinity and fluorescence. In contrast, picoeukaryotes were influenced only by fluorescence. The increased abundance of *Synechococcus* was associated with changes in temperature and oxygen, while *Prochlorococcus* variability was linked to temperature differences. Continued monitoring of these phytoplankton groups and their physical environment is required to detect any trends over time, and to determine if they may be subjected to environmental stress.

Author: Gebe Z (OC Research)

Contributors: Maseti T, Hansraj Y, Mdazuka Y (OC Research)

MONITORING PROGRAMMES

6. LONG-TERM MONITORING OF MICROHABITAT TEMPERATURES IN ELANDS BAY

To better understand the physiological effects of multiple ocean stressors (e.g. warming, acidification, deoxygenation and extreme events) on marine organisms, information on the environmental conditions experienced in their natural habitats is required. Data from long-term monitoring capture *in situ* variability of environmental parameters that are used to design experiments and relate findings back to field conditions. Elands Bay on the west coast of South Africa is a key location for such research and monitoring.

Low pH conditions exist along the west coast due to the effects of upwelling, while cold-bottom waters in Elands Bay often result in low oxygen events responsible for mass walkouts of rock lobster. Additional exposure to extreme stressors such as marine heatwaves can exacerbate impacts on physiological processes. For example, acute thermal stress experienced during a marine heatwave may cause rapid deterioration of cellular processes and performances beyond tolerance limits, affecting survival, growth and development. In South Africa, occurrences of marine heatwaves are increasing along the entire coastline and occur at least once a year on average. Data on temperature extremes are thus important for designing experiments and calculating thermal windows.

We initiated long-term monitoring of inshore environmental parameters in Elands Bay by deploying temperature loggers in representative microhabitat types. These included five intertidal rock pools varying in surface area, volume and position along the shore, as well as one sun-exposed and one subtidal habitat. In rock pools (Fig. 1A), temperature loggers attached to ibolts (Fig. 1B), recorded significantly higher temperatures compared to those housed in moorings (Fig. 1C and D), but were more often subject to theft, with loss of data.



Figure 1. In intertidal rock pools (A), temperature loggers are attached via a cable tie to either an ibolt drilled into the rock (B) or housed inside a mooring block (C–D).

Temperature measurements from November 2022 to September 2024 (Fig. 2) revealed mean autumn-winter minima of 5°C, 11°C and 10°C in sun-exposed, subtidal and rock pool habitats, respectively. Mean spring-summer maxima were 44°C, 24°C and 26°C in sun-exposed, subtidal and rock pool habitats, respectively.

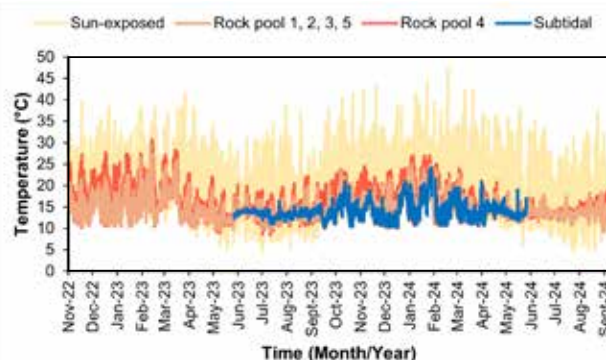


Figure 2. Temperatures of rock pools, a sun-exposed and a subtidal habitat, from November 2022 to September 2024. Data are from the temperature loggers housed inside mooring blocks, which provided a more consistent dataset. Rock pool 4 (ibolt-mooring) was the exception and is therefore plotted separately from other rock pools.

The shallowest rock pool (4), situated furthest inshore, yielded higher temperatures and was also directly in the path of a steady flow of warm estuarine water due to flooding of the Verlorenvlei estuary after a storm in September 2023 (Fig. 2, Table 1).

Table 1. Mean, maximum and minimum temperatures during spring-summer and autumn-winter recorded in the five rock pools during November 2022 to September 2024.

	Spring-Summer		Autumn-Winter	
	Maxima	Mean	Minima	Mean
Rockpool 1	25.15	14.93	10.14	13.86
Rockpool 2	23.53	14.32	10.26	13.63
Rockpool 3	23.50	14.38	10.16	13.66
Rockpool 4	29.04	15.97	9.50	14.14
Rockpool 5	27.45	14.86	10.15	13.84

Maxima and minima temperatures are used in the design of thermal stress experiments investigating the effects of marine heatwaves and cold upwelling events on Cape urchins *Parechinus angulosus*, a keystone benthic invertebrate species. Sessile and semi-motile invertebrates such as urchins are particularly vulnerable to extreme weather events such as storms, floods, and marine heatwaves, since they cannot escape. The importance of the Elands Bay area to commercial fisheries, and the benthic species on which they depend, highlights the need for further monitoring of environmental parameters. Besides temperature, the long-term monitoring of Dissolved Oxygen (DO) has also been initiated in the area through the deployment of three subtidal DO loggers covering the bay.

Authors: Haupt T, Janson L, Williamson R (OC Research); Auerswald L (Fisheries R&D)

Contributor: Samuels K (OC Research)

MONITORING PROGRAMMES

7. EXPLORING THE MICROHABITATS OF THE CAPE URCHIN *PARÉCHINUS ANGULOSUS*

Long-term temperature monitoring captures the local variability and temperature extremes experienced by marine organisms in their natural microhabitats. Such data can be used in physiological research to improve experimental designs and predictions of how marine organisms will fare with changing climatic conditions. This study reports on microhabitat temperatures that were obtained through the deployment of temperature loggers in intertidal rockpools.

The rockpools are situated along Sea Point promenade in Cape Town (Fig. 1A) and are inhabited by Cape urchins *Parechinus angulosus* (Fig. 1B), among other invertebrate species. A sample of these urchins was collected and used in physiological experiments investigating the effects of thermal stress following chronic exposure to low pH conditions. By obtaining in situ temperature data, we could assess what temperature stresses Cape urchins are subjected to in their natural microhabitats, to inform experimental design and interpretation.

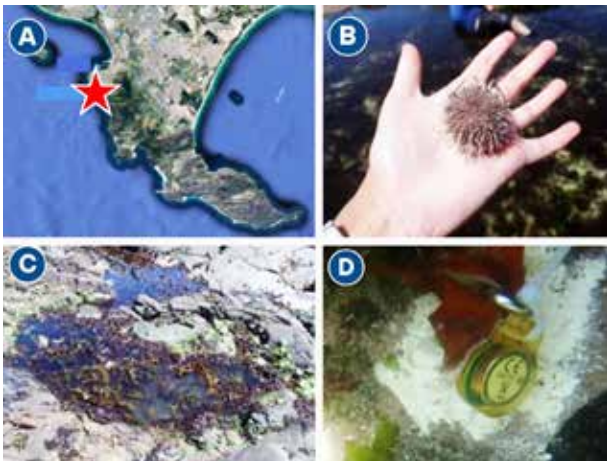


Figure 1. The location of the study site in Sea Point (red star) (A), a Cape urchin *Parechinus angulosus* (B), a rockpool in which temperature loggers were deployed (C) and a HOBO-tidbit temperature logger, attached via an ibolt to a rock (D).

Three prominent rock pools (e.g. see Fig. 1C) were chosen to attach Hobo-tidbit temperature loggers to rocks via bolts (Fig. 1D) and set to record temperature every five minutes. Data have been retrieved monthly. Here we present results of temperature measurements from November 2019 to July 2024 (Fig. 2).

The highest maximum temperature was recorded in spring–summer of 2022 and 2023 (27.9°C), and the lowest minimum temperature during autumn–winter of 2023 (9.14°C). Temperatures in rockpool 1 were consistently higher compared to those of rockpool 3 where narrower temperature ranges were recorded (Fig. 2). These rock pools vary in surface area, volume, and position along the shore, all factors which contribute to the variability in recorded temperatures.

Sessile benthic marine invertebrates such as Cape urchins are particularly vulnerable to thermal stress events since they cannot escape extreme conditions. Preliminary results from experiments showed that Cape urchins that were pre-exposed to chronic low pH conditions (ca. pH 7.3) reached their Critical Thermal Maximum (CTmax) temperature (temperature at which an organism loses locomotory function) at ca. 29°C. This was significantly lower than urchins exposed to normal pH conditions (ca. pH 8), which only reached CTMax at ca. 30°C. This shows that exposure to cumulative stressors may negatively impact Cape urchins and since maximum temperatures recorded in rockpools are as high as 27.9°C, our study shows that these organisms are already living close to their upper thermal limits. These long-term environmental data including daily temperature minima and maxima will be beneficial in further investigations of the effects of extreme weather events, such as marine heat waves and anomalous upwelling, on this important keystone benthic species.

Authors: Janson L, Haupt T (OC Research); Auerswald L (Fisheries R&D)
Contributors: Snyders L (Fisheries R&D); Samuels K (OC Research)

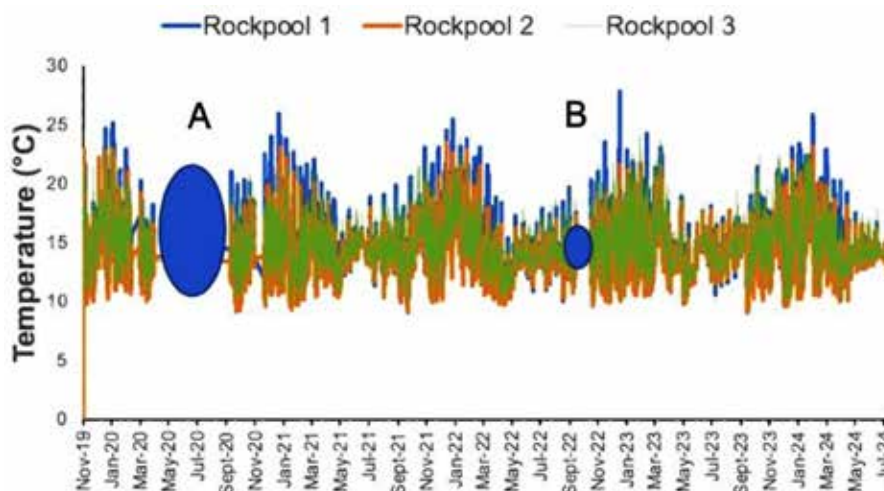


Figure 2. Temperature measurements from November 2019 to July 2024. Blue circles denote gaps in data due to the COVID lockdown period (A) and a damaged logger (B).

MONITORING PROGRAMMES

8. MONITORING MEANDERS IN THREE MAJOR WESTERN BOUNDARY CURRENTS

Western boundary currents (WBCs) are important oceanic pathways for moving heat and salt from the tropics to the poles. Their considerable impact on global climate has sparked intense interest in monitoring their variability. Application of the Tracking Current Cores and Edges (TRACCE) monitoring tool to satellite altimetry data allows simultaneous monitoring of variability within the three largest WBCs. These are the Agulhas Current (AC) off South Africa, the Gulf Stream (GS) off North America and the Kuroshio Current (KC) off Japan (Fig. 1).

The primary source of variability in these systems stems from the meandering of the WBCs. This meandering, described as either shoreward or offshore deviations of the WBCs from their typical paths, is caused by the interaction of mesoscale eddies with the WBCs. To investigate such variability, TRACCE was applied to 30 years (1993–2023) of daily satellite altimetry data in the AC, GS and KC systems. We computed the distance between the coast and the TRACCE-identified WBC cores along selected transects, then used these values as standardised proxies to identify meandering events within the three systems. The selected transects coincided with satellite altimetry ground tracks in the three systems where sufficient in situ data were available to verify the TRACCE-identified WBC cores and edges (Fig. 1a–c). Meanders were identified when the WBC current core moved beyond two standard deviations from its long-term mean position.

TRACCE identified 53 offshore meanders in the AC (Fig. 1d) and 34 offshore meanders in the KC (Fig. 1f). No shoreward meanders were observed in these systems. In contrast, both shoreward (47) and offshore (59) meanders were identified in the GS (Fig. 1e). Along the selected transects, the AC and KC are constrained by the coast (Fig.

1a and c). In contrast, the GS is not (Fig. 1b), allowing for the development of extensive shoreward meanders. The residence time of a meander can influence the intensity of its local impacts. Offshore meanders in the GS resided for 22.59 days on average, whereas the shoreward meanders had a mean residence time of 25.87 days. Although there were fewer offshore meanders overall in the KC, their mean residence time of 44.85 days was ca. double the residence time of meanders in the GS. In contrast, offshore meanders in the AC had a mean residence time of 17.77 days. This suggests that KC meanders are likely to have longer-lasting impacts than meanders in the GS and AC.

WBC meanders have a strong influence on local weather patterns and hydrography, as well as on biological communities and ecosystem dynamics in the adjacent continental shelf regions. Therefore, monitoring their variability is of considerable importance. TRACCE provides a mechanism to monitor the intensity and progression of these meanders within the three WBC systems. It also allows comparison of the variability among the WBCs, which may differ in their response to climate change.

Authors: Russo CS, Lamont T (OC Research)

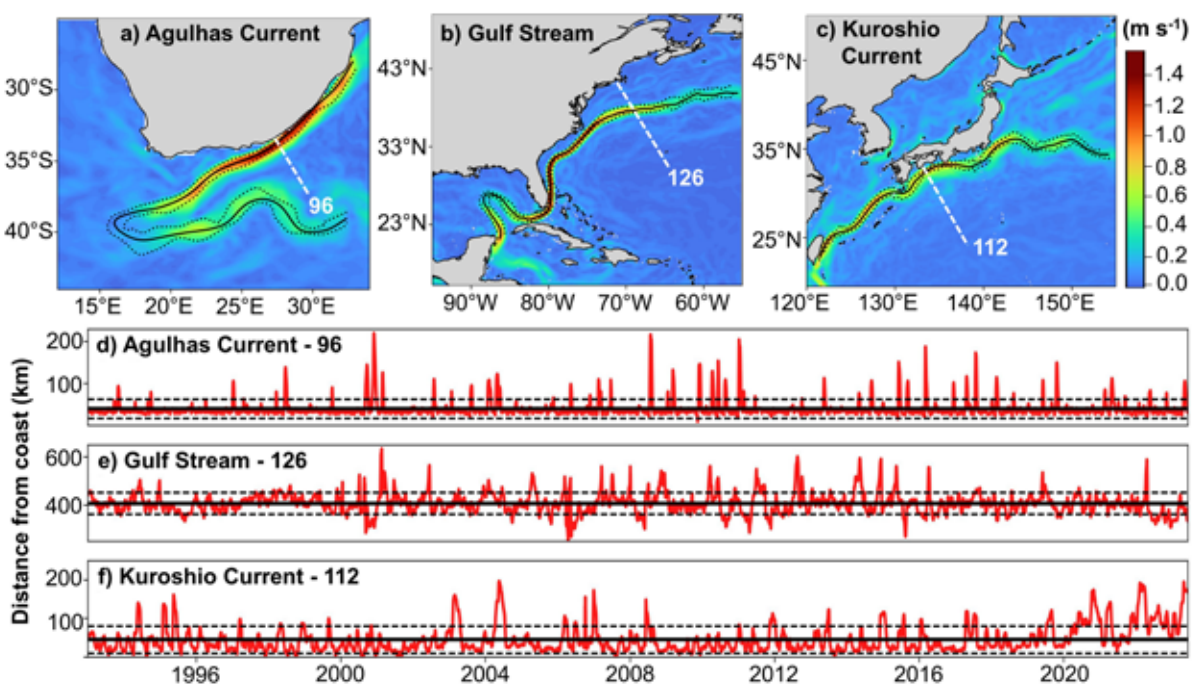


Figure 1. Maps of thirty-year (1993–2023) mean satellite altimetry-derived current speed for (a) the Agulhas Current (AC), (b) the Gulf Stream (GS) and (c) the Kuroshio Current (KC). The locations of satellite altimetry ground tracks (white dashed lines), as well as the TRACCE-identified cores (black solid lines) and edges (black dashed lines) are shown. Time series of the distance between the coast and the TRACCE-identified cores (km) for the (d) AC along track 96, (e) GS along track 126 and (f) the KC along track 112. The mean positions of the cores (solid black lines), as well as two standard deviations above and below the means (dashed black lines) are overlaid.

MONITORING PROGRAMMES

9. LONG-TERM VARIABILITY IN BOTTOM TEMPERATURE ON THE PRINCE EDWARD ISLANDS SHELF

Despite their small size, the Prince Edward Islands (PEIs) provide crucial breeding habitat for vast populations of marine mammals and birds that depend strongly on the ambient oceanographic conditions at and around the islands. While annual relief voyages to re-supply the research base only allow hydrographic data collection during April/May each year, two moorings on the inter-island shelf (Fig. 1) have been providing continuous measurements of bottom temperature since 2014.

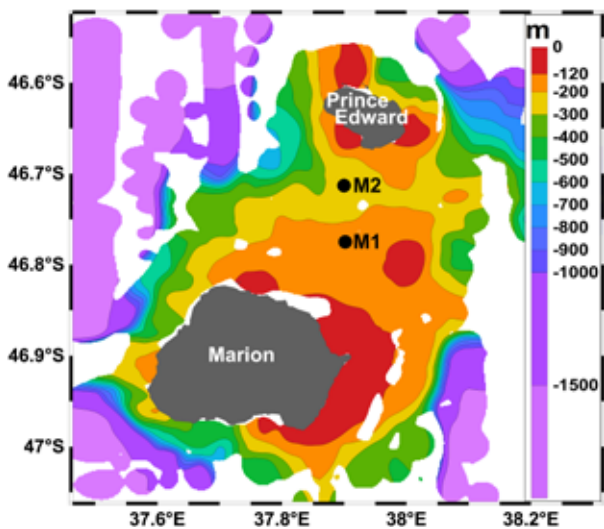


Figure 1. Map of the Prince Edward Islands (PEIs) showing bathymetry (m) on the PEI shelf. Mooring positions M1 and M2 are shown as black dots.

During 2014–2017, overall lower temperatures (below the long-term mean) reflected more frequent northward excursions of the southern branch of the sub-Antarctic Front (S-SAF; Fig. 2). Since 2018, generally elevated temperatures (above the long-term mean) indicate a more southerly location of the S-SAF. During 2023–2024, there were three major events (Fig. 2). A cooling event took place from 12 July to 5 September, when the S-SAF was north of the islands and a cyclonic eddy advected cooler waters toward the PEIs (Fig. 3a). Two warming events occurred from 24 April to 13 June, and from 3 December 2023 to 26 January 2024. These events resulted from cyclonic eddies advecting warmer sub-Antarctic waters toward the PEIs (Fig. 3b). Variations in temperature, and hence food availability, may affect distances that seabirds and marine mammals need to travel from the islands to forage.

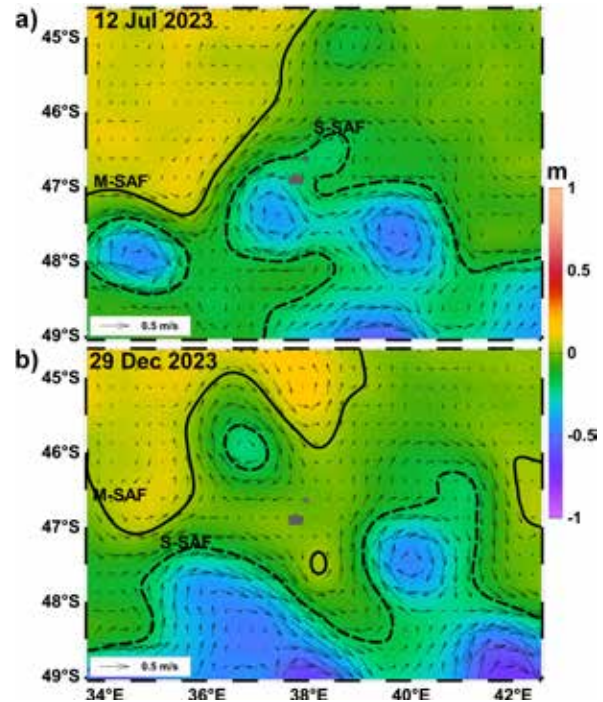


Figure 3. Daily Sea Surface Height (m) on (a) 12 Jul 2023 and (b) 29 December 2023. The middle (M-SAF; solid black contour) and southern (S-SAF; dashed black contour) branches of the sub-Antarctic Front are shown.

This has consequences for time and energy spent foraging, for survival of young that depend on foraging adults, and ultimately for the reproductive success and abundance trends of these populations. Continued warming in 2023–2024 may have meant less food availability at the PEIs, with longer travel times for foraging seabirds and marine mammals.

Authors: van den Berg MA, Lamont T (OC Research)

Contributors: Jacobs L, Louw GS, Masiko O (OC Research)

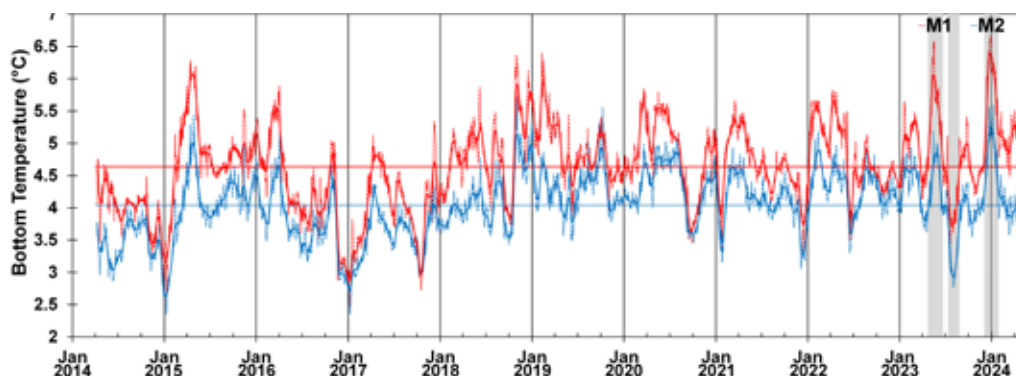


Figure 2. Daily mean bottom temperature (°C) at moorings M1 (red) and M2 (blue). Dashed lines indicate measurements while solid lines show low-pass filtered values. Horizontal lines show mean temperatures for each time series (2014–2024). Grey shading highlights major warming and cooling events during 2023–2024.

MONITORING PROGRAMMES

10. LONG-TERM OBSERVATIONS OF CURRENTS ON THE PRINCE EDWARD ISLANDS SHELF

The Prince Edward Islands (PEIs) are a remote island archipelago in the sub-Antarctic zone of the Southern Ocean. They provide crucial breeding habitat for vast populations of seabirds and marine mammals. It is well-known that there are strong links between the oceanography and biological communities at the PEIs, but observations have been largely limited to periods coinciding with annual relief voyages in April–May. To contribute to long-term oceanographic observations, two moorings deployed on the inter-island shelf (Fig. 1) have been providing continuous measurements of water column current speed and direction since April 2014.

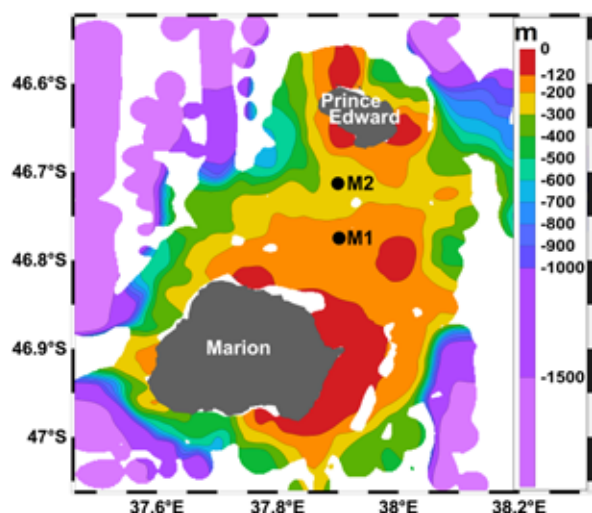


Figure 1. Map of the Prince Edward Islands (PEIs) showing bathymetry (m) on the PEI shelf. Mooring positions M1 and M2 are shown as black dots.

The eastward-flowing Antarctic Circumpolar Current results in much stronger zonal (east/west) than meridional (north/south) flow at the PEIs. During 2014–2024, daily mean current speeds at mooring M1 ranged from 0.01 to 50.90 cm s^{-1} , and those at M2 from 0.03 to 67.32 cm s^{-1} . A Taylor column structure, which is a stationary anticyclonic (anticlockwise) circulation over the shelf, is indicated by westerly flow in the bottom waters at M2 (Fig. 2). This bottom westerly flow is persistent but can be enhanced or interrupted when fronts or mesoscale eddies interact with the shelf. Retention of nutrients and biota by the Taylor column maintains productivity on the shelf, accounting for high concentrations of marine biota at the PEIs.

During 2023–2024, a major cooling event was observed from 12 July to 5 September 2023, while two major warm events occurred from 24 April to 13 June 2023 and from 3 December 2023 to 26 January 2024 (see Report Card 9). During the cooling event, currents changed from easterly to westerly flow as a cyclonic (clockwise) eddy moved northward and interacted with the PEI shelf (Fig. 2). This change was more notable at M1 than at M2, likely due to the location of this cyclonic eddy to the southwest of the PEIs (see Report Card 9, Fig. 3a). Interestingly, while both warming events were also associated with cyclonic eddies, they displayed different circulation patterns. The April–June 2023 event showed a change from westerly to easterly flow as cyclonic eddies located due north and east of the PEIs influenced the flow on the shelf. In contrast, the December 2023 – January 2024 event showed strong westerly flow throughout the water column at both moorings for the duration of the event (Fig. 2).

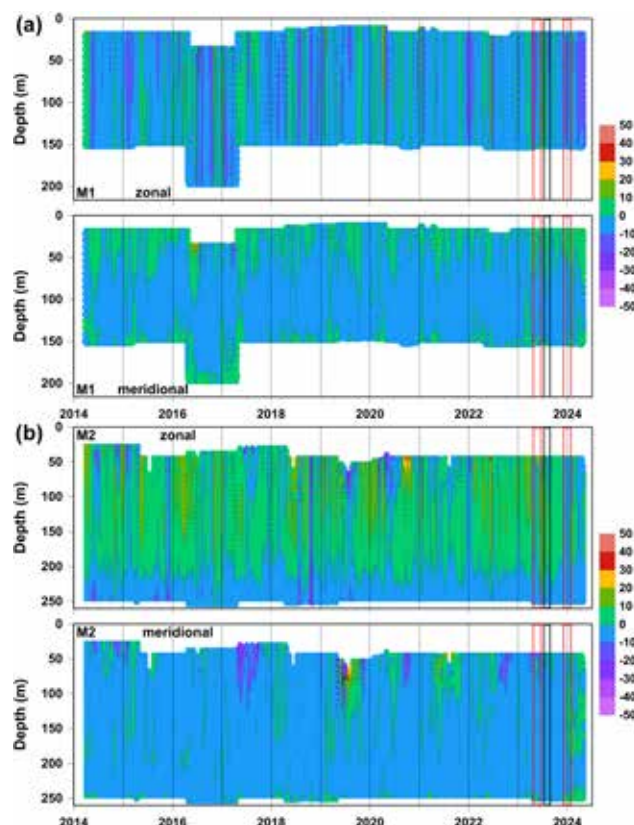


Figure 2. Daily mean zonal and meridional current components (cm s^{-1}) at (a) M1 and (b) M2 during 2014–2024. Positive values denote easterly and northerly flow; negative values denote westerly and southerly flow. Red boxes highlight warming events during April–June 2023 and December 2023 – January 2024, while the black box highlights a cooling event during July–September 2023.

This flow pattern resulted from the location of a cyclonic eddy to the northwest of the PEIs (see Report Card 9, Fig 3b).

Changes in the direction of current flow may influence the distribution of preferred prey, and hence the feeding patterns of seabirds and marine mammals breeding at the PEIs. Detailed comparisons between current patterns and the feeding behaviour, diet, and reproductive performance of selected predators are required to evaluate the impact of these changing flow dynamics on top predators. Our observations do not indicate any clear long-term trends in the current speeds and direction on the PEI shelf. However, these time series are likely too short to adequately reflect such trends. It is therefore crucial to sustain collection of time series to achieve adequate length for accurately detecting long-term trends.

Authors: van den Berg MA, Lamont T (OC Research)

Contributors: Jacobs L, Louw GS, Masiko O (OC Research)

MONITORING PROGRAMMES

11. PATTERNS OF POTENTIAL VULNERABLE MARINE ECOSYSTEMS IN THE SOUTHERN OCEAN

The Southern Ocean (SO) is a vital component of the global climate system and a hotspot for marine biodiversity. The region encompasses ecosystems that are particularly sensitive to anthropogenic activities that interact with the seabed, such as longline fishing for Patagonian toothfish. To this end, the Commission for the Conservation of Antarctic Marine Living Resources (CCAMLR) – the body responsible for resource management in the SO – has developed ecosystem-based management strategies. South Africa has voluntarily adopted these strategies to ensure adequate management of fishing operations in their SO territorial waters around the Prince Edward Islands (PEIs).

To assess the effectiveness of current CCAMLR conservation measures for Vulnerable Marine Ecosystems (VMEs) and gain insights into the ecological health of the regions, we assessed VME bycatch data from within the Exclusive Economic Zone (EEZ) around the PEIs (Fig. 1). The data were obtained from observer records, spanning from 2009 to 2023.

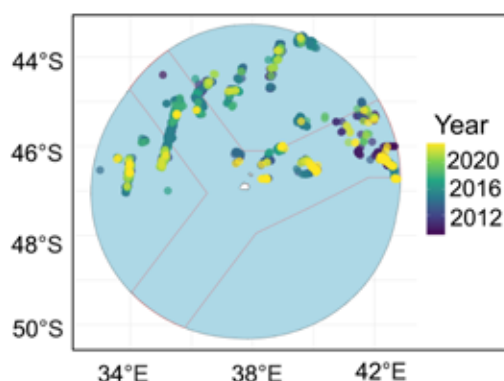


Figure 1. Map showing the distribution of observer data used in this study, in relation to the EEZ of the PEIs and by year (2009–2023). The red lines indicate Marine Protected Area boundaries.

The analysis focused on assessing temporal and spatial patterns of VME indicator species, as defined by CCAMLR (Fig. 2). VME bycatch was identified to the lowest taxonomic level possible following the CCAMLR VME Taxa Identification Guide and recorded with their associated weights per each long-line segment. All 27 taxa (scientific groups) across 12 phyla (taxonomic categories) recognised by CCAMLR as VME indicator species were represented within the 1,703 records of the PEI's bycatch dataset.

Spatially, VME taxa were distributed across a broad area within and around the PEIs Marine Protected Area (MPA). A notable concentration of VME records was found between 44°S and 47°S latitude and 34°E to 42°E longitude (Fig. 1). The temporal distribution of observed VME bycatch weights revealed notable variations (Fig. 3A). The highest bycatch occurred in 2015, coinciding with increased vessel operations in the region. The lowest bycatch was recorded in 2019 and 2020, likely due to reduced fishing activities in the area. Known VME taxa contributed 63% of the VME bycatch weight in 2015, whereas only 26% of known VME taxa were present in 2019 and 2020. Over time, there has been a discernible spatial shift in the locations of VME bycatch, which may partially account for the decline in VME taxa bycatch weight since 2015 (Fig. 3A).



Figure 2. Known VME taxa, where colours are adopted to outline differentiations as represented in the CCAMLR guide.

Bycatch locations were clustered in the northern region during 2015–2017. In contrast, the later years (2021–2023) showed a more dispersed distribution, with some clustering shifting further south (Fig. 3B).

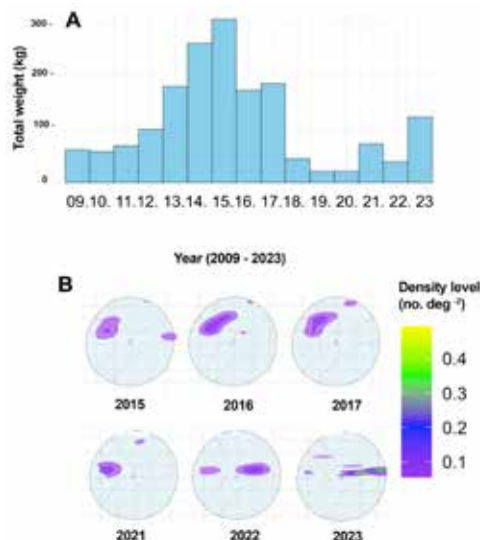


Figure 3. Bycatch of VME indicator species presented as (A) weight per year for 2009–2023, and (B) Kernel Density Estimation heatmaps of VME bycatch events (≤ 15 kg; no. per square degree) for 2015–2017 (top) and 2021–2023 (bottom). Dashed red lines indicate Marine Protected Area boundaries.

This study underscores the critical role of data-driven approaches in understanding the temporal and spatial dynamics of potential VMEs within the PEIs MPA. The observed temporal fluctuations and spatial shifts suggest interplay between fishing activities and ecosystem resilience, and highlight the need for adaptive management strategies.

Authors: Filander Z (OC Research), Somhlaba S (Fisheries R&D), Makhado AB (OC Research)

RESEARCH HIGHLIGHTS

12. A FIRST LOOK AT SEASONAL VARIABILITY OF CURRENTS ON THE PRINCE EDWARD ISLANDS SHELF

Climatologies are long-term means of climate variables, such as ocean temperature or circulation patterns, which provide baselines for understanding climate variations. Data to determine such baselines are being obtained on the inter-island shelf of South Africa's Prince Edward Islands (PEIs) archipelago, where two moorings (M1 and M2; Fig. 1) have been measuring current speed through the water column since 2014. These moorings are in place because it is important to understand and monitor variations in oceanographic conditions at and around the islands, especially because the vast resident breeding populations of marine mammals and seabirds depend on the surrounding marine environment for feeding. Although climatologies are typically only considered accurate when computed from a minimum of 30 years of data, they may still provide useful information when computed using shorter time series.

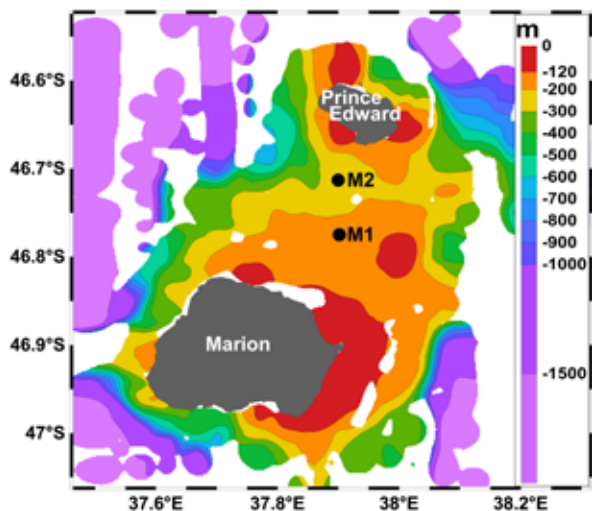


Figure 1. Map of the Prince Edward Islands (PEIs) showing bathymetry on the PEI shelf. Mooring positions M1 and M2 are shown as black dots.

We computed monthly climatologies of current speed from the two PEIs moorings for the period 2014–2024. Zonal speeds indicated westward flow throughout the water column at M1 (Fig. 2a), but westward flow was observed only below 200 m at M2 (Fig. 2b). Seasonal

patterns were opposite at M1 and M2. Zonal speeds indicated strong westward flow, up to 6.55 cm s^{-1} at M1 during December–January and July–August (Fig. 2a), and up to 7.29 cm s^{-1} at M2 in February–May and September–October (Fig. 2b). While eastward current speeds at M1 reached a maximum of 0.19 cm s^{-1} , those at M2 were much stronger (up to 6.19 cm s^{-1}). The weakest mean zonal speeds occurred during April–June at M1 and July–August at M2. Meridional speeds showed stronger southward flow (up to 4.42 cm s^{-1}) at M2 than at M1 (up to 3.91 cm s^{-1}). In contrast, northward flow at M1 (up to 2.52 cm s^{-1}) was stronger than at M2 (up to 0.11 cm s^{-1}) (Fig. 2).

Notably, the mean flow throughout the water column at M1, and below 200 m depth at M2, was westward throughout the year (Fig. 2b). This further substantiates the persistence of a Taylor Column structure that retains water and biota on the shelf (see Report Card 10). These seasonal changes in current speed and direction may have seasonally varying effects on the distribution of food for marine mammals and seabirds.

Authors: Lamont T, van den Berg MA (OC Research)

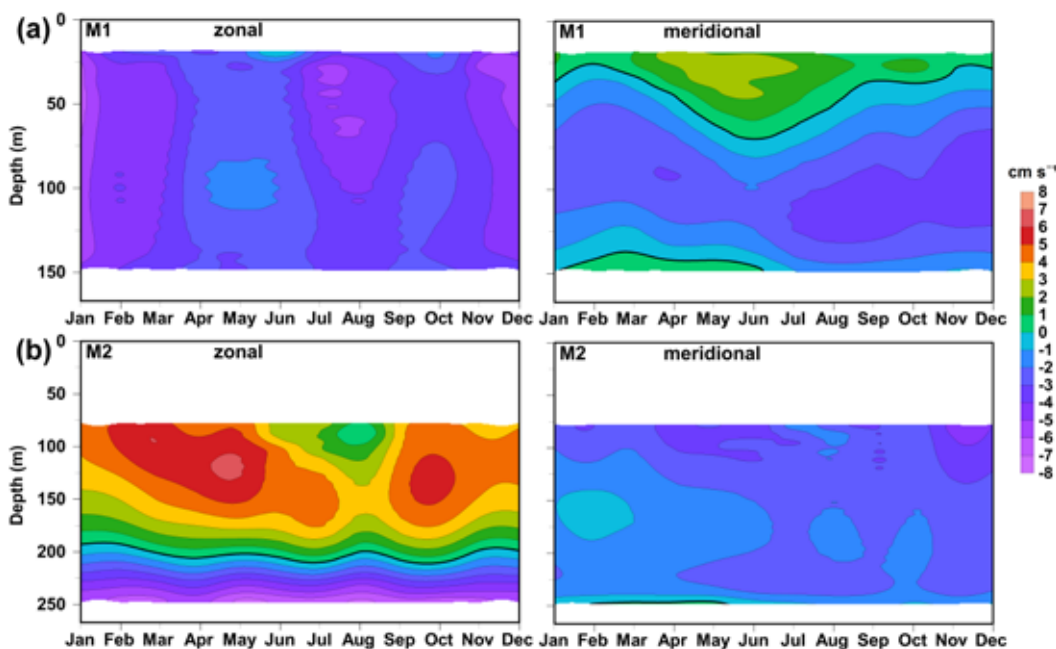


Figure 2. Long-term (2014–2024) climatological monthly mean zonal (east/west) and meridional (north/south) current components (cm s^{-1}) at (a) M1, and (b) M2. Positive values denote eastward (zonal) and northward (meridional) flow; negative values denote westward (zonal) and southward (meridional) flow. The thick black contours indicate 0 cm s^{-1} .

RESEARCH HIGHLIGHTS

13. MICROPLANKTON DIVERSITY IN THE OCEANS SOUTH OF SOUTH AFRICA

Microplankton (phyto- and zooplankton in the size range of 20–200 μm) are a diverse group that are considered robust indicators of the marine environment due to their rapid responses to environmental changes. However, very little is known about their diversity at the Prince Edward Islands (PEIs), which are home to a large number of top predators, and in the Agulhas Current system (Crossroads Monitoring Line) south of South Africa (Fig. 1).

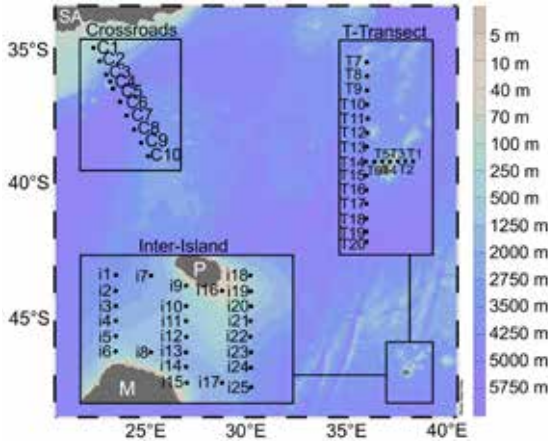


Figure 1. Map indicating stations in the three different sampling regions during the 2023 PEIs relief voyage. SA= South Africa,

At the PEIs, annual sampling occurs in autumn along three inter-island transects on the PEI shelf, and along a larger scale, T-shaped transect further offshore. Sampling also occurs along the Crossroads Monitoring Line and the Agulhas Return Current, which are important for transport of planktonic organisms (Fig. 1). Surface microplankton abundance was assessed using the FlowCam® (which captures images of micro-organisms in water) and associated software.

Total abundance (no. L^{-1}) in 2023 was generally low at most stations (Figs. 2 and 3). Along the Crossroads line, diatoms were more abundant than dinoflagellates and total abundance was fairly uniform (Fig. 2). The exception was station C2 (Fig. 1) where there was a much higher total abundance of diatoms, composed of mainly *Chaetoceros* spp. (Fig. 2). This might be attributed to greater availability of nutrients brought to the surface waters by the Agulhas Current. Interestingly, copepod nauplii were also more abundant at this station

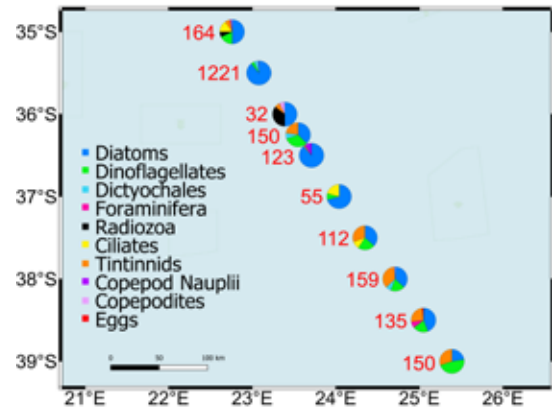


Figure 2. Diversity of microplankton, with total abundance (no. L^{-1}) indicated as red values for each station along the Crossroads monitoring line.

with an absence of both ciliates and tintinnids, suggesting that phytoplankton may be their primary food source at this location (Fig. 2).

In contrast, dinoflagellates were the dominant taxa along the T-Transsect and at the Inter-Island stations (Fig. 3). Dinoflagellates usually grow slower than diatoms and occur in higher numbers once the initial diatom bloom has diminished. Peak total abundance, comprised almost entirely of dinoflagellates and observed furthest away from the islands at station i25 (Figs. 1 and 3), was possibly linked to an influx of nutrients. *Tripos* spp., which often occur in blooms, were the largest contributor to the dinoflagellates at this station.

This study has provided a detailed snapshot of the microplankton variability for these areas during autumn. The low microplankton abundances at most stations was expected since nutrient levels are usually depleted at this time of year.

Authors: Maduray S, Soeker MS, Worship M (OC Research)
Contributors: Kakora H, Mdazuka Y, Mooi G (OC Research)

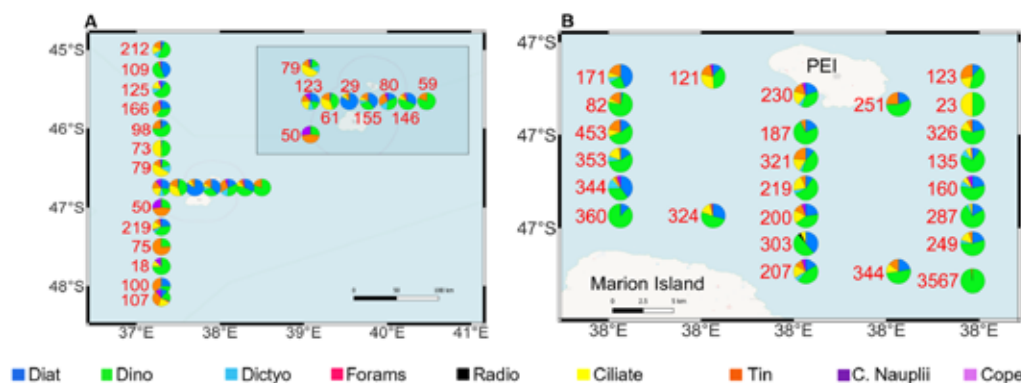


Figure 3. Diversity of microplankton, with total abundance (no. L^{-1}) indicated as red values for each station along the (A) T – Transect, and (B) Inter-Island monitoring lines. Diat: Diatoms, Dino: Dinoflagellates, Dictyo: Dictyochales, Forams: Foraminifera, Radio: Radiozoans, Ciliate: Ciliates, Tin: Tintinnids, C. Nauplii: Copepod nauplii, Cope: Copepodites.

RESEARCH HIGHLIGHTS

14. MACRONUTRIENT DISTRIBUTIONS AROUND GOUGH ISLAND

Phytoplankton species play an important role in regulating climate by facilitating air-sea carbon dioxide (CO₂) exchange. Phytoplankton require macronutrients (such as Nitrate (NO₃⁻), Nitrite (NO₂⁻), phosphate (PO₄³⁻), and Silicate (Si(OH)₄)) for growth. Changes in phytoplankton growth due to macronutrient availability can affect the marine food web and the amount of CO₂ in the atmosphere, which in turn can affect global temperature. It is therefore essential to monitor the distributions and biogeochemistry of macronutrients in the ocean. Here, we describe the first measurements of macronutrient concentrations in the water column around Gough Island (Fig. 1).

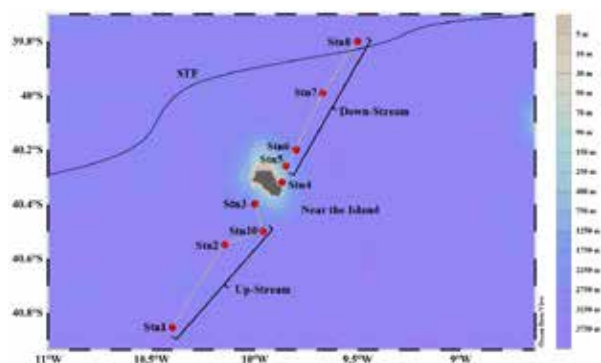


Figure 1. Map showing the cruise track (yellow line with nine stations (red dots)) within three sampling zones (Up-stream, near the Island, and Down-stream). The solid black contour indicates Subtropical Front (STF).

The ranges of macronutrient concentrations in the water column are reported in Table 1. Our results show no significant differences in the highest values among the three zones ($T = 1.12$, $p > 0.05$). In contrast, the low concentrations of NO₃⁻ and Si(OH)₄ near the Island were significantly lower ($T = 2.01$, $p < 0.05$) than in the Up- and Down-stream zones (Table 1). This suggests a more rapid consumption of macronutrients from biological activity, associated with slightly elevated chlorophyll *a* concentrations, near the Island (see Report Card 16).

Water column distributions of NO₃⁻, PO₄³⁻ and Si(OH)₄ concentration were generally low and uniform from the surface to ca. 200 m depth (due to biological uptake).

Table 1. Ranges of macronutrients concentrations within the three zones sampled around Gough Island.

Zones	Macronutrients (μM)			
	NO ₃ ⁻	NO ₂ ⁻	PO ₄ ³⁻	Si(OH) ₄
Up-stream	7.0–33.3	0.03–0.4	0.6–2.2	1.7–61.5
Down-stream	6.1–32.9	0.01–0.4	0.5–2.3	1.5–61.0
Near Island	4.2–32.6	0.03–0.4	0.5–2.2	1.1–61.0

They increased with depth thereafter (due to regeneration of sinking organic matter or upwelling of nutrient-rich deep waters). In contrast, NO₂⁻ concentrations were elevated (0.2–0.4 μM) in the Subtropical Surface Waters and relatively low (<0.15 μM) in the Antarctic Intermediate Waters and in the Upper and Lower Circumpolar Deep Waters (Fig. 2). The highest concentrations of NO₃⁻ (30–35 μM) and PO₄³⁻ (2.0–2.3 μM) were observed within the Upper Circumpolar Deep Waters in association with minimum dissolved oxygen concentrations (see Report Card 16).

Monitoring distributions of macronutrient concentrations is important for understanding how bio-availability of macronutrients drives primary production and the quality of food for phytoplankton growth at the base of the marine food web. This, in turn, has the potential to impact food production for organisms at higher trophic levels (such as fish, seals and whales) around Gough Island.

Authors: Mtshali TN, Tsanwani M (OC Research)

Contributors: Vena K, Kiviets G, Mdokwana B, Britz K (OC Research)

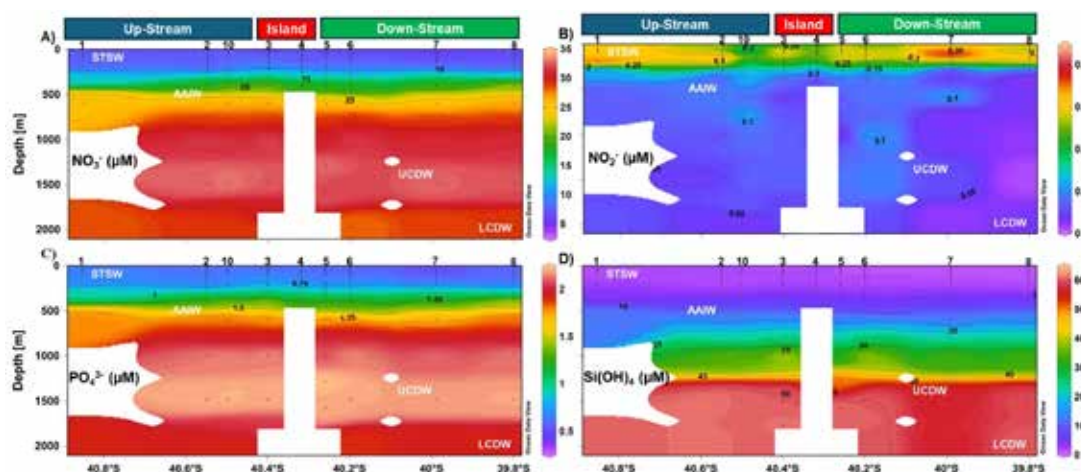


Figure 2. Water column distributions of macronutrients (μM) (a) NO₃⁻, (b) NO₂⁻, (c) PO₄³⁻ and (d) Si(OH)₄ across three zones; Up-stream, near the Island, and Down-stream. Station numbers are indicated above each plot, and the black dots indicate depths of sample collection. Water masses are labelled as follows: Subtropical Surface Waters (STSW; surface – 465 m depth), Antarctic Intermediate Waters (AAIW; 500– 879 m depth), Upper- and Lower Circumpolar Deep Waters (UCDW; 900–1750 m, and LCDW; >1750 m). White blocks below Station 4 indicate the island topography, while the rest of the white shading indicates no data.

RESEARCH HIGHLIGHTS

15. DISTRIBUTIONS OF CARBONATE SYSTEM PARAMETERS AROUND GOUGH ISLAND

The carbonate system in the ocean plays a vital role in absorbing anthropogenic carbon dioxide (CO₂) from the atmosphere by readily reacting with dissolved CO₂ to form bicarbonate ions. The Southern Ocean (SO) accounts for more than 40% of the cumulative global ocean anthropogenic carbon dioxide absorption, making it a key region in terms of CO₂ uptake from the atmosphere. However, the SO is vulnerable to ocean acidification due to increasing atmospheric CO₂ levels. Thus, understanding the distributions of the carbonate parameters in this region is important.

Here, we present the distribution of temperature (°C); salinity (PSU); carbonate parameters, namely total alkalinity (A_T), dissolved inorganic carbon (C_T), pH, and aragonite saturation state (Ω_{arag}); and the partial pressure of CO₂ (pCO₂); in the Gough Island vicinity. Measurements were collected along a transect during the 2023 Gough Island expedition onboard the SA *Agulhas II* (14th September – 17th October 2023) (see Fig. 1, Report Card 14). The transect was divided into three zones: i) Up-stream, where three stations (1, 2, 10) were sampled; ii) Island (meaning near to the island), where there were two stations (3, 4); and iii) Down-stream, where there were four stations (5–8) (Fig. 1). In the results below, the distributions of carbonate parameters and pCO₂ in Fig. 2, are compared with the distributions of temperature and salinity in Fig. 1.

1.75. The high CT, which dominated the down-stream zone in the UCDW, was accompanied by the highest pCO₂ ranging from 550 to 732 μatm, the lowest pH ranging from 7.72 to 7.85, and the lowest Ω_{arag} ranging from 0.64 to 0.80.

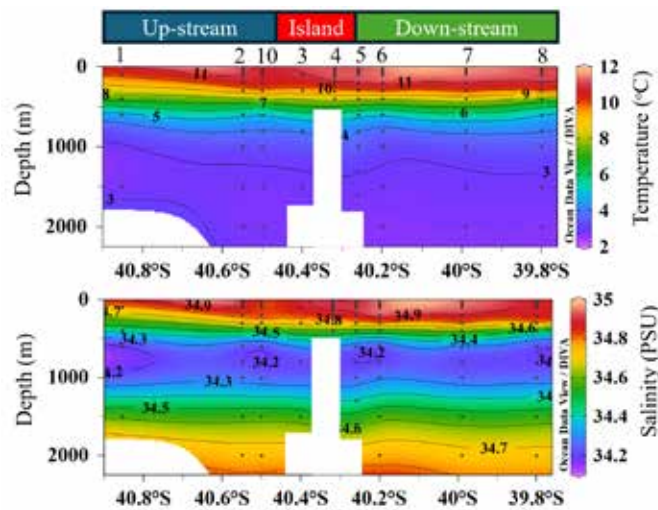


Figure 1. Water column distributions of temperature (°C) and salinity (PSU) along the transect, with the three zones (Up-stream, Island and Down-stream) depicted. The upper surfaces of the white polygons on stations 3–5 indicate bottom depths. STSW = Subtropical Surface Waters, AAIW = Antarctic Intermediate Waters, UCDW = Upper Circumpolar Deep Waters, LCDW = Lower Circumpolar Deep Waters.

Water masses that could be identified include Subtropical Surface Water (STSW), the Antarctic Intermediate Water (AAIW), Upper Circumpolar Deep Water (UCDW) and the Lower Circumpolar Deep Water (LCDW). The CT was lower (2094–2190 μmol kg⁻¹) in the warmer (10–11.58°C) upper 100 m layer, while the AT was lower (2269–2300 μmol kg⁻¹) in the low salinity (34.19–34.3 PSU) AAIW between 500 and 1000 m depth. The CT was highest (2225 to 2253 μmol kg⁻¹) in the UCDW, with high values dominating the down-stream zone, while the AT was highest (>2320 μmol kg⁻¹) below 1500 m in the up-stream and down-stream zones. The upper 100 m layer had low pCO₂ ranging from 289 to 550 μatm, a pH above 8.0, and Ω_{arag} above

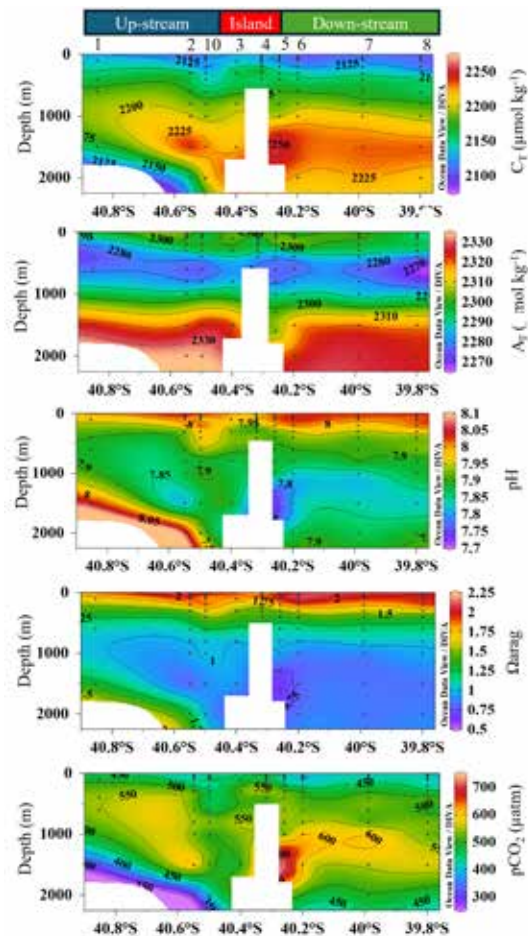


Figure 2. Water column distributions of dissolved CT, AT, pH, Ω_{arag} and pCO₂ along the transect, with the three zones (Up-stream, Island and Down-stream) depicted. The upper surfaces of the white polygons on stations 3–5 indicate bottom depths.

The acidic (pH <7.8) and low Ω_{arag} (<0.75) conditions at depth below station 5 in the down-stream zone could be detrimental to marine life, especially for those with calcium carbonate skeletons (e.g. coral and shellfish). As more anthropogenic CO₂ dissolves in the ocean, C_T and pCO₂ increase and pH and Ω_{arag} decline. These changes in carbonate chemistry may negatively affect the ability of organisms inhabiting the SO to form and maintain their shells.

Authors: Tsanwani M, Mtshali TN, Mdokwana WB (OC Research)
Contributors: Vena K, Kiviets G, Britz K (OC Research)

RESEARCH HIGHLIGHTS

16. CHLOROPHYLL A AND DISSOLVED OXYGEN CONCENTRATIONS AROUND GOUGH ISLAND

Gough Island's phytoplankton bloom is amongst the least studied in the Southern Ocean compared to other subantarctic islands such as the Kerguelen and Crozet Islands. Chlorophyll a (chl a; a pigment for photosynthesis) is an important component of phytoplankton cells and its concentration in water is commonly used as a proxy for phytoplankton biomass. Dissolved oxygen (DO) in the water is an essential requirement for phytoplankton. Its primary sources in water are through diffusion from air and from photosynthesis of phytoplankton. In aquatic systems, chl a and DO concentrations are closely related, with high concentrations of chl a typically indicating a high level of photosynthesis, leading to increased production of DO as a byproduct of the process. Here, we present for the first time the distributions of chl a and DO concentrations in waters around Gough Island.

Data were collected during the Gough Island 2023 expedition onboard the SA *Agulhas II* (14th September – 17th October 2023). Seawater samples were along a transect traversing three zones, namely near the island (referred to as "Island"), Up-stream and Down-stream of the island (see Report Card 14, Figure 1), using a CTD rosette. Thereafter, samples were analysed for chl a and DO measurements.

Along the transect and throughout the water column, chl a and DO concentrations ranged between 0.01–0.6 mg m⁻³ and 4.2–6.5 ml L⁻¹, respectively (Figs. 1 and 2). Chl a concentrations were somewhat uniform from the surface to about 300 m depth, with no subsurface chl a max (Fig. 1a). Elevated chl a concentrations were observed up-stream (0.003–0.61 mg m⁻³) and down-stream (0.001–0.58 mg m⁻³), with low concentrations near the island (0.001–0.42 mg m⁻³). Phytoplankton blooms were observed at two stations up-stream (2, 10) and three stations down-stream (6, 7 and 8) (Fig. 2a). The latter is expected, because water flowing around the island and then converging down-stream may constitute a reliable source of iron (an essential element for phytoplankton growth) from the island mass effect. Alternatively, formation of eddies due to flow disturbance around the island may provide favourable conditions for accumulation of phytoplankton. Upwelling of nutrient-rich waters may explain the up-stream observations.

The DO concentrations were elevated in Subtropical Surface Water with values ranging between 5.75–6.40 ml L⁻¹. Concentrations decreased in Antarctic Intermediate Water (<5.75 ml L⁻¹), with a minimum oxygen zone (MOZ)

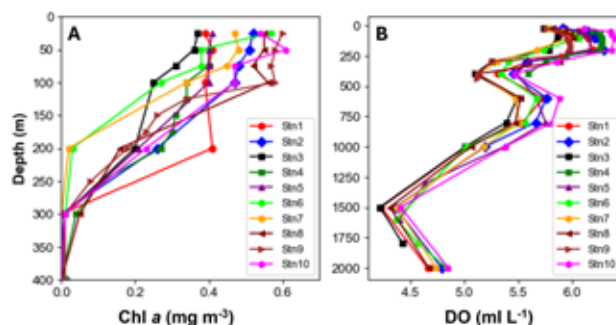


Figure 1. Vertical plots of (A) Chl a (mg m⁻³) and (B) DO (ml L⁻¹) profiles measured along the transect. Note that the y-axis scale is different between plots. Stn = station.

occurring in the Upper Circumpolar Deep Water (isopycnal <4.50 ml L⁻¹). Concentrations increased slightly in Lower Circumpolar Deep Water (isopycnal >4.50 ml L⁻¹) (Figure 2b). High DO concentration in the upper surface waters was more pronounced up-stream and near the island (Fig. 2b). While there seems to be a relationship between chl a and DO (Stations 2, 6, 7, 8 and 10), there appeared to be a mismatch between where the highest concentrations of chl a (down-stream) and DO (up-stream and island) occurred (Fig. 2a and b).

High primary productivity around the island or up- and down-stream of it provides an important food source for both the pelagic and benthic ecosystems. It is therefore critical for sustaining the large breeding colonies of seabirds and seals at the island. Results obtained here provide the baseline for continued monitoring.

Authors: Mtshali TN, Tsanwani M (OC Research)

Contributors: Vena K, Kiviets G, Mdokwana B, Britz K (OC Research)

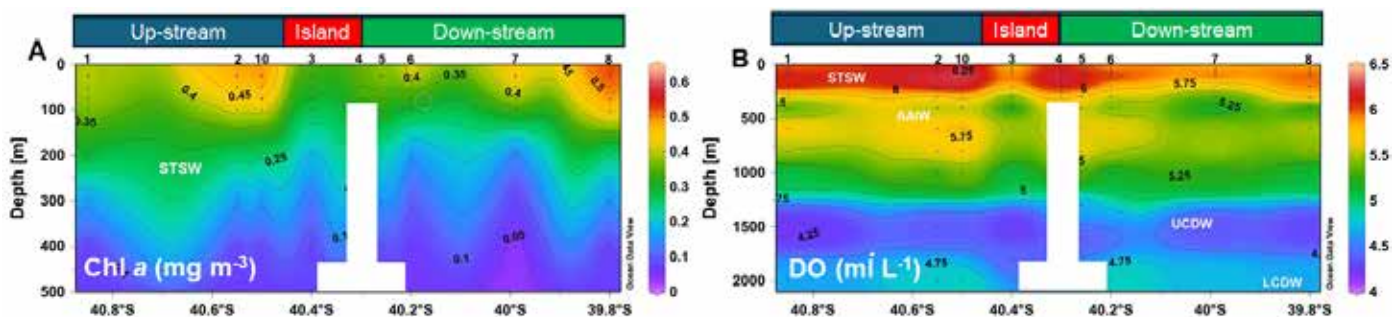


Figure 2. Water column distributions of (A) Chlorophyll a (mg m⁻³) and (B) Dissolved Oxygen (ml L⁻¹). The white bars represent the island bathymetry. Water masses include Subtropical Surface Water (STSW), Antarctic Intermediate Water (AAIW), Upper and Lower Circumpolar Deep Water (UCOW and LCOW, respectively). The numbers above the plots indicate station numbers within the Up-stream (blue bar), near the Island (red bar) and Down-stream transect zones (green bar). Note that the y-axis scales differ for the two parameters.

RESEARCH HIGHLIGHTS

17. DISTRIBUTION OF DISSOLVED TRACE METALS AROUND GOUGH ISLAND

The Southern Ocean (SO) is one of the largest high-nutrient, low-chlorophyll (HNLC) regions in the global ocean, where dissolved trace metals such as iron limit phytoplankton growth, ultimately influencing the Biological Carbon Pump and our climate. Natural exceptions to the HNLC regime occur where wind and current-induced island wakes cause dissolved trace metals from sediments to be mixed into surface waters, enabling large and prolonged phytoplankton blooms (the “Island Mass Effect”; IME) and increased carbon drawdown. Extensive research on trace metal biogeochemistry has been conducted at the sub-Antarctic Kerguelen, South Georgia and Crozet Islands, but no such studies have been undertaken at Gough Island in the Atlantic region of the Southern Ocean. Here, for the first time, we present water column profiles of dissolved trace metals—iron (dFe), manganese (dMn), zinc (dZn), cobalt (dCo), cadmium (dCd) and lead (dPb)—around Gough Island.

Data were collected during the 2023 Gough Island expedition onboard the *SA Agulhas II*, from 14th September to 17th October (see Report Card 14, Fig. 1). Sampling was conducted in three zones: (i) Up-stream (stations 1, 2 and 10), (ii) near the Island (stations 3, 4, and 9), and (iii) Down-stream (stations 5, 6, 7 and 8). Seawater samples were collected using a trace clean GEOTRACES CTD rosette equipped with 12 x 6L clean GoFlo bottles. The samples were filtered through 0.2- μm pore size filters into acid-washed, Low-Density Polyethylene (LDPE) bottles, acidified with 30% HCl (ultrapur) to pH <2. Samples were stored at room temperature for further analysis on land, using on-line SeaFast Inductively Coupled Plasma Mass spectrometry (ICP-MS).

Water column distributions of dissolved trace metals (Fig. 1) typically exhibited nutrient-like distributions, with low concentrations in the upper Subtropical Surface Water (STSW) and increasingly higher concentrations in the deeper Antarctic Intermediate Water (AAIW) and Upper Circumpolar Deep Water (UCDW). Such low upper surface concentrations highlighted strong biological uptake with aggregation of sinking organic matter. Elevated deep-water concentrations can be explained by upwelling of metal-rich deep waters from the sea-floor sediments and diffusive mixing, or remineralisation of sinking organic matter (Figs. 1A, C, D, E and F). Dissolved manganese (dMn) concentrations were an exception, in that they were elevated in the shallower STSW and depleted in the deeper AAIW and UCDW, which is typical for SO dMn profiles (Fig. 1B). Elevated surface dMn concentrations likely indicate a combination of aeolian (wind-borne) inputs from the island and the photo-reduction of Mn oxides. Low values at depth were likely due to the sinking and particle aggregation of Mn oxides, particularly in the UCDW. Slightly higher concentrations of most metals were observed at stations near Gough Island (except for dCd; Fig. 1E), compared to up- and down-stream, highlighting the supply of metals from the IME.

The results show that the up-stream influence of Gough Island appeared to be minor, with down-stream metal concentrations in the range of trace metal-depleted regions of the SO. This is in association with elevated Chl *a* distributions observed down-stream of the island (see Report Card 16). Understanding the impact of IME on distribution, sources and biogeochemical cycles of dissolved trace metals is essential given their interaction with phytoplankton, which, in turn, plays a key role in climate and marine food webs.

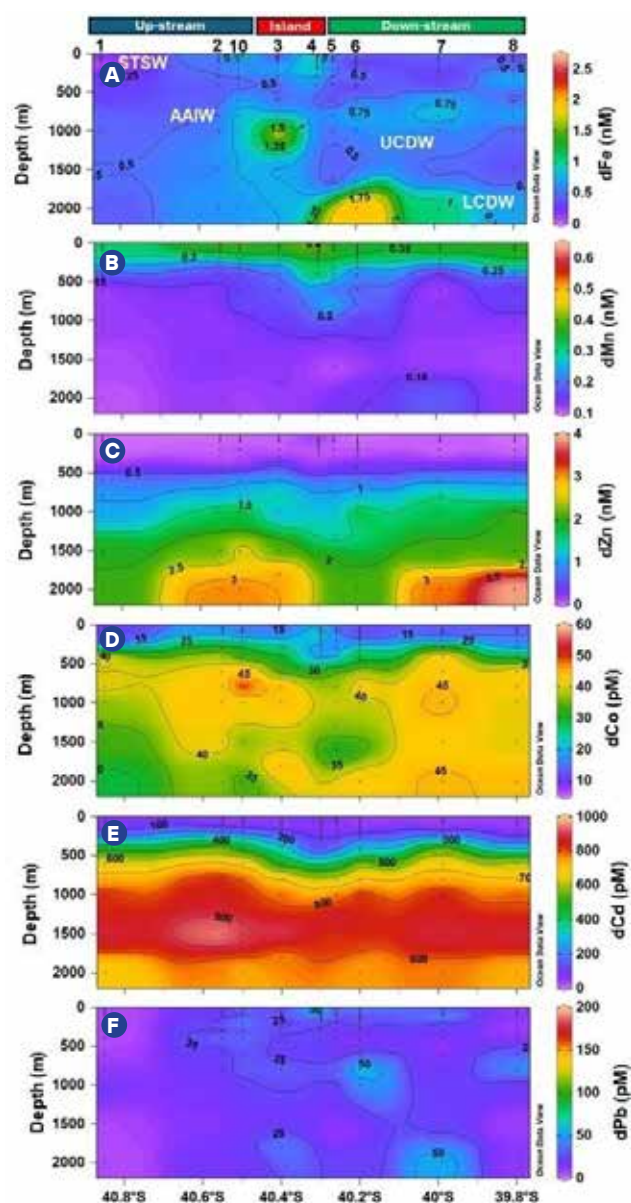


Figure 1. Water column distributions of dissolved metals Fe, Mn, Zn (A, B and C), Co, Cd and Pd (D, E, F; pM). Three sampling zones are indicated as Up-stream (blue block), near the Island (red block) and Down-stream (green block). Water masses identified include Subtropical Surface Water (STSW), Antarctic Intermediate Water (AAIW), Upper Circumpolar Deep Water (UCDW) and Lower Circumpolar Deep Water (LCDW).

Authors: Mtshali TN, Tsanwani M (OC Research)

Contributors: Valk A, Roychoudhury A (SU); Vena K, Kiviets G, Mdokwana B, Britz K (OC Research)

RESEARCH HIGHLIGHTS

18. CHLOROPHYLL A AND PHYTOPLANKTON ABUNDANCE ALONG THE SAMBA MONITORING LINE

Phytoplankton are responsible for more than 45% of global primary production and the sequestration of 5–10 Gt of carbon per year in the global ocean through the biological pump. Consequently, they play an important role in regulating the amount of atmospheric carbon dioxide. Chlorophyll *a* (chl *a*) distribution in seawater is considered a proxy for the biomass of phytoplankton because it is the primary photosynthetic pigment found within phytoplankton. The higher the chl *a* concentration in seawater (especially in the coastal and upwelling zones), the greater the quantity of phytoplankton present. Here, we report on the distribution of chl *a* and phytoplankton abundance at the surface and depth of maximum chl *a* along the South Atlantic Meridional Overturning Circulation Basin-wide Array (SAMBA) Monitoring Line (Fig. 1).

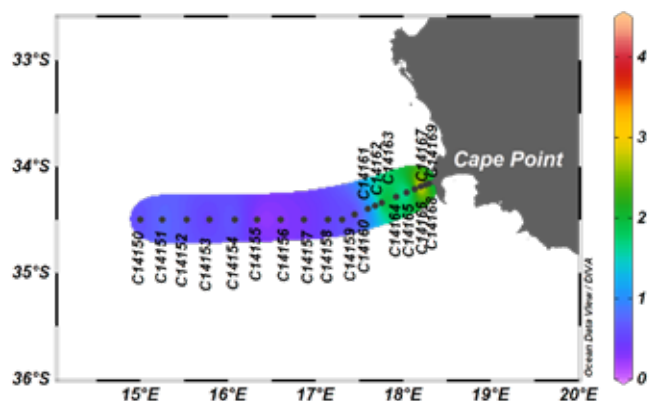


Figure 1. Map showing stations (black dots) sampled along the SAMBA monitoring line in September–October 2024. Colour shading indicates surface chlorophyll *a* concentrations ($\mu\text{g L}^{-1}$).

Seawater samples for chl *a* and phytoplankton analysis were collected along the SAMBA Monitoring Line in September to October 2024, on board the *RS Algoa*, using a CTD rosette. Seawater samples for chl *a* analysis were filtered through 25 mm diameter, 0.7 μm pore size filters, and the filter papers were stored frozen at -80°C . Chl *a* concentration was measured using a Turner Fluorometer, following extraction in 90% acetone. Seawater samples for phytoplankton analysis were collected in triplicate (2 mL per sample), preserved with 25% glutaraldehyde, and stored frozen at -80°C for analysis onshore. Phytoplankton abundance was assessed using the BD Symphony A1 flow cytometer, with subsets of cells selected based on pigment content and cell size, for populations of cells $<10 \mu\text{m}$. Phytoplankton species were characterised according to size as follows: *Prochlorococcus* (0.6 μm), *Synechococcus* (0.9 μm), picoeukaryotes ($<2.0 \mu\text{m}$), and nanoplankton (2–10 μm).

Chl *a* concentrations ranged from 0.15 to 4.05 $\mu\text{g L}^{-1}$ along the monitoring line. At the surface and at the depth of maximum chl *a*, values were higher ($>1.5 \mu\text{g L}^{-1}$) at inshore stations (C14161–C14169) than at open ocean stations (C14150–C14160) where values were $<1.0 \mu\text{g L}^{-1}$ (Fig. 1). This suggests higher nutrient supply from coastal sources (such as dust, river run-off or upwelling of nutrient-rich waters) compared to the open ocean. The smaller-sized *Prochlorococcus* and *Synechococcus* dominated the abundance, followed by picoeukaryotes and nanoplankton, with the latter absent at some stations (Fig. 2).

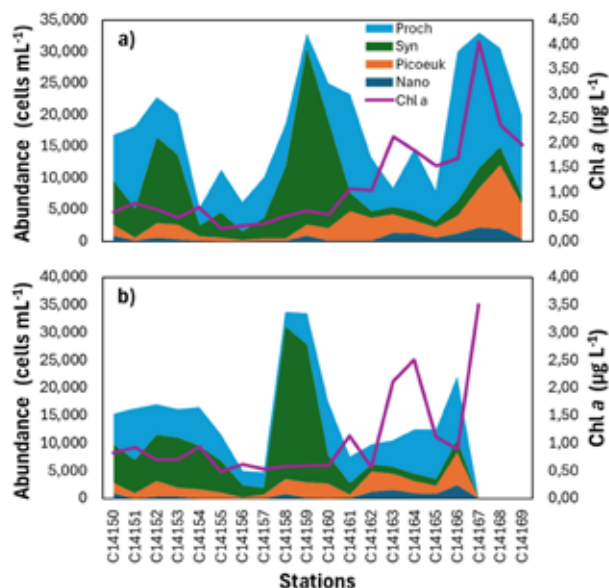


Figure 2. Phytoplankton abundance (cells mL^{-1}) and chlorophyll *a* concentrations ($\mu\text{g L}^{-1}$) along the SAMBA monitoring line from (a) the surface, and (b) the depth of maximum chl *a*. Proch = *Prochlorococcus*, Syn = *Synechococcus*, Picoeuk = Picoeukaryotes, and Nano = nanoplankton.

Abundance of *Prochlorococcus*, picoeukaryotes and nanoplankton was positively correlated with chl *a* at both the surface ($p < 0.001$ for all groups; with $R = 0.63$, $R = 0.73$, and $R = 0.84$, respectively) and at the depth of maximum chl *a* ($p < 0.001$ for all groups; with $R = 0.33$, $R = 0.81$, and $R = 0.88$, respectively). However, *Synechococcus* abundance was negatively correlated with chl *a* ($p < 0.001$ at both depths; with $R = -0.36$, $R = -0.36$, respectively) which could be an indication of the dominance of other accessory pigments within the *Synechococcus* group.

Mismatches between chl *a* and abundance of the smaller phytoplankton, such as at mid-transect stations C14158–C14161, may reflect their relatively low contribution to the total phytoplankton community biomass compared to larger phytoplankton cells ($>10 \mu\text{m}$), for which abundance was not measured. Additionally, size fractionation of chl *a* may provide a better match with the abundance patterns of the smaller phytoplankton species as measured by flow cytometry.

Authors: Vena K, Mtshali T, Gebe Z (OC Research)

Contributors: Ghu T, Hansraj Y, Maseti T, Mdazuka Y (OC Research)

RESEARCH HIGHLIGHTS

19. PARTICLE TRANSPORT ON THE AGULHAS BANK

Determining how water particles disperse and accumulate in the ocean is crucial for various applications, from understanding basic marine ecosystems to addressing pressing socio-environmental challenges. These include but are not limited to predicting pollution dispersal, search-and-rescue operations, fisheries management, improving climate models and coastal management.

The main objective of this study is to demonstrate how satellite-derived Lagrangian Coherent Structures (LCS) and particle density distributions from numerical simulations can be used, and how they compare in their effectiveness, for understanding dispersion and transport of materials in the ocean. LCS are invisible material lines that act as transport barriers and pathways, and which comprise of oceanographic features such as ocean vortices, fronts and filaments. Since particles cannot cross them, LCS determine the flow direction, affecting the dispersion and accumulation of materials.

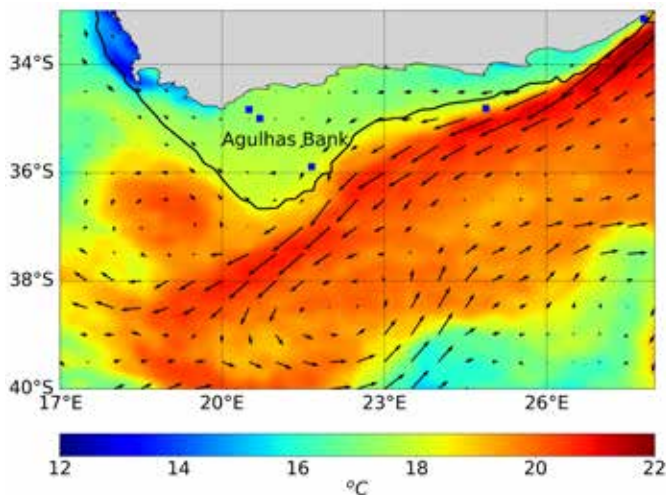


Figure 1. Locations of release sites (blue squares) on the Agulhas Bank. The black contour represents the 200 m isobath. Colour shading represents sea surface temperature and currents are indicated by the vectors (arrow shows direction and vector length indicates current speed).

We used a numerical simulation from the 3 km Coastal and Regional Ocean Community (CROCO) model to simulate the pathways of Cape anchovy and sardine larvae, and compared it to satellite-derived LCS. The aim was to understand how LCS may impact larval recruitment and migration in the spawning region of the Agulhas Bank, south of South Africa (Fig. 1).

Particles representing the fish larvae were randomly released inshore of the 200 m isobath, every first day of October (during the spawning season), at depths between 0 and 25 m, for the 2010–2014 period. They were advected using velocity fields from the CROCO model, and allowed to drift for 30 days. LCS were inferred from the backwards-in-time Finite-Size Lyapunov Exponents (FSLE). High values of FSLE indicate attracting LCS (particle accumulation), while low FSLE values indicate repelling LCS (particle dispersion).

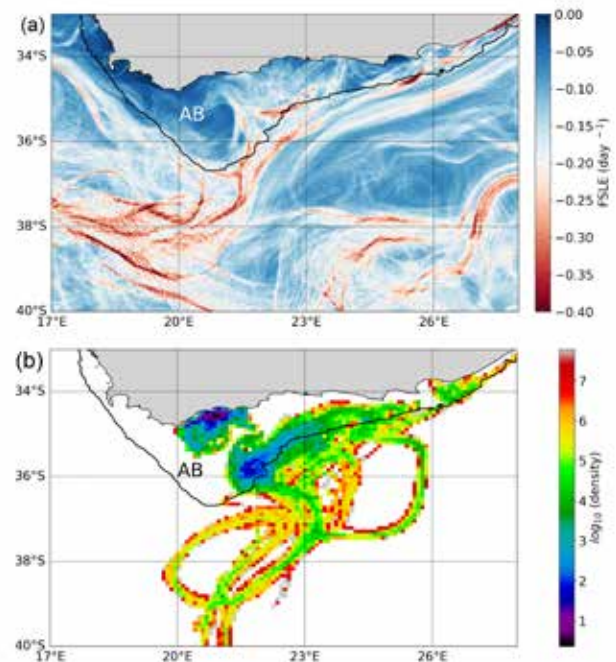


Figure 2. (a) Satellite-derived Finite-Size Lyapunov Exponents (FSLE; day⁻¹), where the red and blue shading represents attracting and repelling LCS, respectively, for 25 October 2014, and (b) Model-simulated particle density (particles km⁻²) shown in log scale for 25 October 2014. The black contour represents the 200 m isobath. AB = Agulhas Bank.

The results show that the LCS derived from satellite observations (Fig. 2a) compare well with the particle density distributions from numerical simulations (Fig. 2b) in terms of predicting material dispersion and accumulation on the Agulhas Bank. Shoreward material accumulation was observed in filament structures, indicated by attracting LCS (red shading in Fig. 2a). This corresponded with regions of high particle density observed inshore of the 200 m isobath (Fig. 2b). Offshore dispersion (blue shading in Fig. 2a) was observed in regions characterised by mesoscale features.

LCS allowed us to map the transport pathways of Cape anchovy and sardine larvae on the Agulhas Bank, identifying regions of larval accumulation, as well as areas where larval dispersal is more likely. This information is useful for identifying fishing grounds and managing stocks sustainably. The transport pathways identified from LCS can also be used for a wide range of additional applications from predicting pollution dispersal to saving lives at sea. Future research will focus on 3-dimensional flow and extended time series to derive interannual variability of particle dispersion.

Authors: Rasehlomi T, Krug M (OC Research)

RESEARCH HIGHLIGHTS

20. AGULHAS CURRENT MEANDERS REDISTRIBUTE INTERMEDIATE WATERS ALONG THE SOUTHEAST COAST OF SOUTH AFRICA

Along the east and southeast coasts of South Africa (Fig. 1), the Agulhas Current (AC) transports substantial amounts of water, heat and salt. It has considerable influence on the weather and climate of the adjacent continent and strongly impacts ecosystem dynamics and variability on the adjacent narrow shelf. The AC is typically located along the continental slope, but on occasion it is displaced offshore (Fig. 1). These offshore displacements, referred to as AC meanders, are comprised of cyclonic (clockwise-rotating) eddies that travel south along the inshore edge of the AC. The upwelling of deep, nutrient-rich waters by these eddies can stimulate substantial ecosystem responses across the shelf, including increased primary production and consequently elevated plankton biomass. We used available *in situ* observations and hydrodynamic model output to investigate the effects of AC meanders on the vertical structure of continental slope and shelf waters to improve our understanding of their impacts on ecosystem functioning.

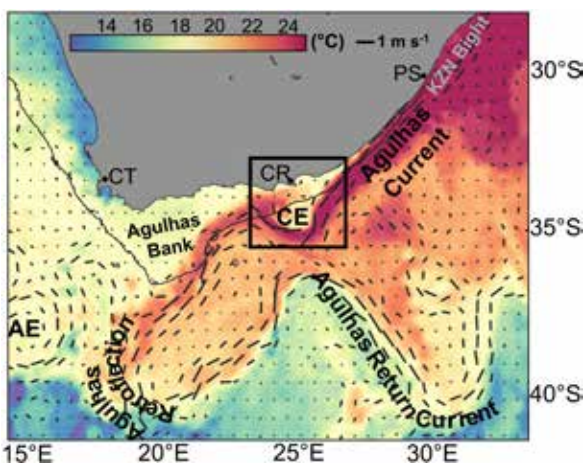


Figure 1. Sea surface temperature map overlaid with velocity vectors. Larger vectors indicate stronger currents. CE indicates a cyclonic eddy, while AE indicates an anticyclonic eddy. Cape Town (CT), Cape Recife (CR) and Port Shepstone (PS) are labelled. The black box indicates the focus region for our study and the black contour indicates the 1000 m isobath.

We focussed on intermediate waters, including Red Sea Water (RSW) and Antarctic Intermediate Water (AAIW), which typically occur at 500–1500 m depth. Although both are rich in nutrients, RSW is older than AAIW and contains less dissolved oxygen. When the AC is located against the continental slope, RSW occurs along the inshore edge of the AC, while AAIW occurs offshore of the AC (Fig. 2a). During these situations, cross-stream water exchange (from east to west of the AC, and vice versa) is restricted to depths well below 1500 m. However, during AC meanders, the cyclonic eddies enable cross-stream exchange of waters, resulting in the occurrence of AAIW inshore of the AC. When the eddy centres were located on the slope, larger proportions of intermediate waters were uplifted and advected onto the shelf (Fig. 2b). In contrast, when the eddy centres were further offshore, these waters were uplifted to shallower depths but were not advected onto the shelf (Fig. 2c).

Larger proportions of AAIW inshore of the AC during meanders are likely important for oxygenation of bottom waters and biological communities on the shelf. Importantly, our observations were restricted to a limited latitudinal area (Fig. 1), and thus further research is required to determine if similar impacts occur along the entire South African east coast.

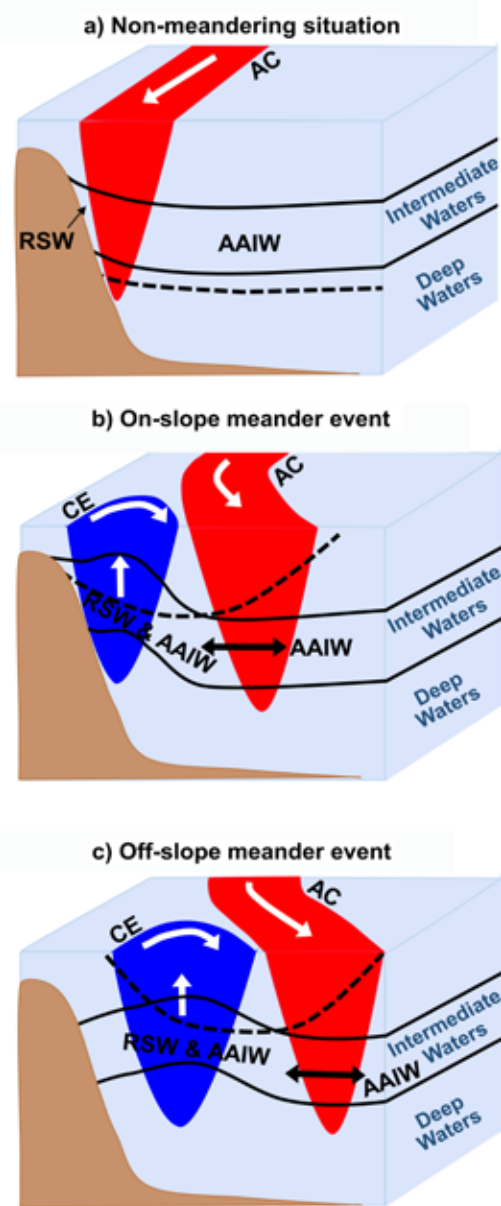


Figure 2. Schematic illustration of the influence of Agulhas Current meanders on the distribution of intermediate waters during (a) non-meandering situations, (b) an on-slope meander, and (c) an off-slope meander event. The dashed black line indicates the depth below which cross-stream mixing occurs.

Authors: Lamont T, Russo CS, Halo I (OC Research)

RESEARCH HIGHLIGHTS

21. A COMPLEMENTARY OPTICAL-MOLECULAR APPROACH TO EXPLORING ZOOPLANKTON COMMUNITIES

Cyclonic mesoscale eddies (ca. 10–100 km wide) can influence ocean productivity through upwelling in their cores, and by entraining and transporting biota. In June/July 2022, a cyclonic eddy was located between the continental shelf edge and the Agulhas Current (Fig. 1). A training cruise on the SA *Agulhas II* provided the opportunity to explore the composition of the zooplankton community within the eddy, using a combination of imaging and molecular analyses.

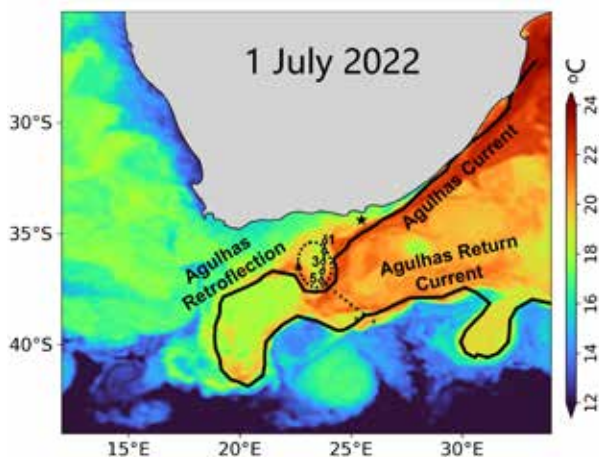


Figure 1. Sea surface temperature (°C) map showing stations across a cyclonic eddy (dashed circle) located along the inshore edge of the Agulhas Current, sampled from 30 June to 1 July 2022. The solid line indicates the core of the Agulhas Current, Agulhas Retroflection and Agulhas Return Current identified by the Location of the Agulhas Current's Core and Edges (LACCE) algorithm. The star marks the position of a reference shelf station.

Sampling was conducted at five stations across the eddy (Fig. 1). Duplicate meso- and macrozooplankton samples were collected in the upper 200 m, using 200 and 500 μm -mesh Bongo nets, respectively. One set of samples was imaged using a ZooScan (optical analysis), yielding abundance data at a coarse taxonomic level. Images were validated using EcoTaxa (<https://ecotaxa.obs-vlfr.fr/>), with assistance from expert taxonomists. The second set of samples was processed using DNA metabarcoding (bulk molecular analysis), yielding a detailed species list for most taxa.

Abundance data from imaging showed that both meso- and macrozooplankton communities were dominated

by copepods (Fig. 2), with greatest abundance near the eddy core. Mesozooplankton ($>200 \mu\text{m}$) were ca. 10 times more abundant than macrozooplankton ($>500 \mu\text{m}$). Euphausiids, chaetognaths and larger gelatinous zooplankton (GZ), such as cnidarians and thaliaceans, were relatively more abundant in the macrozooplankton community. In contrast, the meso-GZ were dominated by the smaller-sized appendicularians. Along with the larger thaliaceans, these filter-feeders are important contributors to carbon flux. GZ was also more abundant in the eddy compared to the shelf (Fig. 2a). In total, 300 zooplankton species were detected using DNA metabarcoding, after matching sequences with reference barcodes on online databases. The most species were recorded for Copepoda (89), followed by Teleostei (52), Cnidaria (31), Mollusca (31), Euphausiacea (25), Decapoda (24), Chaetognatha (13), Ostracoda (11) and Echinodermata (10). Most of the species detected by metabarcoding occur in the western and/or eastern Indian Ocean, suggesting southwestward dispersal from these regions and subsequent entrainment into the eddy. Entrainment of shelf water into the eddy was highlighted by the presence of *Calanus agulhensis*, a resident Agulhas Bank copepod, in all eddy samples.

Metabarcoding can detect fragile species that break apart in nets, and those with cryptic life history stages that are difficult to identify visually. Imaging provides quantitative data on abundance, size and developmental stage, but rarely to species level. Combining these techniques provides complementary information and new insights into community diversity and functioning.

Authors: Huggett JA (OC Research); Thibault D (Aix-Marseille Univ, France); Govender A, Groeneveld J (ORI)

Contributors: Maseti T, Russo CS (OC Research); Gibbons MJ (UWC); Isari M (IMR, Norway)

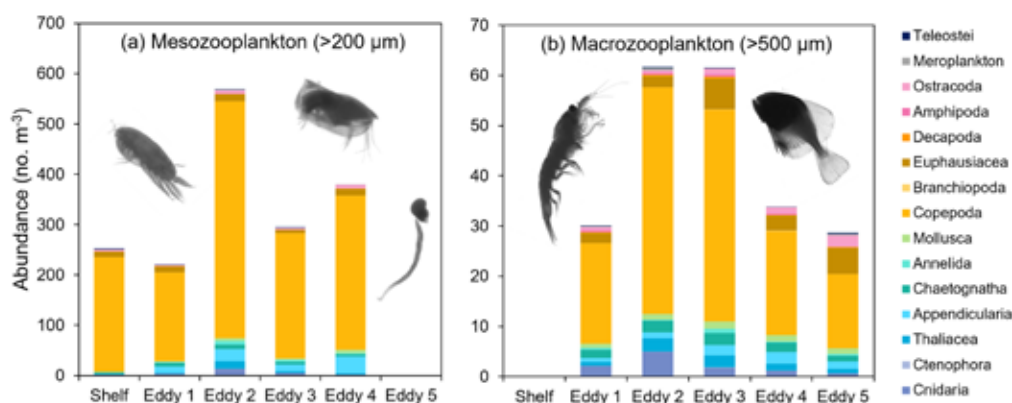


Figure 2. Abundance of (a) mesozooplankton and (b) the larger macrozooplankton taxa at each station during the study. Image insets from left to right: (a) calanoid copepod *Calanus agulhensis*, ostracod, appendicularian; (b) euphausiid *Euphausia* sp., juvenile scombrid (not to scale).

RESEARCH HIGHLIGHTS

22. MODELLING DISTRIBUTIONS AND DRIVERS OF SPONGE TAXA

Marine sponges (phylum Porifera) have been around for approximately 600 million years and are essential components of marine benthic ecosystems. They occupy a wide range of marine habitats, from shallow intertidal zones to deep-sea plains, and play an important role as ecosystem engineers. Sponge-dominated habitats are frequently classified as vulnerable marine ecosystems (VMEs), requiring protection from anthropogenic pressures such as fishing and deep-sea mining. Despite their ecological importance, sponge biodiversity and distribution are poorly studied, particularly in places affected by human activity. Effective conservation and management efforts are hampered by a lack of comprehensive biodiversity inventories, integrated databases, and realistic monitoring techniques for sponges and their environments.

We address some of these knowledge gaps by modelling the geographical distribution of sponge fauna caught as bycatch during routine research bottom trawl surveys off South Africa's west and south coasts. Surveys spanned areas with bottom depths between 20 and 500 m, with ca. 100 trawls conducted annually. Data from 2007–2009, 2011, 2012, 2016, 2019 and 2024 were used in the study. Sponge specimens were identified to species level using both morphological characteristics and genetic barcoding. Occurrence records were used to model the spatial distribution of species with at least five encounters, of which there were seven species in total (Fig. 1). Environmental data used in the model were obtained from Bio-ORACLE, a global environmental dataset. Parameters included mean bottom temperature, mean bottom salinity and mean and range of bottom current velocity.

Predicted distribution patterns varied, with some species showing a wider distribution extending from nearshore to the shelf edge, e.g. *Ectyonopsis pluridentata* and *Suberites dandelena*, and others having a narrower distribution, e.g. *Clathria (Thalysia) lissoclada* and *Acanthascus (Rhabdocalyptus) baculifer* (Fig. 1). Bottom temperature was the most important predictor of distribution for all species except *Ectyonopsis pluridentata*, for which bottom salinity was the most important environmental variable (Fig. 2).

By identifying highly suitable habitats, many overlapping with trawling grounds, this study highlights sponge habitats' vulnerability to bottom-contact fishing like trawling. Our findings can contribute to: (i) defining Key

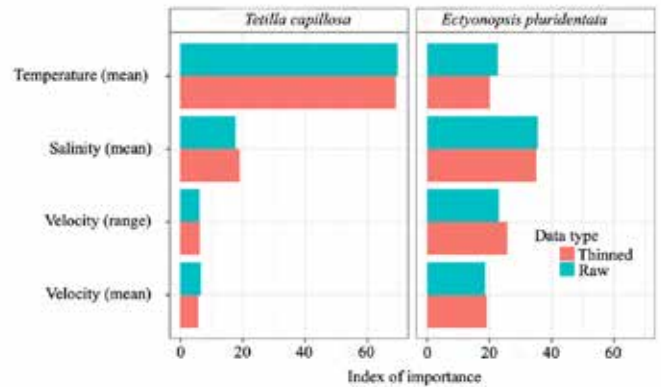


Figure 2. Index of relative importance of the four environmental variables that influence the distribution of sponge species for both the raw and “thinned” data comparison. To reduce spatial bias in species occurrence records, spatial thinning was applied (closely spaced occurrence records were removed) and the model was the thinned and raw data sets.

Biodiversity Areas for conservation and guiding trawl exclusion zones or bycatch mitigation, thereby reducing direct impacts on these vulnerable habitats; and (ii) supporting stronger VME protection under international agreements and integrating sponge habitats in area-based management in South Africa. Incorporating climate projections into habitat models will help anticipate sponge distribution shifts due to changing drivers like sea temperature, informing adaptive management for dynamic marine ecosystems.

Authors: Samaai T (OC Research); Yemane D (Fisheries R&D); Kirkman SP (OC Research)

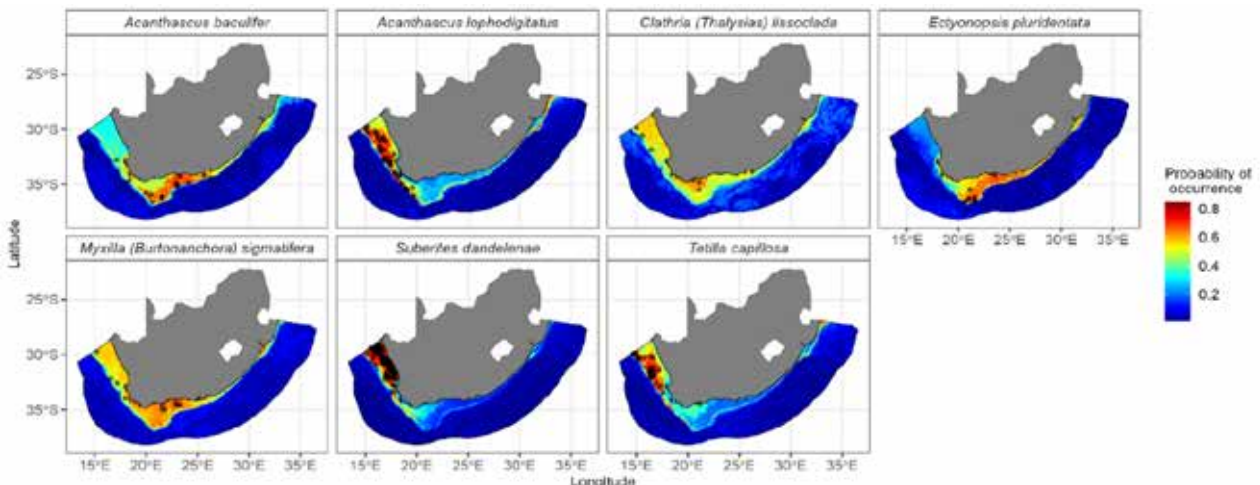


Figure 1. Predicted probability of occurrence (colour scale) for seven sponge species overlaid with observed occurrences (black dots).

RESEARCH HIGHLIGHTS

23. CROSS-SHELF EXCHANGES AROUND DIEPGAT SUBMARINE CANYON IN THE NORTHERN KWAZULU-NATAL

Submarine canyons that incise the edge of the continental shelf, known as shelf-break canyons, are prominent bathymetric features along the northeast coast of KwaZulu-Natal in South Africa (Fig. 1). Characterised by high biodiversity, these closely-spaced canyons are important sanctuaries within the iSimangaliso Marine Protected Area. The ecological integrity of these canyons depends on the oceanographic conditions driving the water circulation over the continental shelf, and the exchange of physical, chemical and biological material between the nearshore and the deep offshore oceanic environments.

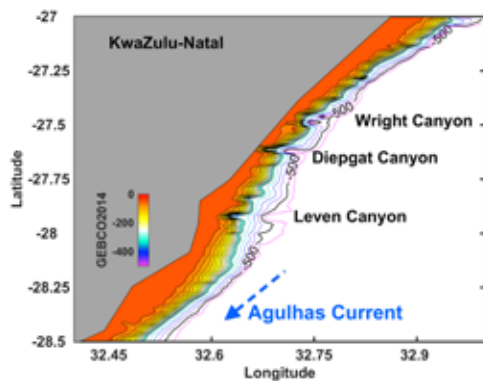


Figure 1. Nearshore bathymetry along the northern KwaZulu-Natal shelf showing several shelf-break submarine canyons. The black contour line indicates the 500 m isobath. The blue arrow indicates the general direction of flow for the Agulhas Current.

Using output from the Coastal Regional Ocean Community model simulation with a 1 km resolution (Fig. 2), we assessed the oceanic forces driving the water circulation to determine how they could impact water property exchanges between the offshore and nearshore environments in the Diepgat Canyon area. The pressure gradient force (Fig. 2a) is positive, indicating that this force is expected to move water parcels from areas of higher pressure (typically deeper water columns, i.e. offshore) to areas of lower pressure (typically shallower water columns, i.e. nearshore). This force is weakest inshore of the 50 m isobath in the northwest (Fig. 2a). The Coriolis force (Fig. 2b) is negative in the Southern Hemisphere, indicating that water parcels are deflected to the left of their direction of movement. The strongest Coriolis force, illustrating the strongest leftward deflection of water parcels, occurs along the continental slope between the 50 and 450 m isobaths, upstream and downstream of the Canyon. There is a notable decrease in this leftward deflection where the Canyon incises the slope (Fig. 2b), showing clearly that the Canyon influences shelf circulation. Figure 2c shows that ageostrophic forcing (computed as the sum of the pressure gradient (Fig. 2a) and Coriolis (Fig. 2b) forces) is mainly negative, which means that the resulting water movement is southwestward across most of the region. The small area of positive ageostrophic forcing values in the northwest indicates northeastward movement of water inshore of the 50 m isobath (Fig. 2c). This suggests that colder, nutrient-rich waters are likely to be upwelled at this location and then transported southwestward along the 50 m isobath, with accelerated southwestward flow clearly visible at the Canyon head (Fig. 2c).

Horizontal advective forcing (Fig. 2d) illustrates the transport of properties by the motion of the water, while

surface and bottom frictional forces (Fig. 2e) usually act to decelerate water movement. In the Diepgat Canyon area, horizontal advective forces (Fig. 2d) and surface and bottom frictional forces (Fig. 2e) are close to zero, showing little influence on water movement. This means that the overall acceleration of water (Fig. 2f) is sustained by ageostrophic forcing (Fig. 2c), indicating that high-frequency variations control the circulation and cross-shelf exchanges. Thus, monitoring of oceanographic parameters must be done at high spatial (<1 km) and temporal (at least daily) resolution to be able to capture these variations. This analysis enabled spatial mapping that pinpointed precise locations of upwelling and enhanced shoreward water movement, improving our ability to locate and monitor changes in these processes in response to climate variability.

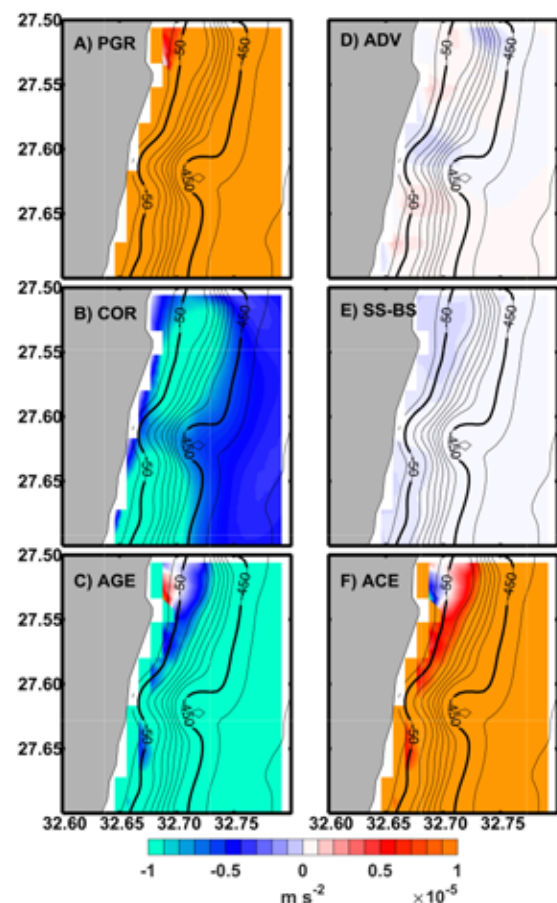


Figure 2. Oceanic forces around the Diepgat Canyon, (A) pressure gradient (PGR), (B) Coriolis (COR), (C) Ageostrophic (AGE), (D) Advection (ADV), (E) Surface and bottom friction (SS-BS), (F) Acceleration (ACE). The contours are isobaths.

Authors: Halo I, Lamont T (OC Research); Rautenbach G (SAEON/NMU)

RESEARCH HIGHLIGHTS

24. UNEXPECTED PATTERNS IN DENSITIES OF LIMPETS AND OYSTERS BETWEEN NO-TAKE AND HARVESTED SITES AT DWESA-CWEBE MPA

Intertidal rocky shores in South Africa are faced with high harvesting pressure due to the increasing human population. Limpets, mussels and oysters are harvested as food by subsistence harvesters and as bait by fishermen, with mussels dominating the catch. Stocks of these organisms were reported to be overexploited in the 1990s, with some stocks reported as depleted. Growing concern about the impacts of harvesting led to the establishment of the Dwesa-Cwebe Marine Reserve in the Eastern Cape, which was re-proclaimed as a Marine Protected Area (MPA) in 2000. The MPA was originally no-take but was rezoned in 2015 to allow for fishing/harvesting in certain controlled zones.

To assess the impacts of harvesting on the populations of goat's eye limpet *Cymbula oculus* and Natal rock oyster *Saccostrea cucullata*, both no-take and harvested areas of the MPA were sampled. Three transect lines were set up from the top shore to the low shore inside the no-take area, and similarly, three in each of the harvested areas of the MPA. Two additional harvested sites outside the MPA were also set up for monitoring, namely at Nqabarha and Nkanya. During surveys, 50 x 50 cm quadrats were surveyed along each transect line to determine the density of each species. Thirty individuals (if available) were measured for size along the transect lines in each area.

Limpets were absent along transect lines in the no-take area of the MPA and also at one of the harvested areas outside of the MPA (Nkanya), but were present in both harvested areas inside the MPA and the remaining harvested area outside of the MPA. The greatest density of limpets was found at one of the harvested areas inside of the MPA (MPA harvested 2) (Fig. 1).

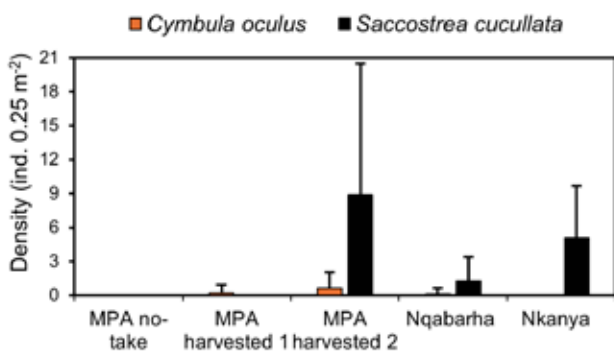


Figure 1. Density of *Cymbula oculus* and *Saccostrea cucullata* in one no-take area and two harvested areas within Dwesa-Cwebe MPA, and at two sites that fall outside of the MPA (Nkanya and Nqabarha).

On average, individuals of *C. oculus* were largest in one of the harvested areas inside the MPA (MPA harvested 2; Fig. 2) and in one of the areas outside of the MPA (Nqabarha). For *S. cucullata*, individuals in the harvested areas inside the MPA were larger on average than those in areas outside of the MPA.

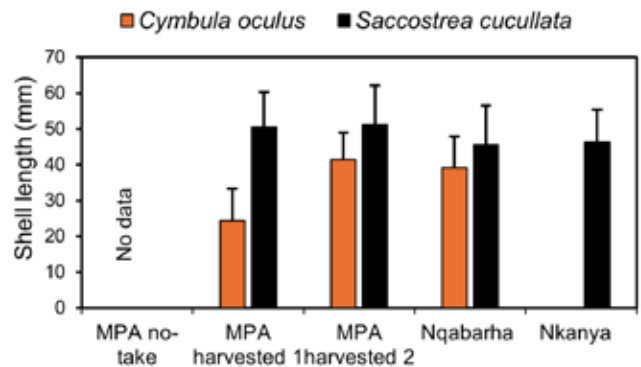


Figure 2. Shell length of *Cymbula oculus* and *Saccostrea cucullata* in one no-take area and two harvested areas within Dwesa-Cwebe MPA, and at two sites that fall outside of the MPA (Nkanya and Nqabarha).

Past comparisons of limpets inside versus outside the MPA (which was then entirely no-take) demonstrated significantly greater density and size of individuals inside of the MPA, compared with the harvested areas outside. The absence of limpets in the no-take area of the MPA in this study was therefore unexpected. Oysters were also absent.

No-take areas are intended to reduce harvesting pressure, promote stock recovery, and maintain healthy adult populations that can supply larvae to nearby harvested areas. A possible explanation for the lack of limpets in the no-take areas is that illegal harvesters were attracted to the high density and large size of limpets in the no-take area and stripped the area of these organisms.

Illegal harvesting is a significant factor in population declines of marine living resources and compromises the effectiveness of MPA no-take areas. The findings of this study point to the need for enhanced enforcement of the Dwesa-Cwebe no-take area (e.g. more frequent patrols) and raising awareness in the local community regarding the potential long-term benefits of respecting the no-take area.

Authors: Baliwe N, Mushanganyisi K (OC Research)

RESEARCH HIGHLIGHTS

25. POPULATION REDISTRIBUTION AND LONGEVITY OF CAPE GANNETS IN THE BENGUELA ECOSYSTEM

Cape gannets *Morus capensis* are endemic to the Benguela Upwelling Ecosystem of southern Africa, where they breed at six localities—three in Namibia (Mercury Island, Ichaboe Island and Possession Island) and three in South Africa (Lambert’s Bay, Malgas Island and Bird Island in Algoa Bay). Since 1956/57, the total population has declined from ca. 254,000 pairs to ca. 145,000 pairs in 2023/24. The species is listed by the International Union for Conservation of Nature (IUCN) as Endangered due to the declining population size.

Concurrently with the population decline, there has been a shift in distribution of the population, anticlockwise around the southern African coast: whereas most Cape gannets bred in Namibia in 1956/57, by 1978/79 numbers in Namibia and South Africa were approximately equivalent and thereafter, most birds nested in South Africa (Fig. 1). Currently, ca. 70% of the population occurs at Bird Island in Algoa Bay off the southeast coast of South Africa

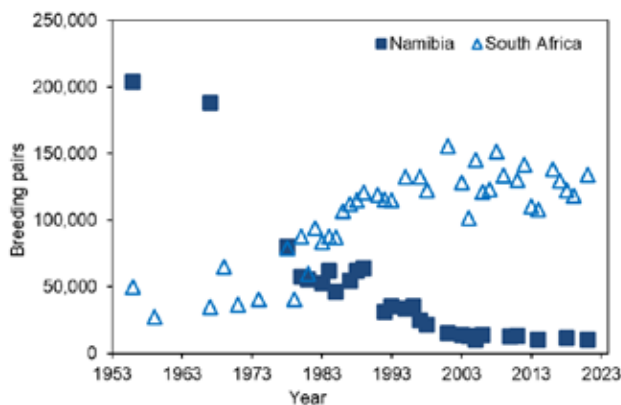


Figure 1. Numbers of Cape gannet breeding pairs in Namibia and South Africa between 1956–2024.

While numbers have continued to decline in Namibia, there has been some stabilisation of numbers in South Africa’s colonies. Apart from Bird Island in Algoa Bay, which is the largest Cape gannet colony, there has been an increase of the Malgas Island colony (situated at the northern entrance to Saldanha Bay), from ca. 20,000 pairs in 2018 to ca. 30,000 pairs in 2024. In the mid-1990s, there were 50,000 pairs at this colony. The breeding colony at Lambert’s Bay was stable for decades, but has increased from 8,000 in 2018 to 12,000 in 2024—this is the highest number of breeding pairs yet recorded for this colony.

Since the inception of DFFE’s Cape gannet monitoring programme in 1978, there has been a mark-recapture effort (using uniquely numbered rings) to determine the longevity and migratory movement patterns of Cape gannets between breeding colonies, amongst other objectives. A Cape gannet that was ringed as a chick in February 1983 was recaptured on Malgas Island in October 2020 (Fig. 2). This individual was resighted on only one other occasion, on 10 March 1992. The length of time between ringing and the 2020 recapture was 37 years, 8 months and 4 days, several years longer than the previous greatest longevity recorded for Cape gannets, which was 30 years and 7 months. It is also the greatest longevity recorded for any of the three gannet species, globally.



Figure 2. A Cape gannet that was recaptured at Malgas Island with one of the oldest bands on record.

The longevity of gannets relates to their high adult annual survival rate, which is estimated at ca. 0.94 and ca. 0.95 for northern and Australasian gannets, respectively, and 0.83–0.90 for Cape gannets, as determined during a period of gradually decreasing populations at three breeding colonies. Gannets show high fidelity to their breeding colonies, but as highly mobile predators they may abandon their colony to avoid detrimental conditions that can cause mortality, such as disturbance or predation. This is illustrated in the mass abandonment (ca. 5,000 breeding pairs) of the colony at Lambert’s Bay during the 2005/06 breeding season, after disturbance of the colony and predation of adults by Cape fur seals *Arctocephalus pusillus pusillus*. Similarly, ca. 10% of the breeding pairs at Malgas Is. abandoned the colony after seal attacks in 2017/18. In both cases, birds returned to colonies over the next few years, following the removal of damage-inflicting seal individuals.

In periods of scarcity of preferred prey, Cape gannets are able to buffer against reduced adult survival by feeding on poor-quality prey such as offal discarded by demersal trawlers, but this is at the cost of lower reproductive success. Hence recruitment, rather than adult survival, seems to be the most important limiting factor for the population.

Author: Makhado AB (OC Research)

Contributors: Visagie L, Masotla MM, Cebekhulu T, Dyer B (OC Research)

RESEARCH HIGHLIGHTS

26. UNUSUAL PREDATORY BEHAVIOUR BY MOLE SNAKES ON AFRICAN PENGUINS AT ROBBEN ISLAND

Robben Island (33.81°S, 18.37°E) is home to some of South Africa's most important seabird populations, including large breeding colonies of African penguins *Spheniscus demersus* and Bank cormorants *Phalacrocorax neglectus*. Significant populations of Cape cormorants *P. capensis*, crowned cormorants *P. coronatus*, African black oystercatchers *Haematopus moquini*, Hartlaub's gulls *Chroicocephalus hartlaubii* and greater-crested terns *Sterna bergii* also inhabit the island. African penguins are listed as Critically Endangered (CE) on the IUCN Red List of Threatened species, and both bank and Cape cormorants are listed as Endangered. Also inhabiting the island are snake populations including mole snakes *Pseudaspis cana* (Fig. 1), which are native to the island, and introduced olive house snakes *Lamprophis inornatus*.

Adult mole snakes grow to a maximum length of over 2 m and a girth of about 158 mm. On the South African mainland, their diet consists mostly of rodents (mice, rats and moles) and small amphibians or reptiles. At Robben Island, mole snakes have frequently been observed to prey on eggs within colonies of smaller seabirds such as greater-crested terns and Hartlaub's gulls. During the 2024 breeding season ca. 6,600 and over 1,100 pairs of these two species bred at Robben Island, respectively. Recently, mole snakes have been observed to target the



Figure 1. A mole snake with its belly bulging after swallowing an African penguin egg on Robben Island, June 2024.

larger eggs of African penguins at Robben Island (Fig. 1), as well as their chicks. One individual was observed to attack and kill two chicks after which it attempted to swallow them but failed on account of their large size. The same individual was later observed strangling and then attempting to swallow an adult African penguin (Fig. 2). These incidents occurred approximately two months after the breeding peak of the terns and gulls. The observed shift in diet from tern and gull eggs to African penguin eggs and chicks therefore reflects the seasonal shift in the relative availability of these prey species. Robben Island is the only island where mole snakes and African penguins are known to co-exist. However, attempts by mole snakes to prey on adult penguins have not been documented



Figure 2. A mole snake in the act of preying on an adult African penguin at its nest on Robben Island, June 2024.

before. It is possible that this atypical behaviour may have been influenced by warm spells (e.g. 27°C) experienced during the winter months of 2024. That is, unusually warmer days at the onset of winter may have allowed for a longer hunting window at a time when mole snakes are usually inactive. Their inactivity at this time of the year in typical years may explain why such predatory activities between mole snakes and breeding African penguins have not been observed before. Interactions between the two species may therefore be expected to increase with warming and anomalous temperature fluctuations due to climate change.

Mole snakes preying on African penguins, including adults, is a newly detected phenomenon and the latest addition to the myriad of threats faced by this CE species. This discovery highlights the importance of active monitoring and the need for management interventions to mitigate this new threat to the population.

Authors: Masotla MJ, Cebekhulu T, Upfold L, Makhado AB (OC Research)
Contributors: Dyer BM, Bawuli A (ex-OC Research)

RESEARCH HIGHLIGHTS

27. OVERLAP IN FEEDING AREAS OF CAPE FUR SEALS AND AFRICAN PENGUINS

Understanding competition between Cape fur seals (seals) *Arctocephalus pusillus pusillus* and African penguins *Spheniscus demersus* (penguins) for breeding habitat and forage resources is critical for conservation management. The two species are sympatric breeders at Vondeling Island and two other localities in South Africa (Fig. 1). They also target similar prey: anchovy *Engraulis encrasicolus* and sardine *Sardinops sagax*. To date, this is the first study to demonstrate the degree of overlap in their core feeding areas.



Figure 1. Distribution of African penguin colonies in South Africa. Red dots indicate colonies where both penguins and seals breed, and blue dots indicate penguin-only colonies.

To address this, we analysed satellite telemetry data from seven lactating female seals and five breeding (on eggs or with chicks) penguins tagged at Vondeling Island in September 2017 (Fig. 2). The objective was to calculate the horizontal movement overlaps of their home ranges and core feeding areas. Seals and penguins completed 32 and 38 return trips with a median distance from the colony of 86.9 and 41.9 km respectively. Seals had a larger home range (158,486 km² vs 40,495 km² for penguins) and core foraging area (25,682 km² vs 7,865 km² for penguins). Home ranges and core foraging areas overlapped by 78% and 86% between the two species, respectively. Although core foraging areas overlapped in the vicinity of Vondeling Island, the penguins' core foraging area extended southward (Fig. 3a) along the 16 Mile Beach Marine Protected Area towards Yzerfontein. The seals' core foraging area extended northward (Fig. 3b) to coincide with the waters of the Cape Columbine upwelling cell.

Core foraging areas identified for Vondeling Island's penguins also overlapped with those of their conspecifics breeding at other localities such as Dassen Island and Robben Island. This was the first phase in investigating interactions between the two species at Vondeling Island. More work is underway to investigate other aspects of their interactions, including how they mitigate competition.



Figure 2. African penguin (top left) and a Cape fur seal (bottom) on Vondeling Island, showing deployed satellite tags.

In summary, seals had a larger home range and core foraging area than penguins. Seals are able to travel further from their breeding colonies than penguins are able to, due to differences in morphology and reproductive physiology between the two taxa. This bestows seals with a competitive advantage over penguins during the breeding season when both adopt a central place foraging strategy.

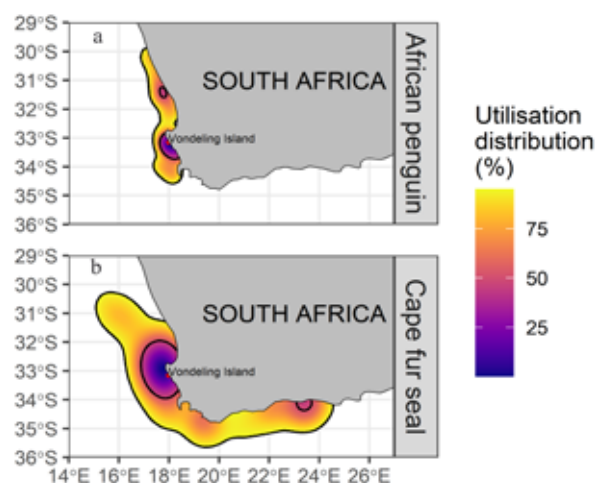


Figure 3. Overall utilization distributions (0-95%) of (a) African penguins, and (b) Cape fur seals. Outer black contours represent 95% (home ranges) and inner black contours indicate 50% (core areas).

Authors: Seakamela SM, Kotze D, McCue SA, Makhado AB (OC Research); Dyer B (ex-OC Research); Carpenter-Kling T (NMU); Dakwa F, Underhill L (UCT)
Contributors: Du Plessis G (Steenberg Vets); Coetzee T (SMS); Kirkman SP, Lentswana S, Ngwenze Z, (OC Research)

SCIENCE TO POLICY

28. EVALUATING THE ENHANCED BATHTUB MODEL FOR COASTAL FLOOD RISK ASSESSMENT IN TABLE BAY, SOUTH AFRICA

The Geographic Information Systems (GIS) based enhanced BathTub Model (eBTM) enables the identification of flood risk areas by producing coastal inundation extents that are hydrologically connected to the coast. It also presents water pathways as a baseline for coastal flood mitigation and/or adaptation strategies. This study aimed to establish the methodological robustness of the eBTM, by analysing flooding at eight sites (Fig. 1) during a storm event in Table Bay, Cape Town.



Figure 1. Study site locations and the respective maximum wave run-up heights recorded during the storm event on 16 September 2023.



Figure 2. Inundation in Bloubergstrand during the storm event that occurred on 16 September 2023. Photograph credit: FJ van Coller.

The eBTM data inputs require wave run-up heights, a high-resolution Digital Surface Model (DSM), and a water source to produce inundation extents. As such, a 1 m resolution DSM, and a 0 m contour line representing the water source, was produced using the first return points of a light detection and ranging (LiDAR) dataset provided by the City of Cape Town. Wave run-up heights per site were represented by a randomised point selection using the ground-validated flooded areas and the vertical elevation of the DSM (Fig. 1).

The ground validation component relied on data collected after the storm event that occurred on 16 September 2023, where the compounded effects of strong winds, high rainfall, storm surge and the equinox spring tide resulted in substantial flooding. Across the eight study sites, a total of 332 coordinates were recorded, using a GPS, with accompanying photographic validation of the inland flood extents (Fig. 2). These coordinates were loaded into the ArcGIS Pro software for comparison with the eBTM modelled flood extents. Results showed that 74% of the validation points achieved a horizontal spatial modelling error less than 6 m, while 56% of the validation points had

an error less than 3 m. The root mean square error (RMSE) for all sites was less than 10 m (horizontal distance), with an average of 4.88 m.

In order to examine the eBTM's applicability to different coastal morphologies, these results were further assessed by classifying the sites into morphology classes and evaluating these classes against the RMSE (Table 1). Results showed that sites with intertidal or subtidal reefs produced above average RMSE values, indicating that these reefs may have a dampening effect on the flooding, which the eBTM cannot account for. Therefore, the eBTM may be more applicable to coasts where wave propagation is uninterrupted. Since a horizontal error of less than 10 m was achieved at all sites, the eBTM is considered relevant for use within the context of coastal risk assessments, particularly where more sophisticated models are unavailable.

Authors: Williams LL (OC Research); Lück-Vogel M (CSIR); van Coller FJ (SU)

Table 1. Study site morphologies and site-specific Root Mean Square Errors (RMSE).

Study sites	Classification	Local RSME
a Melkbosstrand North	Shallow wide sandy shore + reef	6.52
b Melkbosstrand South	Shallow narrow sandy shore	4.54
c Bloubergstrand	Shallow narrow sandy shore + reef	7.61
d Lagoon Beach	Shallow narrow sandy shore with estuary mouth	1.04
e Muelle Point	Highly modified shore + reef	8.68
f Sea Point	Highly modified shore + reef	6.07
g Camps Bay	Shallow wide sandy shore	3.0
h Bakoven Beach	Steep rocky shore	1.61

SCIENCE TO POLICY

29. SOUTH AFRICAN (MACRO-, MESO-, MICRO-) PLASTICS PROGRAMME (SAMP)

One of the targets of the Sustainable Development Goals, SDG 14, "Life below water", is to prevent and significantly reduce marine pollution of all kinds, particularly that produced by activities carried out on land, including plastic debris. To achieve this objective, indicator 14.1.1.b "Density of Plastic Waste" was established. This indicator includes several parameters that are to be monitored and reported, including measures of plastic debris in beach sand and floating on the sea surface. It is important for policy making and implementation that these parameters are based on actual data. Of concern is that several techniques that are not comparable are being used to estimate these parameters. The South African (Macro-, Meso-, Micro-) Plastic (SAMP) programme aims to standardise the collection, analysis and data reporting of plastic pollution. Established by Ocean Research, DFFE, SAMP is a monitoring programme consisting of a network of voluntary researchers from eight provinces in South Africa (Fig. 1).

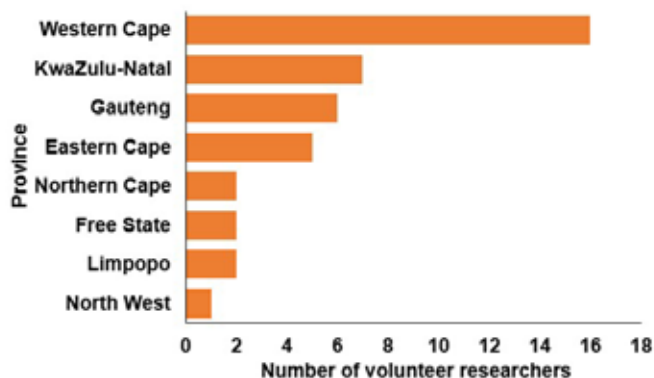


Figure 1. Number of SAMP members across eight provinces in South Africa.

People interested in participating in the programme were asked to complete an online form. The 44 responses received were used to gather baseline information on macro-, meso- and micro-plastic research in South Africa. More effort is needed to find volunteers in some provinces, particularly Mpumalanga, from which there are currently no representatives. Nevertheless, current volunteer scientists are established and already conducting plastics research in different environments (Fig. 2), thus incorporating a range of expertise into the SAMP network.

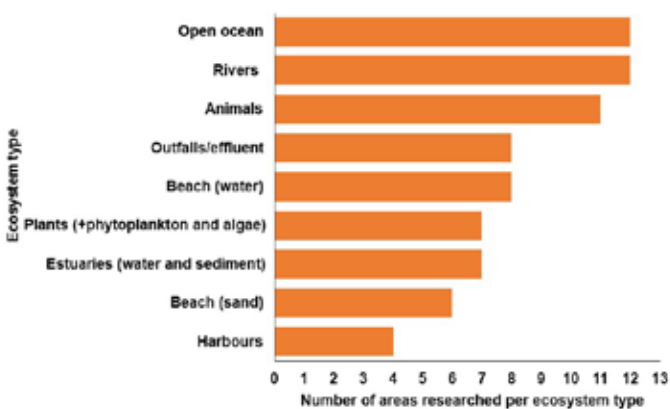


Figure 2. Number of areas per ecosystem type in which SAMP volunteer researchers have conducted plastic pollution monitoring.

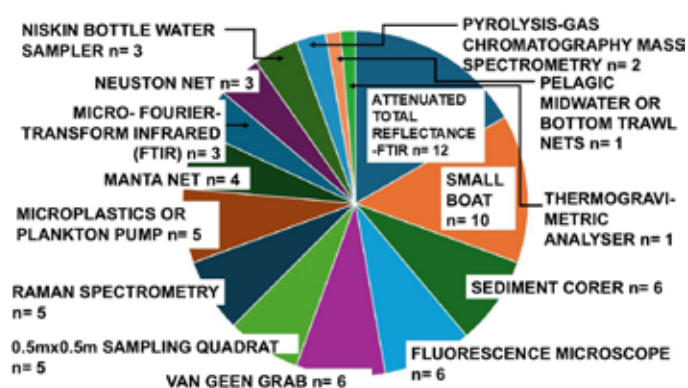


Figure 3. Instrumentation and tools, including number (n) available to conduct plastic pollution monitoring under SAMP.

The baseline information gathered shows that South Africa is not lacking in infrastructure for monitoring plastic pollution, with a multitude of tools and technologies being employed (Fig. 3). The online survey also indicated that 92% of researchers are willing to use a standardised methodology to generate information for All SAMP data will be housed in the South African Marine Information Management System (MIMS) which is an open data repository that archives and publishes datasets (<https://data.ocean.gov.za/>). MIMS is directly linked to SDG reporting and all but one of the researchers responded positively to housing their data in MIMS.

The first SAMP meeting was held online in December 2024 outlining the national need for comparable data for SDG 14 reporting in South Africa. The meeting recording remains available to all new members.



Author: Pillay K (OC Research)

SCIENCE TO POLICY

30. INITIATING A GLOBAL MICROPLASTICS DATABASE

Plastic pollution is a widespread issue impacting marine, freshwater, and terrestrial ecosystems worldwide, posing a significant threat to environmental sustainability, biodiversity, and human well-being. Once plastics enter the environment, they break down into smaller particles known as microplastics (MPs)—an emerging type of persistent contaminant that is of global concern due to the widespread distribution of MPs throughout the world’s oceans. The NUTEC Plastics initiative (NUclear TEChnology for Controlling Plastic Pollution) was launched by the United Nations International Atomic Energy Agency (IAEA) in 2021, with the overall objective of assisting the IAEA Member States in their effort to address the challenges of plastic pollution.

The NUTEC Plastics initiative aims to establish the Global NUTEC Plastics Monitoring Network by 2026, comprising specialised laboratories located in the Member States. By standardising and enhancing their capabilities, instrumentation, and expertise in characterising and quantifying marine MPs, these laboratories should have the capacity to assess risks posed by marine MPs to ecosystems and livelihoods. It is anticipated that this will aid the development of global policies and actions for sustainability of seas and oceans around the world. Currently, 99 Member States have agreed to use a standard approach and generate comparable data. To date, OC Research has participated in several international meetings aimed at standardising these approaches.

Following the first co-ordination meeting of adhering Member States, held at the IAEA Headquarters in Vienna, Austria during July 2024 (Fig. 1), two additional meetings were held there during October 2024 (Fig. 2). These focused on standardisation of data collection, and on tailoring database infrastructure to meet the data requirements, respectively. The expected outcomes of these meetings were to:

- Determine the content, architecture, and extent of the database;
- Shape decisions on data management policies, user rights, and responsibilities;
- Ensure the interconnectivity of the database with other existing platforms from NUTEC partners;
- Promote international collaboration and knowledge sharing;
- Support the reporting of SDG 14 (Life Below Water) by providing a hub for collected data;
- Incorporate insights from other database experiences;
- Prevent duplication of efforts.

The main agreements from the three meetings were:

- Development of harmonised sampling protocols and analytical procedures in laboratories as well as a set of relevant vocabulary for researchers, laboratories and any data collection initiatives;
- Data centre development with the data ingestion system that captures all available information, including data made available from the other databases.
- To establish a systematic tool for Quality Assurance and Quality Control for the reported data.
- Creation of global datasets on the specific indicators (e.g. MPs in surface water, beach sand, and sediments)

that are ready to be visualised under the Global Partnership on Plastic Pollution and Marine Litter (GPML) Digital Platform, and that can inspire policy actions.



Figure 1. First co-ordination meeting of adhering member states. To help guide discussions, South Africa (Keshnee Pillay) was requested to make presentations on our ongoing microplastic monitoring and on the Marine Information Management Systems (MIMS database) and National Oceans and Coastal Information Management System (OCIMS).

The agreements will inform the curation of ocean plastic data on the Department’s Marine Information Management System (MIMS). These meetings also emphasised the need for funding to sustain monitoring activities that will ensure continuity of data collection and analysis, particularly in low to middle income countries.



Figure 2. Second (scientific development) and third (NUTEC database development) meetings. South Africa was represented in meetings on science (Keshnee Pillay, DFFE) and data systems architecture (Mark Jacobson, SAEON).

Author: Pillay K (OC Research)

SCIENCE TO POLICY

31. A BIODIVERSITY SECTOR PLAN FOR MARINE SPATIAL PLANNING

Target 1 of the Convention on Biological Diversity’s Kunming–Montreal Global Biodiversity Framework (GBF) is for all land and sea areas to be under biodiversity-inclusive spatial planning. The term “biodiversity-inclusive” emphasises the need for policies, plans and projects to do more than simply acknowledge biodiversity considerations, by taking a proactive stance and embedding them at the core of decision-making processes and practices. The basis for this is that healthy biodiversity is crucial for long-term environmental and societal resilience and prosperity.

This rationale underlies objectives for the future development of South Africa’s (SA’s) marine biodiversity sector through Marine Spatial Planning (MSP). These objectives are presented in the Marine Biodiversity Sector Plan, produced in 2024. The Sector Plan advances the need for adequate management of biodiversity priority areas through MSP, thus aiming to ensure biodiversity-inclusiveness of MSP in line with GBF Target 1. Provision for this is also made in the MSP Act (Act 16, 2018), with a primary objective of conserving the ocean for current and future generations, by allocating areas where biodiversity management is prioritised.

The tool presented by the Sector Plan to achieve its development objectives is zoning with spatial regulations, as prescribed in the National Framework for MSP. Thus, the Sector Plan defines an integrated set of priority spatial biodiversity areas along with required management specifications for them. This approach was influenced by a priority action for improving the state of marine biodiversity in the most recent (2018) National Biodiversity Assessment (NBA). This called for the coastal and marine Critical Biodiversity Areas (CBA) Map for SA (Fig. 1) to be applied in MSP to mitigate pressures in priority areas. This map, a product of the National Coastal and Marine Spatial Biodiversity Plan produced by NMU, SANBI and DFFE, delineates areas identified as critical to ensure the future persistence of biodiversity. It includes areas of known importance for biodiversity and ecosystem services, such as Ecologically or Biologically Significant Marine Areas. Outside of existing Marine Protected Areas (which have their own regulations), it describes two categories of CBAs (natural/near-natural, or in a modified state) and Ecological Support Areas (ESAs; other areas of importance for ecological processes and ecosystem services). Guidelines were developed for each category indicating the types of sea uses that should or should not be allowed (or allowed only under specific conditions) for sites to maintain their state.

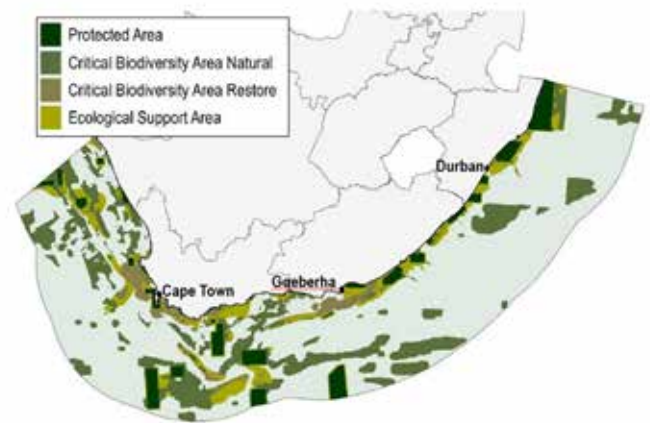


Figure 1. The coastal and marine CBA Map for mainland SA. for sites to maintain their state.

The CBA Map and associated sea use guidelines have directly informed the zoning and regulations that are proposed in the Marine Biodiversity Sector Plan (Fig. 2). Zones for strict biodiversity conservation (informed by CBAs) and for impact management (informed by ESAs) are included. For sea uses assessed to be incompatible with maintaining areas in their desired state, prohibiting these uses, or giving consent only under certain conditions of practice, are specified. In the development of Marine Area Plans, this proposal will have to be evaluated against the spatial interests and requirements of other sectors (e.g. fishing, aquaculture, oil and gas, cultural heritage and others) to achieve an integrated plan that will balance socio-economic, cultural and biodiversity priorities.

Author: Kirkman SP (OC Research)
Contributors: Ramakulukusha M (Fisheries Management); Holness S, Sorgenfrei R (MARISMA); Langa Z (OCS); Majiedt P, Sink K (SANBI)

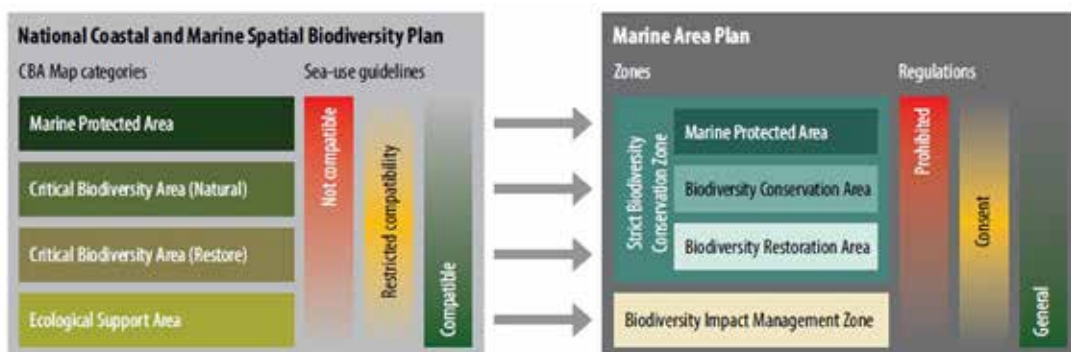


Figure 2. The relationship of CBA Map categories and sea use guidelines to proposed biodiversity zones and management specifications.

PLATFORMS, TECHNOLOGY & INNOVATION

32. FILLING IN THE BLANKS – IMPROVED BATHYMETRIC OBSERVATIONS AT THE PRINCE EDWARD ISLANDS

Accurate bathymetric (sea floor) observations are crucial not only for safe navigation of vessels at sea, but also for numerous research and monitoring applications. These include determining locations for oceanographic mooring deployments; creating hydrodynamic models for investigating oceanic properties; mapping of sediments, glacial deposits, and habitats of benthic biota; monitoring impacts of climate change and variability such as beach erosion, subsidence, and sea level rise; and others. In 2017, international recognition of the importance of bathymetric observations resulted in the launch of the Nippon Foundation-GEBCO Seabed 2030 Project. In 2021, this project was formally endorsed as a flagship programme and a Decade Action of the United Nations (UN) Decade of Ocean Science for Sustainable Development. The Seabed 2030 Project is a global citizen science initiative that seeks to map the sea floor of the global ocean by 2030.

In 2022, collaborative efforts between OC Research, UNISA and the University of Fort Hare resulted in the development of a high spatial resolution *in situ* bathymetry data source for the Prince Edward Islands (PEIs) region (Fig. 1a). This map was produced using 10 years (2013–2022) of data from single beam scientific transducers (38, 120, and 200 kHz), bottom tracking pings from a Ship-mounted Acoustic Doppler Current Profiler (S-ADCP), and a combination of CTD pressure and altimeter measurements. These data were collected during annual April/May voyages of the SA *Agulhas II* to re-supply the research base at Marion Island. Despite a decade of data collection, there were still extensive areas where no bathymetry data were available, indicated as white shaded areas in Figure 1a. Drawing on recommendations from the 2022 OC Annual Science Report, and in line with the UN Ocean Decade Action to map the global sea floor, OC Research has endeavoured to conduct systematic surveys of the PEI region to improve the *in situ* bathymetry data coverage.

In 2023, two research and monitoring cruises (the April Marion Island re-supply voyage, and the November Summer Survey of seabirds, mammals and benthic biota)

allowed the collection of additional CTD, S-ADCP, and scientific transducer measurements in the region. These data, together with the 18 kHz transducer measurements (used mainly for navigational purposes), were combined with existing data to produce an updated bathymetry map for the region (Fig. 1b). In the updated map, data coverage has been substantially expanded in the eastern section of the region and the majority of the eastern slope of the PEI shelf can now be clearly visualised. The same is true for the shelf and slope regions north of Prince Edward Island and south of Marion Island. Nevertheless, much work still needs to be done to fill in the remaining data gaps. On the shallower PEI shelf, relatively broad regions with no data still exist along the northern boundaries of Marion and Prince Edward Islands, mainly because these regions are too shallow and too close to the islands for the SA *Agulhas II* to navigate safely. In addition to continuing data collections in deeper waters, we recommended small boat-based bathymetry surveys to map these nearshore regions more effectively.

Authors: van den Berg MA, Lamont T, Tutt GCO (OC Research); Hedding D (UNISA); Nel W (UFH)
Contributors: Anders DA (OC Research); Frémand A (BAS, UK Polar Data Centre)

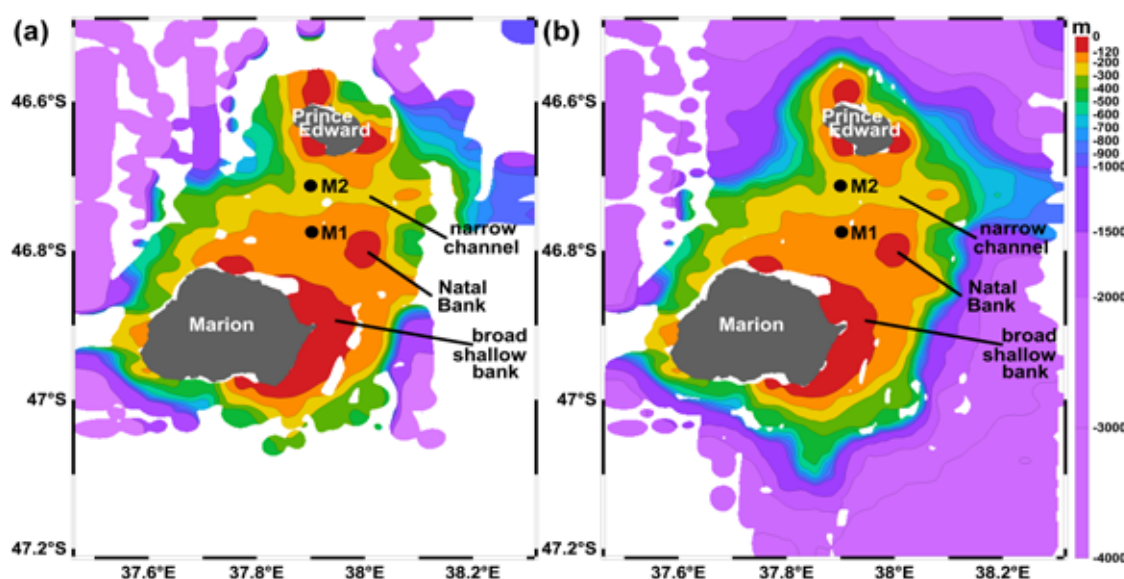
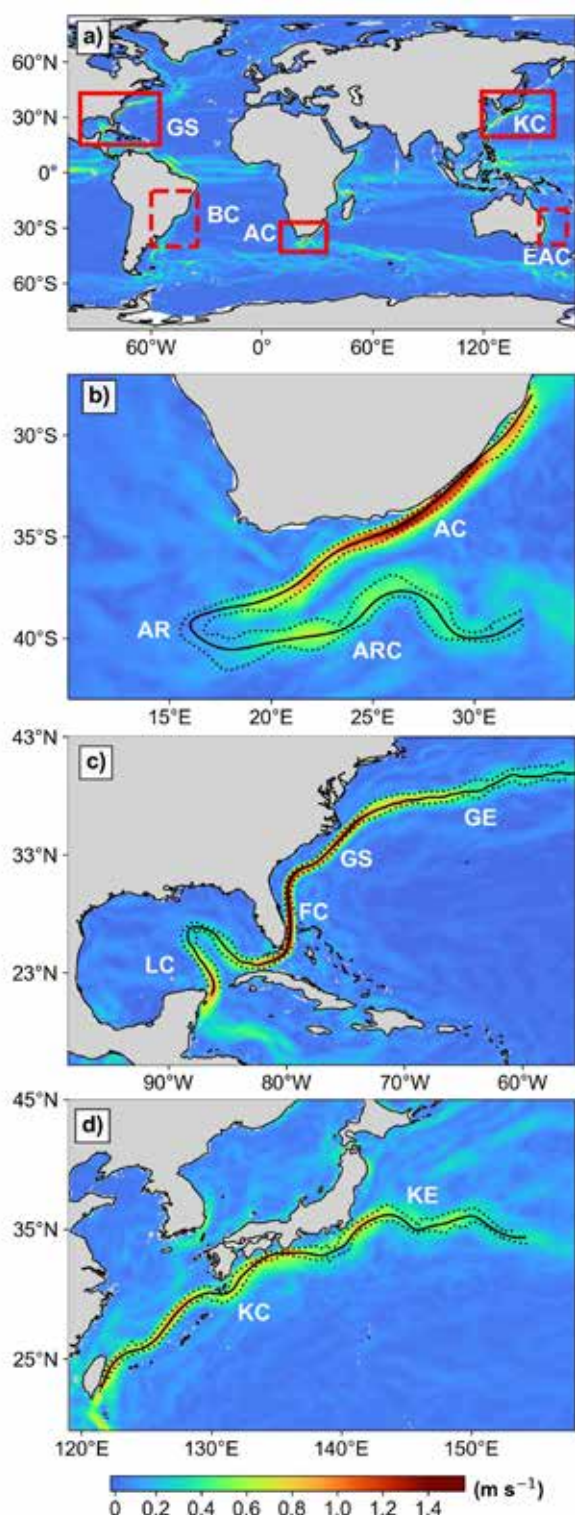


Figure 1. Maps of the Prince Edward Islands (PEIs) showing *in situ* bathymetry on and around the PEI shelf, gridded from data collected during (a) 2013–2022, and (b) 2013–2023. White shading indicates areas of no data.

PLATFORMS, TECHNOLOGY & INNOVATION

33. TRACKING CURRENT CORES AND EDGES (TRACCE) OF MAJOR WESTERN BOUNDARY CURRENTS

The five major western boundary currents (WBCs) include the Agulhas Current (AC) system off South Africa, the Brazil Current (BC) system off South America, the Gulf Stream (GS) system off North America, the Kuroshio Current (KC) system off Japan, and the East Australian Current (EAC) system off Australia (Fig. 1a). These systems strongly influence global climate, local marine ecosystems and coastal dynamics, and interest in understanding their variability has increased in recent years. In 2019, satellite altimetry data was used to develop and implement the LACCE (Location of the Agulhas Current Core and Edges) monitoring tool to investigate and routinely monitor variability in the AC system (Fig. 1b). Here, we evaluate the suitability of LACCE, now renamed TRACCE, for application in the remaining four major WBC systems.



The application of TRACCE to the BC and EAC systems was highly complex and ultimately unsuccessful. This was due to the multiple recurrent, and occasionally stationary, mesoscale eddies (clockwise and anticlockwise circulating features) that diminish the intensity and continuity of the mean WBC flow in these two systems. The weaker flow of these WBCs (Fig. 1a) makes it impossible to use gridded satellite altimetry data to distinguish them objectively from the surrounding mesoscale features throughout their entire domains. In contrast, TRACCE was effectively adapted to work in the GS and KC. It successfully captured all the components of the respective current systems throughout their entirety, with the Loop Current, Florida Current, GS and Gulf Extension, in the GS system (Fig. 1c) and the KC and the Kuroshio Extension in the KC system (Fig. 1d).

Our finding that TRACCE could only be successfully applied to three of the five major WBCs is in line with previous studies that demonstrated a similar inability to apply their respective identification methods to all five major WBCs simultaneously. However, successful application of TRACCE to the AC, GS, and KC now provides a useful tool to objectively identify the cores and edges of these three WBCs. This enables us to compare the variability in and among these systems. Such comparisons are critical to determine and monitor whether these WBC systems respond to climate-driven changes in the same way, and to better understand how local factors, such as coastal bathymetry and wind patterns, could potentially alter the expected climate-driven responses in each system.

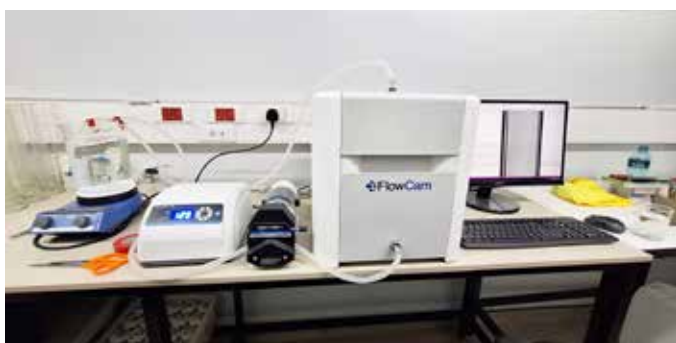
Authors: Russo CS, Lamont T (OC Research)

Figure 1. Maps of thirty-year (1993–2023) mean altimetry-derived current speed. (a) Global map outlining the Agulhas Current (AC), Gulf Stream (GS) and Kuroshio Current (KC) systems where TRACCE was successfully applied (solid red boxes), as well as the Brazil Current (BC) and East Australian Current (EAC) systems where its application was unsuccessful (dashed red boxes). The TRACCE-identified current cores (solid black lines) and edges (dotted black lines) for the (b) AC, (c) GS and (d) KC systems. The system components, including the AC, Agulhas Retroflection (AR) and Agulhas Return Current (ARC) in the AC system; the Loop Current (LC), Florida Current (FC), GS and Gulf Extension (GE) in the GS system; and the KC and Kuroshio Extension (KE) in the KC system, are labelled.

PLATFORMS, TECHNOLOGY & INNOVATION

34. PICTURE PERFECT: RAPID CLASSIFICATION OF MESOZOOPLANKTON

Picture Perfect is a United Nations (UN) Ocean Decade project under the programme Marine Life 2030 (<https://oceandecade.org/actions/picture-perfect-rapid-classification-of-plankton>), which is aimed at increasing the world's biodiversity information. This project is developing rapid techniques for image analysis of plankton with a size range of 0.2–50 mm, to ensure there are data to inform decision-making in a short space of time. In earlier years, traditional microscopy was used to identify these organisms, but due to their high biomass and the time-consuming nature of the work, imaging technology is now more widely used. Three instruments have been identified to be tested for rapid analysis of plankton within three size classes. Here, we present our technical assessment of the Yokogawa Fluid Imaging Flowcam Macro instrument (Fig. 1) for protocol development of rapid image analysis of mesozooplankton (0.2–20 mm).



During instrument assessment and protocol testing, solutions were found to a number of challenges:

- 1. Challenge:** Too many air bubbles.
Solution: Ensure the sample and the instrument are at a similar temperature. Elevate the sample inlet pipe ensuring that there are no dips. This allows gravity to assist rather than hinder the process. Then prime the sample (Fig. 2A).
- 2. Challenge:** Dense samples require more than one run, which is not ideal.
Solution: As the sample is running, re-fill the beaker using a funnel and pipe. This introduces the sample slowly, decreasing air bubbles, and thus preventing a rush of organisms that cannot be captured by the camera (Fig. 2B and C).
- 3. Challenge:** Condensation on the flow cell.
Solution: Reduce humidity in the laboratory.
- 4. Challenge:** Destruction of organisms. The system uses a pump with rollers. If connected correctly the sample is imaged well, but organisms >1 mm are destroyed by the pump. If the sample is required for archival purposes (as at DFFE), there is currently no off-the-shelf solution.
Solution: Our in-house solution was to attach a sample container with a 0.2 mm mesh to the outlet, and to submerge this in water. This allows the correct flow rate to be maintained without destruction of organisms (Fig. 2A). We found that using a vacuum pump with a sample retention reservoir could not maintain the flow rate required to image dense samples.

- 5. Challenge:** Animal retention within the system due to the large volume of water used. If sample is comprised of organisms <1 mm, the system can be used as is, but animal retention is an issue.
Solution: Attaching the outlet pipe to a collecting sieve allows the water to drain out, while animals are retained on the mesh (Fig. 2D).
- 6. Challenge:** Camera quality for organisms ranging in size from 0.2–20 mm.
Assessment: The camera calibrates automatically and can easily adjust between sizes while maintaining image quality. There is no need to fractionate samples into different size classes.
- 7. Challenge:** Speed of sample analysis.
Assessment: There is no need to sub-sample; multiple samples can be run daily as the flow-through system is rapid.

OC Research is working closely with Yokogawa Fluid Imaging Technologies as they are very interested in our in-house solutions and methods. Standard operating procedures will be shared as open source after finalisation as a protocol under the UN Ocean Best Practices.



Figure 2. (A) Modified setup of the FlowCam Macro, (B) and (C) re-filling the beaker to minimise air bubbles, and (D) retention of the sample by separation of animals and water at the outlet.

Author: Pillay K (OC Research)

Contributors: Hansraj Y, Setati S, van der Poel J (OC Research)

PLATFORMS, TECHNOLOGY & INNOVATION

35. MIMS MASTER DATA MANAGEMENT PLAN GUIDE: A FRAMEWORK FOR FAIR AND TRUSTWORTHY MARINE AND COASTAL DATA FOR DFFE

The Marine Information Management System (MIMS) Master Data Management Plan (MDMP) guide serves as a framework for ensuring that the data produced by DFFE: Ocean and Coastal Research is FAIR (Findable, Accessible, Interoperable and Reusable) and trustworthy. The guide provides instructions on how to develop a MDMP to align with these principles, ensuring that both the data and the MIMS meet the highest standards of data stewardship. This is especially crucial for institutions that manage accredited Associate Data Units (ADUs), such as DFFE, which manages MIMS.

As an International Oceanographic Data and Information Exchange (IODE) accredited ADU, MIMS aligns its data management practices with both local and international standards. By following the guide, MDMPs that are developed for marine research projects within DFFE will ensure data management practices that adhere to both local and international standards, fostering transparency and trust (see Fig. 1 for other benefits of developing a MDMP).

Interoperability is promoted by encouraging the use of standardised formats, which ensures that data integrates seamlessly with global marine data and systems. The MDMP guide also emphasises the importance of maintaining data reusability through detailed documentation of datasets for future research and decision-making.

Additionally, the guide highlights the need for comprehensive protocols that address data validation, error checking, and thorough documentation, including the methods used in data collection and processing. It further supports the development of long-term data preservation strategies within the MDMP, ensuring ongoing accessibility and usability of data even after project completion. Ultimately, the guide helps DFFE and MIMS contribute to the advancement of ocean science, promoting global collaboration, and safeguarding marine ecosystems for future generations.

Authors: Mahanjana A, Rasmeni B, Khoza I, Rasehlomi T (OC Research)

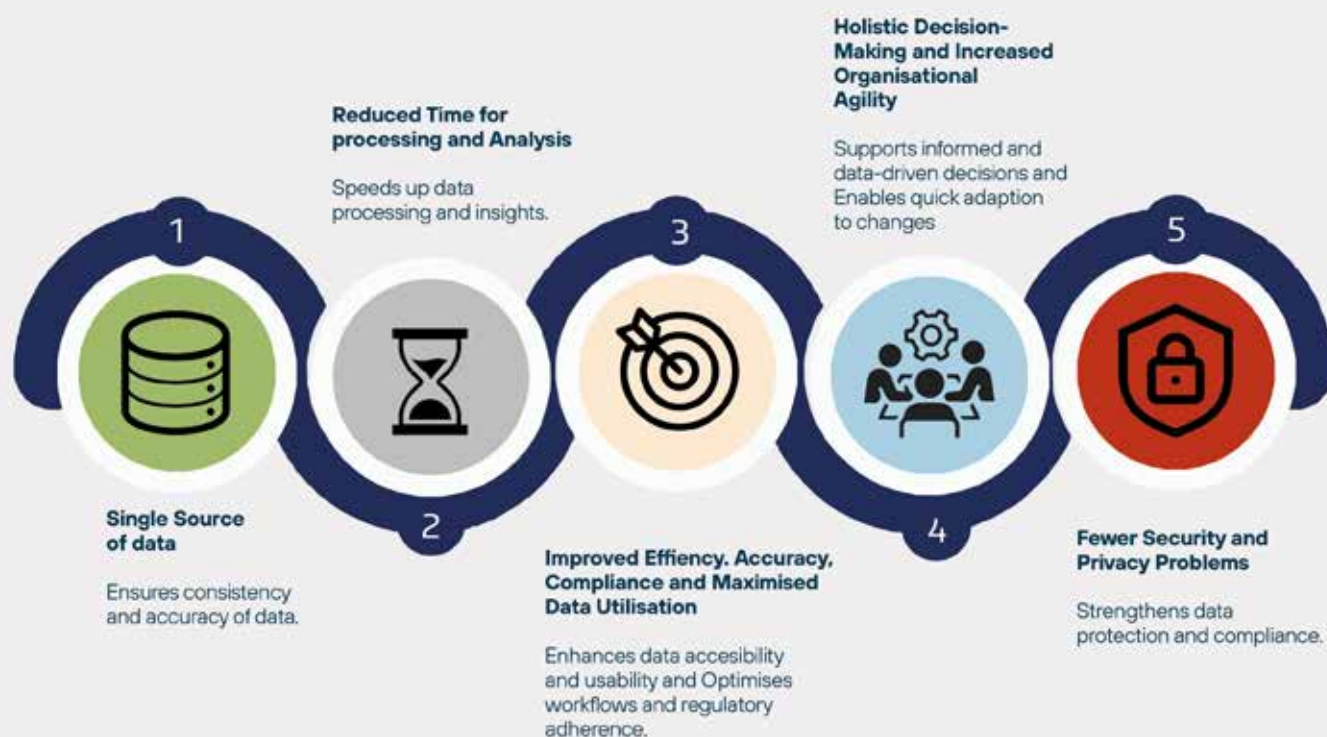


Figure 1. Flowchart illustrating the benefits of a having a Master Data Management Plan, based on a schematic diagram by R Rajpal (<https://www.softwaresuggest.com/blog/erp-and-plm/>).

TRAINING & OUTREACH

36. FLOW CYTOMETRY TRAINING FOR MARINE MICROBIAL ANALYSIS

Flow cytometers have long been used in medical research to measure and analyse multiple properties of single particles in a fluid stream through a laser light. Since its introduction to marine science in the 1980s, the flow cytometer has been used to enumerate picophytoplankton (microbial organisms ranging from 0.2–2.0 μm), due to its ability to take up water samples and arrange each cell according to size and fluorescence (emission of light). Despite being widespread and abundant in marine ecosystems, these microbes had previously gone unnoticed in epifluorescence microscopic analyses due to their small size.

The BD (Becton, Dickinson) FACSymphony A1, a high-performance cell analyser developed by BD Biosciences for flow cytometry application (Fig. 1a), was acquired for microbial oceanography analyses in 2024. Training was facilitated to enhance participants' understanding of flow cytometry and its applications to improve the team's capabilities to use the flow cytometer quickly and efficiently (Fig. 1b). The training spanned three days and included theory, a hands-on instructor-led session (with a BD Instrument Specialist) and a one-day workshop on "virtual gating". Virtual gating is the process of visualising certain cell populations without having to physically separate them. Through this process, a particular cell subset and its characteristics can be observed. Within a sample, the flow of fluid through the instrument suspends cells, after which they pass through a laser beam and are sorted and counted according to pigment, size and shape. Various cell types, as well as the number of cells within a sample, can then be determined via analysis using FlowJo or BD FACSDiva software.

Trainees learnt how to use the flow cytometer to analyse cells and were also given the opportunity to work on existing data. For each project, an experiment was created with the collection of organisms that emit pigments detected by chosen lasers. Organisms (cells) were counted and grouped together as clusters of dots. Once the sample analysis was completed, the analysed dot plots were "gated" using FlowJo software (Fig. 2a). A fully analysed monitoring line during the 2024 August Integrated Ecosystem Programme (IEP) cruise off the west coast is used as an example, accompanied by isosurface plots of the gated picophytoplankton groups (Fig. 2b). To date, the team has independently analysed samples from five scientific cruises, totalling over a thousand individual samples. This approach will now be implemented by DFFE for routine monitoring of marine microbes, to assess ecosystem status and health.

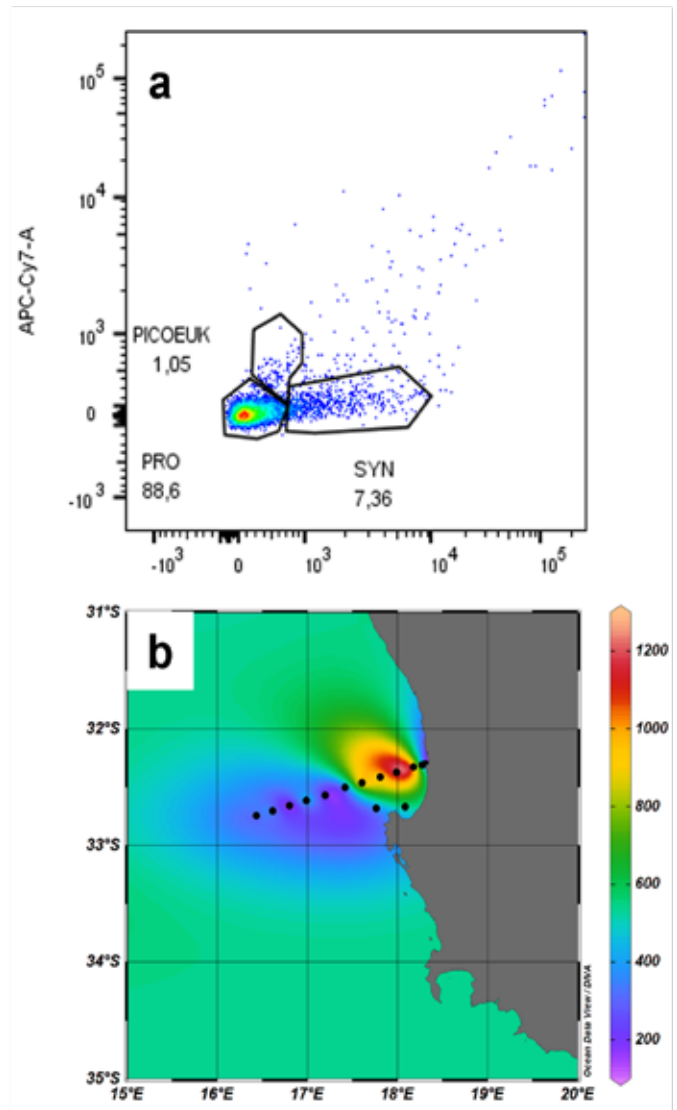


Figure 2. (a) A FlowJo cytogram plot with phycocyanin (blue pigment) on the y-axis (APC-Cy7-A), and phycoerythrin (red pigment) on the x-axis (PE-A) showing different phytoplankton groups: picoeukaryotes (PICOEUK), *Synechococcus* (SYN) and *Prochlorococcus* (PRO). (b) Gated populations of picophytoplankton abundance (cells mL^{-1}) along the IEP monitoring line.

Authors: Mdazuka Y, Hansraj Y, Maseti T, Gebe Z (OC Research)
Contributor: Adams R (BD Biosciences).



Figure 1. (a) The BD FACSymphony A1 Flow Cytometer setup, and (b) the Microbial Oceanography team receiving hands-on flow cytometry training.

TRAINING & OUTREACH

38. HARMONISING COLLECTION OF MICROPLASTICS IN BEACH SAND AND SURFACE WATER IN AFRICA UNDER THE UN IAEA INITIATIVE

The third engagement of the United Nations International Atomic Energy Agency (IAEA) regional hands-on training initiative was hosted by the Government of Tunisia, in June 2024, through the Institut National des Sciences et Technologies de la Mer (INSTM) RAF 1010 project for member states. Sixteen African countries were provided with knowledge and skills for sampling (Fig. 1) and analysis (Fig. 2) of microplastics of 0.3-5 mm size fraction in beach sand and surface water, and for country reporting to United Nations (UN) Sustainable Development Goals (SDGs). This is a priority for DFFE as the national reporter of SDG 14.



Figure 1. Participants undergoing boat-based training on collection of surface microplastics samples using a manta trawl, sample preservation and data recording.

The two-week “Regional Training Course on Monitoring of Microplastics in Tunisia” focused on sample collection of surface water (using manta trawl) and beach sand, sample preparation, microscopic identification and polymer characterisation. The harmonised protocol that was used was developed at the 2nd meeting of RAF1010 and will be implemented in the Nuclear Technology for Controlling Plastic Pollution (NUTEC) global project with 99 adhered member states. The participating laboratories will have to undergo this training to certify each of them as an Intermediate Level Laboratory in the NUTEC Global Monitoring Network.

The key outcomes from the training course were:

1. Understanding microplastics: participants gained an understanding of microplastics, including their sources, types, and environmental impact;
2. Nuclear analytical techniques: the course emphasised the use of nuclear analytical techniques for monitoring microplastics for the next phase or advanced level of laboratory grading. South Africa (DFFE: OC) has been ear-marked to be an advanced NUTEC laboratory;
3. Practical sampling methods: attendees learnt and practised various sampling methods, ensuring they can effectively collect microplastic samples in different environments;
4. Laboratory analysis: the course included laboratory work where participants analysed samples using techniques such as Attenuated Total Reflection-Fourier Transform Infrared spectroscopy (ATR-FTIR) for polymer characterisation, thus enhancing their analytical capabilities;

5. Data reporting and presentation: participants were trained in calculating, reporting, and presenting their findings, which is crucial for scientific communication and collaboration;
6. Collaborative learning: the course fostered collaboration through group activities, discussions and presentations, allowing participants to learn from each other and build professional networks; and
7. Country-specific insights: through country presentations, participants shared and learnt about national capacities and approaches, gaining insights into practices and challenges within Africa, and fostering an African network.



Figure 2. Laboratory-based training and analysis.

Knowledge gained from the regional training course will be used to harmonise sampling techniques within South Africa to ensure that several institutions can produce comparable data for national UN SDG reporting. This will enable DFFE to understand the extent of microplastic pollution along beaches and to identify hotspots. Additionally, by integrating these practices, we can improve our understanding and management of microplastic pollution, ultimately helping to protect marine environments and public health. This harmonised approach has been registered as a UN Ocean Decade Project, and is led by South Africa (<https://oceandecade.org/actions/comparable-microplastics-monitoring-of-oceans/>).

Authors: Pillay K, Worship MM (OC Research)

OUTPUTS FOR 2024

PEER-REVIEWED PUBLICATIONS

- Amjad F, Ahusan M, Amir H, de Villiers NM, Gress E, Mah CL, Naeem S, Rico-Seijo N, Samaai T, Afzal MS, Woodall LC, Stefanoudis PV. 2024. An underwater imagery identification guide for shallow, mesophotic and deep-sea benthos in Maldives. *Biodiversity Data Journal* 12: e120128. doi: [10.3897/BDJ.12.e120128](https://doi.org/10.3897/BDJ.12.e120128).
- Bentley LK, Phillips RA, Carpenter-Kling T, Crawford RJM, Cuthbert RJ, Delord K, Dilley BJ, Makhado AB, Miller PI, Opper S, Pistorius PA, Ryan PG, Schoombie S, Weimerskirch H, Manica A. 2024. Habitat preferences of *Phoebastria* albatrosses in sympatry and allopatry. *Journal of Biogeography* 51: 1986–1998. doi: [10.1111/jbi.14966](https://doi.org/10.1111/jbi.14966).
- Brandt P, Bordbar MH, Coelho P, Koungue RAI, Körner M, Lamont T, Lübbecke JF, Morholz V, Prigent A, Roch M, Schmidt M, van der Plas AK, Veitch J. 2024. Chapter 9. Physical drivers of Southwest African coastal upwelling and its response to climate variability and change. In: von Maltitz GP, Midgley GF, Veitch J, Brümmer C, Rotter RP, Viehberg FA, Veste M (Eds.) *Sustainability of Southern African ecosystems under global change: Science for Management and Policy Interventions*. Ecological Studies Volume 248. Cham: Springer. pp. 221–257. doi: [10.1007/978-3-031-10948-5_9](https://doi.org/10.1007/978-3-031-10948-5_9).
- Dugenne M, Corrales-Ugalde M, Luo JY, Kiko R, O'Brien TD, Irisson J-O, Lombard F, Stemmann L, Stock C, Anderson CR, Babin M, Bhaiy N, Bonnet S, Carlotti F, Cornils A, Crockford ET, Daniel P, Desnos C, Drago L, Elineau A, Fischer A, Grandrémy N, Grondin P-L, Guidi L, Guieu C, Hauss H, Hayashi K, Huggett JA, Jalabert L, Karp-Boss L, Kenitz KM, Kudela RM, Lescot M, Marec C, McDonnell A, Mériguet Z, Niehoff B, Noyon M, Panaïotis T, Peacock E, Picheral M, Riquier E, Roesler C, Romagnan J-B, Sosik HM, Spencer G, Taucher J, Tilliette C, Vilain M. 2024. First release of the Pelagic Size Structure database: global datasets of marine size spectra obtained from individual imaging devices. *Earth System Science Data* 16: 2971–2999. doi: [10.5194/essd-16-2971-2024](https://doi.org/10.5194/essd-16-2971-2024).
- Dyer BM, Masotla M, Little W, Crawford RJM, Makhado AB. 2024. The longest living gannet *Morus* spp. at Malgas Island, South Africa. *Biodiversity Observations* 14: 81–83. doi: [10.15641/bo.1618](https://doi.org/10.15641/bo.1618).
- Filander ZN, Sink KJ, Kitahara MV, Cairns SD, Lombard A. 2024. Diversity patterns of the South African azooxanthellate scleractinians (Cnidaria: Anthozoa), with considerations of environmental correlates. *PLoS ONE* 19: e0296188. doi: [10.1371/journal.pone.0296188](https://doi.org/10.1371/journal.pone.0296188).
- Hood RR, Coles VJ, Huggett JA, Landry MR, Levy M, Moffett JW, Rixen T. 2024. Chapter 13. Nutrient, phytoplankton and zooplankton variability in the Indian Ocean. In: Ummenhofer CC, Hood RR (Eds.) *The Indian Ocean and its Role in the Global Climate System*. Elsevier. pp 293–327. doi: [10.1016/B978-0-12-822698-8.00020-2](https://doi.org/10.1016/B978-0-12-822698-8.00020-2).
- Katharoyan C, Peer N, Landschoff J, Griffiths CL, Samaai T, Beeslaar D. 2024. Kelp holdfasts in the Great African Seafloor provide habitat for diverse assemblages of macroinvertebrates. *Aquatic Biology* 33: 33–45. doi: [10.3354/ab00766](https://doi.org/10.3354/ab00766).
- Lamont T, Halo I, Russo CS. 2024. Impacts of Agulhas Current meanders on intermediate water masses along the adjacent continental slope and shelf. *Continental Shelf Research* 274: article 105197. doi: [10.1016/j.csr.2024.105197](https://doi.org/10.1016/j.csr.2024.105197).
- Mann BQ, Jordaan GL, Dalton WN, Daly R, Soekoe M, Potts WM, Smale MJ, Swart L. 2024. Movement and growth of the spotted gully shark *Triakis megalopterus* in South African waters. *African Journal of Marine Science* 46: 1–15. doi: [10.2989/1814232X.2024.2355868](https://doi.org/10.2989/1814232X.2024.2355868).
- Martin B, Auel H, Bode-Dalby M, Dudeck T, Duncan S, Ekau W, Fock HO, Hagen W, Heinatz K, Kaufmann MJ, Koppelman R, Lamont T, Louw D, Moloto T, Sell AF, Thomalla S, van der Lingen CD. 2024. Chapter 11. Studies of the ecology of the Benguela Current Upwelling System – the TRAFFIC approach. In: von Maltitz GP, Midgley GF, Veitch J, Brümmer C, Rotter RP, Viehberg FA, Veste M (Eds.) *Sustainability of Southern African ecosystems under global change: Science for Management and Policy Interventions*. Ecological Studies Volume 248. Cham: Springer. pp. 277–312. doi: [10.1007/978-3-031-10948-5_11](https://doi.org/10.1007/978-3-031-10948-5_11).
- McInnes AM, Weideman EA, Carpenter-Kling T, Barham P, Christian M, Day K, Glencross JS, Hagen C, Kock A, Lawrence C, Ludynia K, Makhado A, Pichegru L, Shannon L, Sherley RB, Smith C, Steinfurth A, Stander N, Upfold L, Waller L. 2024. Commercial fishery no-take zones for African penguins minimize fisheries losses at the expense of conservation gains. *ICES Journal of Marine Science* 81: 1632–1646. doi: [10.1093/icesjms/fsae109](https://doi.org/10.1093/icesjms/fsae109).
- Meiritz LC, Rixen T, van der Plas AK, Lamont T, Lahajnar N. 2024. The influence of zooplankton and oxygen on the particulate organic carbon flux in the Benguela Upwelling System. *Biogeosciences* 21: 5261–5276. doi: [10.5194/bg-21-5261-2024](https://doi.org/10.5194/bg-21-5261-2024).
- Payne RP, Ngwakum B, Teske PR, Landschoff J, Samaai T. 2024. The first hermit crab-associated sponge from South Africa, *Suberites ambulodomus* sp. nov. (Porifera, Demospongiae, Suberitida, Suberitidae), and its relationship with the hermit crab *Pagurus liochele*. *Systematics and Biodiversity* 22: article 2346829. doi: [10.1080/14772000.2024.2346829](https://doi.org/10.1080/14772000.2024.2346829).
- Payne RP, Samaai T, Janson L, Kerwath SE, Gibbons MJ. 2025. Eleven new heteroscleromorph Demospongiae (Porifera), and a new record of the tetractinellid *Ancorina corticata*, from Walters Shoal, a shallow seamount on the Madagascar Ridge in the South West Indian Ocean (SWIO). *Zootaxa* 5575:1–56. doi: [10.11646/zootaxa.5575.1.1](https://doi.org/10.11646/zootaxa.5575.1.1).

OUTPUTS FOR 2024

- Pichegru L, Sherley RB, Malan T, Barham BJ, Ludynia K, Geldenhuys D, Amos K, Barham PJ, Drost E, Hahndiek V, Hufke A, Hugo C, Lawrence C, McGeorge C, McInnes AM, Makhado AM, Mashau M, Milne R, Purves A, Slier M, van der Merwe C, van Wilgen NJ, Waller L. 2024. Decades of artificial nests towards African penguin conservation—Have they made a difference? *Ecological Solutions and Evidence* 5: e12388. doi: [10.1002/2688-8319.12388](https://doi.org/10.1002/2688-8319.12388).
- Puccinelli E, Filander Z, Lamont T. 2024. The influence of the Cape Canyon on the food web structure of the southern Benguela upwelling system. *Journal of Marine Systems* 244: article 103965. doi: [10.1016/j.jmarsys.2024.103965](https://doi.org/10.1016/j.jmarsys.2024.103965).
- Rixen T, Lahajnar N, Lamont T, Koppelman R, Martin B, Meiritz L, Siddiqui C, van der Plas AK. 2024. Chapter 25. The marine carbon footprint: Challenges in the quantification of CO₂ uptake by the biological carbon pump in the Benguela Upwelling System. In: von Maltitz GP, Midgley GF, Veitch J, Brümmer C, Rotter RP, Viehberg FA, Veste M (Eds.) *Sustainability of Southern African ecosystems under global change: Science for Management and Policy Interventions*. Ecological Studies Volume 248. Cham: Springer. pp. 729–757. doi: [10.1007/978-3-031-10948-5_25](https://doi.org/10.1007/978-3-031-10948-5_25).
- Sell AF, von Maltitz GP, Auel H, Biastoch A, Bode-Dalby M, Brandt P, Duncan SE, Ekau W, Fock HO, Hagen W, Huggett JA, Koppelman R, Körner M, Lahajnar N, Martin B, Midgley GF, Rixen T, van der Lingen CD, Verheye HM, Wilhelm MR. 2024. Chapter 2. Unique southern African terrestrial and oceanic biomes and their relation to steep environmental gradients. In: von Maltitz GP, Midgley GF, Veitch J, Brümmer C, Rötter RP, Viehberg FA, Veste N (Eds.) *Sustainability of Southern African Ecosystems under Global Change*. Ecological Studies. Volume 248. Cham: Springer. pp 23–88. doi: [10.1007/978-3-031-10948-5_2](https://doi.org/10.1007/978-3-031-10948-5_2).
- Shabangu FW, Daniels R, Jordaan RK, de Bruyn PJN, van den Berg MA, Lamont T. 2024. Killer whale acoustic patterns respond to prey abundance and environmental variability around the Prince Edward Islands, Southern Ocean. *Royal Society Open Science* 11: article 230903. doi: [10.1098/rsos.230903](https://doi.org/10.1098/rsos.230903).
- Shabangu FW, Munoz T, van Uffelen L, Estabrook BJ, Yeman D, Stafford KM, Branch TA, Vermeulen E, van den Berg MA, Lamont T. 2024. Diverse baleen whale acoustic occurrence around two sub-Antarctic Islands: A tale of residents and visitors. *Scientific Reports* 14: article 21663. doi: [10.1038/s41598-024-72696-2](https://doi.org/10.1038/s41598-024-72696-2).
- Sherley RB, Makhado AB, Crawford RJM, Hagen C, Kemper J, Ludynia K, Masotla MJ, McInnes A, Pichegru L, Tom D, Upfold L, Waller LJ. 2024. The African Penguin *Spheniscus demersus* should be considered critically endangered. *Ostrich* 95: 181–187. doi: [10.2989/00306525.2024.2355618](https://doi.org/10.2989/00306525.2024.2355618).
- Siddiqui C, Rixen T, Lahajnar N, Lamont T, van der Plas AK. 2024. Simulating potential impacts of bottom trawling on the biological carbon pump: A case study in the Benguela Upwelling System. *Frontiers in Marine Science* 11: article 1387121. doi: [10.3389/fmars.2024.1387121](https://doi.org/10.3389/fmars.2024.1387121).
- Tree B, Olbers J, Seyboth E, Seakamela SM, Cockcroft VG, Vermeulen E, Findlay KP. 2024. Migratory movement of photo-identified humpback whales *Megaptera novaeangliae* along the southeastern coast of Africa. *African Journal of Marine Science* 46: 191–203. doi: [10.2989/1814232X.2024.2380882](https://doi.org/10.2989/1814232X.2024.2380882).

PRESENTATIONS AT SYMPOSIA, CONFERENCES AND WORKSHOPS

- Bucklin A, Blanco-Bercial L, Escribano R, Falkenhaug T, Hirai J, Huggett J, Martinez P, Peijnenburg K, Suter L, Weydmann-Zwolicka A, Batta-Lona P, Dubbeldam S, Ershova E, Gonzalez CE, Govender A, Groeneveld J, Khodami S, MacDonald A, Mioduchowska M, Polanowski A, Renz J, Wiebe P, O'Brien T. 2024. Metabarcoding Zooplankton Diversity: MetaZooGene Intercalibration Experiment (MZG-ICE). *International Council for the Exploration of the Sea and the North Pacific Marine Science Organization (ICES-PICES) 7th International Zooplankton Production Symposium, Hobart, Tasmania, Australia, 17–22 March 2024*.
- Chioze CA, Huggett JA, Isari S, Malauene BS, Roberts M. 2024. The abundance and distribution of mesozooplankton communities on the Mozambique shelf. *International Council for the Exploration of the Sea and the North Pacific Marine Science Organization (ICES-PICES) 7th International Zooplankton Production Symposium, Hobart, Tasmania, Australia, 17–22 March 2024*.
- Daniels R, Lamont T, Shabangu FW. 2024. Interannual variability of the acoustic occurrence of killer whales around the Prince Edward Islands. *4th African Bioacoustics Community (ABC) Conference, The Breakwater Lodge, Cape Town, South Africa, 1–6 September 2024*. Daniels R, Lamont T, Shabangu FW. 2024. Interannual variability of the acoustic occurrence of killer whales around the Prince Edward Islands. *7th International Marine Conservation Congress (IMCC7), Cape Town International Convention Centre, Cape Town, South Africa, 13–18 October 2024*.
- du Preez SA, Lamont T, Huggett JA. 2024. Zooplankton variability around the sub-Antarctic Prince Edward Islands and the influence of the environment. *International Council for the Exploration of the Sea and the North Pacific Marine Science Organization (ICES-PICES) 7th International Zooplankton Production Symposium, Hobart, Tasmania, Australia, 17–22 March 2024*.
- du Preez S, Lamont T, Huggett J. 2024. Zooplankton variability around the sub-Antarctic Prince Edward

OUTPUTS FOR 2024

- Islands and the influence of the environment. *Hobart 2024 workshop on WP1.3. The Pelagic realm of the subantarctic Indian and Southern Indian Ocean, Hobart, Tasmania, Australia, 25–26 March 2024.*
- du Preez SA, Lamont T, Huggett JA, Ansorge I. 2024. Zooplankton variability around the sub-Antarctic Prince Edward Islands and the influence of the environment. *7th International Marine Conservation Congress (IMCC7), Cape Town International Convention Centre, Cape Town, South Africa, 13–18 October 2024.*
- Esquivel-Garrote O, Gregory L, Worship M, Inck C, Huggett J, Johns D, Muxagata E. 2024. Brazil - South Africa Continuous Plankton Recorder results. *Atlantic Ecosystems Assessment, Forecasting & Sustainability (AtlantECO) General Assembly 2024 (GA24), Vigo, Spain, 16–21 September 2024.*
- Govender A, Huggett J, Maseti T, Thibault D, Cedras R, Groeneveld J. 2024. An integrated approach to exploring zooplankton assemblages in a cyclonic eddy. *International Council for the Exploration of the Sea and the North Pacific Marine Science Organization (ICES-PICES) 7th International Zooplankton Production Symposium, Hobart, Tasmania, Australia, 17–22 March 2024.*
- Halo I, Lamont T, Penven P. 2024. Spatial and temporal variability of the oceanic circulation in the greater Agulhas Current System. *Research Seminar, Institute of Marine Science, Bergen, Norway, 31 October 2024.*
- Halo I, Lamont T, Rautenbach G. 2024. Modelling the shelf and slope currents in submarine canyons off northern KwaZulu-Natal, east coast of South Africa. *7th International Marine Conservation Congress (IMCC7), Cape Town International Convention Centre, Cape Town, South Africa, 13–18 October 2024.*
- Haupt T, Janson L, Auerswald L. 2024. Monitoring of inshore temperatures to support physiological research. *International Conference on: Integrated Responses to the Intensification of Extreme Climate and Weather Events in Developing Economies, Stellenbosch, South Africa, 22–24 May 2024.*
- Haupt T, Reismann M, Macey B, Auerswald L. 2024. A compromised immune system: The Cape urchin in a rapidly acidifying World. *7th International Marine Conservation Congress (IMCC7), Cape Town International Convention Centre, Cape Town, South Africa, 13–18 October 2024.*
- Holliday NP, Ansorge I, Burmeister K, Campos EJD, Chidichimo MP, DeYoung B, Heymans JJ, Hounkpé J, Jackson LC, Lamont T, Lee S-K, Perez RC, Sams C, Snowden J, Zinkann A-C. 2024. Social and economic impacts of changes in the Atlantic Meridional Overturning Circulation. *Ocean Sciences Meeting, New Orleans, Louisiana, USA, 18–23 February 2024.*
- Huggett JA. 2024. Ocean observations off Southern Africa and priorities for the Indian Ocean. Challenge: 7 Expand the Global Ocean Observing System. *Indian Ocean Regional Decade Conference 2024: Bridging Billions to Barcelona, Hyderabad, India, 1–3 February 2024.*
- Huggett JA. 2024. Overview of SIBER and WIOMSA. *IOCINDIO-led Special Session: Synergizing Regional Frameworks of the IOR. Indian Ocean Regional Decade Conference 2024: Bridging Billions to Barcelona, Hyderabad, India, 1–3 February 2024.*
- Huggett JA. 2024. South African activities in support of the IIOE-2. *7th Second International Indian Ocean Expedition (IIOE-2) Steering Committee meeting, International Indian Ocean Science Conference 2024, Lombok, Indonesia, 4–8 March 2024.*
- Huggett JA, Groeneveld J, Govender A. 2024. Zooplankton Metabarcoding Initiatives in South Africa. *Scientific Committee on Oceanic Research Working Group (SCOR WG) 157 MetaZooGene 2024 Annual meeting, Hobart, Australia, 20 March 2024.*
- Huggett J, Lamont T, Carstensen J, Jakobsen HJ, Møller EF, Coetzee J. 2024. Eat, prey, love: can functional traits provide insight into bottom-up vs top-down forcing and long-term distribution patterns of copepods on the Agulhas Bank? *International Council for the Exploration of the Sea and the North Pacific Marine Science Organization (ICES-PICES) 7th International Zooplankton Production Symposium, Hobart, Tasmania, Australia, 17–22 March 2024.*
- Huggett J, Mdluli N, du Preez S. 2024. Zooplankton sampling near the Prince Edward Islands - past, present and future initiatives. *Hobart 2024 workshop on WP1.3. The Pelagic realm of the subantarctic Indian and Southern Indian Ocean, Hobart, Australia, 25–26 March 2024.*
- Huggett J, Worship M. 2024. CPR surveys in the Indian subantarctic south of Africa. *Hobart 2024 workshop on WP1.3. The Pelagic realm of the subantarctic Indian and Southern Indian Ocean, Hobart, Australia, 25–26 March 2024.*
- Janson L, Haupt T, Auerswald L. 2024. Exploring the microhabitats of the Cape urchin, *Parechinus angulosus*. *7th International Marine Conservation Congress (IMCC7), Cape Town International Convention Centre, Cape Town, South Africa, 13–18 October 2024.*
- Lamont T, Halo I, Russo CS. 2024. Agulhas Current meanders redistribute Intermediate waters along the South African southeast coast. *Ocean Sciences Meeting, New Orleans, Louisiana, USA, 18–23 February 2024.*
- Lamont T, Russo CS. 2024. From LACCE to WBC TRACCE: Tracking Current Core and Edges. *Agulhas Current Observing System Design Workshop, The President Hotel, Bantry Bay, Cape Town, 9–12 September 2024.*
- Lamont T, van den Berg MA, Louw G, Dong S, Speich S, Ansorge I. 2024. GoodHope and CrossRoads transects – status and plans. *10th South Atlantic Meridional Overturning (SAMOC) Workshop, Online, 21–22 May 2024.*

OUTPUTS FOR 2024

- Lamont T, van den Berg MA, Louw G, Jacobs L, Russo CS, Perez R, Dong S, Speich S, Ansorge I. 2024. South Atlantic Meridional Overturning Circulation Basin-wide Array – status and plans. *10th South Atlantic Meridional Overturning (SAMOC) Workshop, Online, 21–22 May 2024.*
- Mdluli N, Carrasco N, Huggett J, Harris S, Lombard AT. 2024. Zooplankton assemblages associated with submarine canyons off the east coast of South Africa. *International Council for the Exploration of the Sea and the North Pacific Marine Science Organization (ICES-PICES) 7th International Zooplankton Production Symposium, Hobart, Tasmania, Australia, 17–22 March 2024.*
- Muxagata E, Bruneta M, Esquivel-Garrote O, Gregory L., Huggett J, Inck C, Worship M, Johns DG. 2024. Progress & challenges of CPR data analysis in the context of AtlantECO. *Atlantic Ecosystems Assessment, Forecasting & Sustainability (AtlantECO) General Assembly 2024 (GA24), Vigo, Spain, 16–21 September 2024.*
- Nkadimeng TN, Lamont T, Ansorge I, Halo I, Russo CS. 2024. Eddy variability in the southeast Atlantic Ocean: A comparison of the northern and southern Benguela eddy fields. *Nansen-Tutu Centre Science Day and Students Symposium, All Africa House, University of Cape Town, Cape Town, South Africa, 6 November 2024.*
- Russo CS, Lamont T. 2024. Investigating variability in the Agulhas Current System using the LACCE monitoring tool. *Ocean Sciences Meeting, New Orleans, Louisiana, USA, 18–23 February 2024.*
- Russo CS, Lamont T, Halo I. 2024. Monitoring variability of Western Boundary Currents and their impact on adjacent coastlines. *7th International Marine Conservation Congress (IMCC7), Cape Town International Convention Centre, Cape Town, South Africa, 13–18 October 2024.*
- Swart L, Nemanashe E. 2024. Galjoen catch per unit effort and dispersal between exploited and unexploited zones of the Table Mountain National Park MPA. *6th Southern African Marine Linefish Symposium, Mpekweni Beach Resort, Eastern Cape, South Africa, 19–23 August 2024.*
- van den Berg MA, Lamont T. 2024. Long-term hydrographic variability on the Prince Edward Islands shelf in the Southern Ocean. *Ocean Sciences Meeting, New Orleans, Louisiana, USA, 18–23 February 2024.*
- Anders D, Frantz F, Jacobs L, van den Berg M, Lamont T. 2024. Raw underway Thermosalinograph (TSG) observations from the South Atlantic Meridional Overturning Circulation Basin-wide Array (SAMBA) on Algoa Voyage 265, September 2019. DFFE. doi: [10.15493/DEA.MIMS.13492023](https://doi.org/10.15493/DEA.MIMS.13492023).
- Anders D, Jacobs L, van den Berg MA, Lamont T. 2024. Processed underway Thermosalinograph (TSG) observations from the Integrated Ecosystem Programme: Southern Benguela (IEP:SB) on Algoa Voyage 235, February 2017. DFFE. doi: [10.15493/DEA.MIMS.13362023](https://doi.org/10.15493/DEA.MIMS.13362023).
- Anders D, Jacobs L, van den Berg M, Lamont T. 2024. Raw underway Thermosalinograph (TSG) observations from the Integrated Ecosystem Programme: Southern Benguela (IEP:SB) on Algoa Voyage 235, February 2017. DFFE. doi: [10.15493/DEA.MIMS.13372023](https://doi.org/10.15493/DEA.MIMS.13372023).
- Filander Z, Lamont T. 2024. Cape Canyon Benthic Invertebrates Tissue samples. DFFE. doi: [10.15493/DEA.MIMS.12642023](https://doi.org/10.15493/DEA.MIMS.12642023).
- Filander Z, Lamont T. 2024. Cape Canyon Suspended Particulate Matter CTD water sample. DFFE. doi: [10.15493/DEA.MIMS.12652023](https://doi.org/10.15493/DEA.MIMS.12652023).
- Haupt T, Janson L, Auerswald L. 2024. Raw seawater temperature data from intertidal rockpools in Elands Bay, 9 November 2022 to 13 March 2023. DFFE. doi: [10.15493/DEA.MIMS.13922023](https://doi.org/10.15493/DEA.MIMS.13922023).
- Haupt T, Janson L, Auerswald L. 2024. Seawater temperature data from intertidal rockpools in Elands Bay, 9 to 30 November 2022. DFFE. doi: [10.15493/DEA.MIMS.13932023](https://doi.org/10.15493/DEA.MIMS.13932023).
- Haupt T, Janson L, Auerswald L. 2024. Seawater temperature data from intertidal rockpools in Elands Bay, 1 to 31 December 2022. DFFE. doi: [10.15493/DEA.MIMS.13942023](https://doi.org/10.15493/DEA.MIMS.13942023).
- Haupt T, Janson L, Auerswald L. 2024. Seawater temperature data from intertidal rockpools in Elands Bay, 1 to 31 January 2023. DFFE. doi: [10.15493/DEA.MIMS.13952023](https://doi.org/10.15493/DEA.MIMS.13952023).
- Haupt T, Janson L, Auerswald L. 2024. Seawater temperature data from intertidal rockpools in Elands Bay, 1 to 28 February 2023. DFFE. doi: [10.15493/DEA.MIMS.13962023](https://doi.org/10.15493/DEA.MIMS.13962023).
- Haupt T, Janson L, Auerswald L. 2024. Seawater temperature data from intertidal rockpools in Elands Bay, 1 to 31 March 2023. DFFE. doi: [10.15493/DEA.MIMS.13972023](https://doi.org/10.15493/DEA.MIMS.13972023).
- Haupt T, Janson L, Auerswald L. 2024. Raw temperature data from an exposed habitat in Elands Bay, 8 November 2022 to 13 March 2023. DFFE. doi: [10.15493/DEA.MIMS.13982023](https://doi.org/10.15493/DEA.MIMS.13982023).
- Haupt T, Janson L, Auerswald L. 2024. Temperature data from an exposed habitat in Elands Bay, 11 to 30 November 2022. DFFE. doi: [10.15493/DEA.MIMS.13992023](https://doi.org/10.15493/DEA.MIMS.13992023).
- Haupt T, Janson L, Auerswald L. 2024. Temperature data from an exposed habitat in Elands Bay, 1 to 31 December 2022. DFFE. doi: [10.15493/DEA.MIMS.14002023](https://doi.org/10.15493/DEA.MIMS.14002023).
- Haupt T, Janson L, Auerswald L. 2024. Temperature data

PUBLISHED DATASETS

- Anders D, Frantz F, Jacobs L, van den Berg M, Lamont T. 2024. Processed underway Thermosalinograph (TSG) observations from the South Atlantic Meridional Overturning Circulation Basin-wide Array (SAMBA) on Algoa Voyage 265, September 2019. DFFE. doi: [10.15493/DEA.MIMS.13482023](https://doi.org/10.15493/DEA.MIMS.13482023).

OUTPUTS FOR 2024

- from an exposed habitat in Elands Bay, 1 to 31 January 2023. DFFE. doi: [10.15493/DEA.MIMS.14012023](https://doi.org/10.15493/DEA.MIMS.14012023).
- Haupt T, Janson L, Auerswald L. 2024. Temperature data from an exposed habitat in Elands Bay, 1 to 28 February 2023. DFFE. doi: [10.15493/DEA.MIMS.14022023](https://doi.org/10.15493/DEA.MIMS.14022023).
- Haupt T, Janson L, Auerswald L. 2024. Temperature data from an exposed habitat in Elands Bay, 1 to 31 March 2023. DFFE. doi: [10.15493/DEA.MIMS.14032023](https://doi.org/10.15493/DEA.MIMS.14032023).
- Haupt T, Janson L, Auerswald L. 2024. Raw seawater temperature data from intertidal rockpools in Elands Bay, 13 March to 5 June 2023. DFFE. doi: [10.15493/DEA.MIMS.14042023](https://doi.org/10.15493/DEA.MIMS.14042023).
- Haupt T, Janson L, Auerswald L. 2024. Seawater temperature data from intertidal rockpools in Elands Bay, 1 to 30 April 2023. DFFE. doi: [10.15493/DEA.MIMS.14062023](https://doi.org/10.15493/DEA.MIMS.14062023).
- Haupt T, Janson L, Auerswald L. 2024. Seawater temperature data from intertidal rockpools in Elands Bay, 1 to 31 May 2023. DFFE. doi: [10.15493/DEA.MIMS.14072023](https://doi.org/10.15493/DEA.MIMS.14072023).
- Haupt T, Janson L, Auerswald L. 2024. Seawater temperature data from intertidal rockpools in Elands Bay, 1 to 30 June 2023. DFFE. doi: [10.15493/DEA.MIMS.14082023](https://doi.org/10.15493/DEA.MIMS.14082023).
- Haupt T, Janson L, Auerswald L. 2024. Raw temperature data from an exposed habitat in Elands Bay, 14 March to 5 June 2023. DFFE. doi: [10.15493/DEA.MIMS.14092023](https://doi.org/10.15493/DEA.MIMS.14092023).
- Haupt T, Janson L, Auerswald L. 2024. Temperature data from an exposed habitat in Elands Bay, 1 to 30 April 2023. DFFE. doi: [10.15493/DEA.MIMS.14112023](https://doi.org/10.15493/DEA.MIMS.14112023).
- Haupt T, Janson L, Auerswald L. 2024. Temperature data from an exposed habitat in Elands Bay, 1 to 31 May 2023. DFFE. doi: [10.15493/DEA.MIMS.14122023](https://doi.org/10.15493/DEA.MIMS.14122023).
- Haupt T, Janson L, Auerswald L. 2024. Temperature data from an exposed habitat in Elands Bay, 1 to 30 June 2023. DFFE. doi: [10.15493/DEA.MIMS.14142023](https://doi.org/10.15493/DEA.MIMS.14142023).
- Haupt T, Janson L, Auerswald L. 2024. Raw seawater temperature data from intertidal rockpools in Elands Bay, 5 June to 18 October 2023. DFFE. doi: [10.15493/DEA.MIMS.14152023](https://doi.org/10.15493/DEA.MIMS.14152023).
- Haupt T, Janson L, Auerswald L. 2024. Seawater temperature data from intertidal rockpools in Elands Bay, 1 to 31 July 2023. DFFE. doi: [10.15493/DEA.MIMS.14172023](https://doi.org/10.15493/DEA.MIMS.14172023).
- Haupt T, Janson L, Auerswald L. 2024. Seawater temperature data from intertidal rockpools in Elands Bay, 1 to 31 August 2023. DFFE. doi: [10.15493/DEA.MIMS.14182023](https://doi.org/10.15493/DEA.MIMS.14182023).
- Haupt T, Janson L, Auerswald L. 2024. Seawater temperature data from intertidal rockpools in Elands Bay, 1 to 30 September 2023. DFFE. doi: [10.15493/DEA.MIMS.14192023](https://doi.org/10.15493/DEA.MIMS.14192023).
- Haupt T, Janson L, Auerswald L. 2024. Seawater temperature data from intertidal rockpools in Elands Bay, 1 to 31 October 2023. DFFE. doi: [10.15493/DEA.MIMS.14202023](https://doi.org/10.15493/DEA.MIMS.14202023).
- Haupt T, Janson L, Auerswald L. 2024. Raw temperature data from an exposed habitat in Elands Bay, 5 June to 18 October 2023. DFFE. doi: [10.15493/DEA.MIMS.14212023](https://doi.org/10.15493/DEA.MIMS.14212023).
- Haupt T, Janson L, Auerswald L. 2024. Temperature data from an exposed habitat in Elands Bay, 1 to 31 July 2023. DFFE. doi: [10.15493/DEA.MIMS.14232023](https://doi.org/10.15493/DEA.MIMS.14232023).
- Haupt T, Janson L, Auerswald L. 2024. Temperature data from an exposed habitat in Elands Bay, 1 to 31 August 2023. DFFE. doi: [10.15493/DEA.MIMS.14242023](https://doi.org/10.15493/DEA.MIMS.14242023).
- Haupt T, Janson L, Auerswald L. 2024. Temperature data from an exposed habitat in Elands Bay, 1 to 30 September 2023. DFFE. doi: [10.15493/DEA.MIMS.14252023](https://doi.org/10.15493/DEA.MIMS.14252023).
- Haupt T, Janson L, Auerswald L. 2024. Temperature data from an exposed habitat in Elands Bay, 1 to 31 October 2023. DFFE. doi: [10.15493/DEA.MIMS.14262023](https://doi.org/10.15493/DEA.MIMS.14262023).
- Haupt T, Janson L, Auerswald L. 2024. Raw seawater temperature data from a subtidal habitat in Elands Bay, 5 June to 18 October 2023. DFFE. doi: [10.15493/DEA.MIMS.14272023](https://doi.org/10.15493/DEA.MIMS.14272023).
- Haupt T, Janson L, Auerswald L. 2024. Seawater temperature data from a subtidal habitat in Elands Bay, 5 to 30 June 2023. DFFE. doi: [10.15493/DEA.MIMS.14282023](https://doi.org/10.15493/DEA.MIMS.14282023).
- Haupt T, Janson L, Auerswald L. 2024. Seawater temperature data from a subtidal habitat in Elands Bay, 1 to 31 July 2023. DFFE. doi: [10.15493/DEA.MIMS.14292023](https://doi.org/10.15493/DEA.MIMS.14292023).
- Haupt T, Janson L, Auerswald L. 2024. Seawater temperature data from a subtidal habitat in Elands Bay, 1 to 31 August 2023. DFFE. doi: [10.15493/DEA.MIMS.14302023](https://doi.org/10.15493/DEA.MIMS.14302023).
- Haupt T, Janson L, Auerswald L. 2024. Seawater temperature data from a subtidal habitat in Elands Bay, 1 to 30 September 2023. DFFE. doi: [10.15493/DEA.MIMS.14312023](https://doi.org/10.15493/DEA.MIMS.14312023).
- Haupt T, Janson L, Auerswald L. 2024. Seawater temperature data from a subtidal habitat in Elands Bay, 1 to 31 October 2023. DFFE. doi: [10.15493/DEA.MIMS.14322023](https://doi.org/10.15493/DEA.MIMS.14322023).
- Haupt T, Janson L, Auerswald L, Williamson R. 2024. Raw seawater temperature data from intertidal rockpools in Elands Bay, 18 October 2023 to 13 February 2024. DFFE. doi: [10.15493/DEA.MIMS.14332023](https://doi.org/10.15493/DEA.MIMS.14332023).
- Haupt T, Janson L, Auerswald L, Williamson R. 2024. Seawater temperature data from intertidal rockpools in Elands Bay, 1 to 30 November 2023. DFFE. doi: [10.15493/DEA.MIMS.14352023](https://doi.org/10.15493/DEA.MIMS.14352023).
- Haupt T, Janson L, Auerswald L, Williamson R. 2024. Seawater temperature data from intertidal rockpools in Elands Bay, 1 to 31 December 2023. DFFE. doi: [10.15493/DEA.MIMS.14362023](https://doi.org/10.15493/DEA.MIMS.14362023).
- Haupt T, Janson L, Auerswald L, Williamson R. 2024. Seawater temperature data from intertidal rockpools in Elands Bay, 1 to 31 January 2024. DFFE. doi: [10.15493/DEA.MIMS.14372023](https://doi.org/10.15493/DEA.MIMS.14372023).

OUTPUTS FOR 2024

- Haupt T, Janson L, Auerswald L, Williamson R. 2024. Seawater temperature data from intertidal rockpools in Elands Bay, 1 to 13 February 2024. DFFE. doi: [10.15493/DEA.MIMS.14382023](https://doi.org/10.15493/DEA.MIMS.14382023).
- Haupt T, Janson L, Auerswald L, Williamson R. 2024. Raw temperature data from an exposed habitat in Elands Bay, 18 October 2023 to 13 February 2024. DFFE. doi: [10.15493/DEA.MIMS.14392023](https://doi.org/10.15493/DEA.MIMS.14392023).
- Haupt T, Janson L, Auerswald L, Williamson R. 2024. Temperature data from an exposed habitat in Elands Bay, 1 to 30 November 2023. DFFE. doi: [10.15493/DEA.MIMS.14412023](https://doi.org/10.15493/DEA.MIMS.14412023).
- Haupt T, Janson L, Auerswald L, Williamson R. 2024. Temperature data from an exposed habitat in Elands Bay, 1 to 31 December 2023. DFFE. doi: [10.15493/DEA.MIMS.14422023](https://doi.org/10.15493/DEA.MIMS.14422023).
- Haupt T, Janson L, Auerswald L, Williamson R. 2024. Temperature data from an exposed habitat in Elands Bay, 1 to 31 January 2024. DFFE. doi: [10.15493/DEA.MIMS.14432023](https://doi.org/10.15493/DEA.MIMS.14432023).
- Haupt T, Janson L, Auerswald L, Williamson R. 2024. Temperature data from an exposed habitat in Elands Bay, 1 to 13 February 2024. DFFE. doi: [10.15493/DEA.MIMS.14442023](https://doi.org/10.15493/DEA.MIMS.14442023).
- Haupt T, Janson L, Auerswald L, Williamson R. 2024. Raw seawater temperature data from a subtidal habitat in Elands Bay, 18 October 2023 to 13 February 2024. DFFE. doi: [10.15493/DEA.MIMS.14452023](https://doi.org/10.15493/DEA.MIMS.14452023).
- Haupt T, Janson L, Auerswald L, Williamson R. 2024. Seawater temperature data from a subtidal habitat in Elands Bay, 1 to 30 November 2023. DFFE. doi: [10.15493/DEA.MIMS.14472023](https://doi.org/10.15493/DEA.MIMS.14472023).
- Haupt T, Janson L, Auerswald L, Williamson R. 2024. Seawater temperature data from a subtidal habitat in Elands Bay, 1 to 31 December 2023. DFFE. doi: [10.15493/DEA.MIMS.14482023](https://doi.org/10.15493/DEA.MIMS.14482023).
- Haupt T, Janson L, Auerswald L, Williamson R. 2024. Seawater temperature data from a subtidal habitat in Elands Bay, 1 to 31 January 2024. DFFE. doi: [10.15493/DEA.MIMS.14492023](https://doi.org/10.15493/DEA.MIMS.14492023).
- Haupt T, Janson L, Auerswald L, Williamson R. 2024. Seawater temperature data from a subtidal habitat in Elands Bay, 1 to 13 February 2024. DFFE. doi: [10.15493/DEA.MIMS.14502023](https://doi.org/10.15493/DEA.MIMS.14502023).
- Haupt T, Janson L, Williamson R, Auerswald L. 2024. Long-term monitoring of inshore temperatures in Elands Bay to support physiological research. DFFE. doi: [10.15493/DEA.MIMS.13912023](https://doi.org/10.15493/DEA.MIMS.13912023).
- Haupt T, Snyders L, Samaai T, Janson L, Parker D, Williams L. 2024. Benthic invertebrate fauna, associated habitats and potential factors influencing their distribution and abundance in the Southern Benguela Ecoregion, Algoa Voyage 263, August 2019. DFFE. doi: [10.15493/DEA.MIMS.200521-1](https://doi.org/10.15493/DEA.MIMS.200521-1).
- Ismail H, van den Berg MA, Lamont T. 2024. Raw temperature data for long-term observations of bottom temperatures at Ystervarkpunt (August 2022 - December 2023). DFFE. doi: [10.15493/DEA.MIMS.03062024](https://doi.org/10.15493/DEA.MIMS.03062024).
- Ismail H., van den Berg MA, Lamont T. 2024. Long-term observations of hourly bottom temperatures at Ystervarkpunt (August 2022 - December 2023). DFFE. doi: [10.15493/DEA.MIMS.03052024](https://doi.org/10.15493/DEA.MIMS.03052024).
- Ismail H, van den Berg MA, Lamont T. 2024. Raw temperature data for long-term observations of bottom temperatures at Sodwana Bay (August 2022 - February 2023). DFFE. doi: [10.15493/DEA.MIMS.05082024](https://doi.org/10.15493/DEA.MIMS.05082024).
- Ismail H, van den Berg MA, Lamont T. 2024. Raw temperature data for long-term observations of bottom temperatures at Sodwana Bay (February 2023 - November 2023). DFFE. doi: [10.15493/DEA.MIMS.05102024](https://doi.org/10.15493/DEA.MIMS.05102024).
- Ismail H, van den Berg MA, Lamont T. 2024. Long-term observations of hourly bottom temperatures at Sodwana Bay (August 2022 - February 2023). DFFE. doi: [10.15493/DEA.MIMS.05072024](https://doi.org/10.15493/DEA.MIMS.05072024).
- Ismail H, van den Berg MA, Lamont T. 2024. Long-term observations of hourly bottom temperatures at Sodwana Bay (February 2023 - November 2023). DFFE. doi: [10.15493/DEA.MIMS.05092024](https://doi.org/10.15493/DEA.MIMS.05092024).
- Ismail H, van den Berg MA, Lamont T. 2024. Raw temperature data for long-term observations of bottom temperatures at North East Madagascar (February 2012 - April 2013). DFFE. doi: [10.15493/DEA.MIMS.61072024](https://doi.org/10.15493/DEA.MIMS.61072024).
- Ismail H, van den Berg MA, Lamont T. 2024. Long-term observations of hourly bottom temperatures at North East Madagascar (February 2012 - April 2013). DFFE. doi: [10.15493/DEA.MIMS.60072024](https://doi.org/10.15493/DEA.MIMS.60072024).
- Ismail H, van den Berg MA, Lamont T. 2024. Raw temperature data for long-term observations of bottom temperatures at Seychelles site A (December 2003 - April 2004). DFFE. doi: [10.15493/DEA.MIMS.73072024](https://doi.org/10.15493/DEA.MIMS.73072024).
- Ismail H, van den Berg MA, Lamont T. 2024. Long-term observations of hourly bottom temperatures at Seychelles site A (December 2003 - April 2004). DFFE. doi: [10.15493/DEA.MIMS.72072024](https://doi.org/10.15493/DEA.MIMS.72072024).
- Ismail H, van den Berg MA, Lamont T. 2024. Raw temperature data for long-term observations of bottom temperatures at Seychelles site B (December 2003 - April 2004). DFFE. doi: [10.15493/DEA.MIMS.75072024](https://doi.org/10.15493/DEA.MIMS.75072024).
- Ismail H, van den Berg MA, Lamont T. 2024. Raw temperature data for long-term observations of bottom temperatures at Seychelles site B (April 2004 - July 2004). DFFE. doi: [10.15493/DEA.MIMS.77072024](https://doi.org/10.15493/DEA.MIMS.77072024).
- Ismail H, van den Berg MA, Lamont T. 2024. Long-term observations of hourly bottom temperatures at Seychelles site B (December 2003 - April 2004). DFFE. doi: [10.15493/DEA.MIMS.74072024](https://doi.org/10.15493/DEA.MIMS.74072024).
- Ismail H, van den Berg MA, Lamont T. 2024. Long-term observations of hourly bottom temperatures at Seychelles site B (April 2004 - July 2004). DFFE. doi: [10.15493/DEA.MIMS.76072024](https://doi.org/10.15493/DEA.MIMS.76072024).
- Ismail H, van den Berg MA, Lamont T. 2024. Raw temperature data for long-term observations of bottom temperatures off Trou-aux-Biches, Mauritius (March 2014 - November 2016). DFFE. doi: [10.15493/DEA.MIMS.26112024](https://doi.org/10.15493/DEA.MIMS.26112024).

OUTPUTS FOR 2024

- Ismail H, van den Berg MA, Lamont T. 2024. Long-term observations of hourly bottom temperatures off Trou- aux- Biches, Mauritius (March 2014 - November 2016). DFFE. doi: [10.15493/DEA.MIMS.25112024](https://doi.org/10.15493/DEA.MIMS.25112024).
- Ismail H, van den Berg MA, Lamont T. 2024. Raw temperature data for long-term observations of bottom temperatures at Moheli, Comoros (September 2004 - October 2007). DFFE. doi: [10.15493/DEA.MIMS.28112024](https://doi.org/10.15493/DEA.MIMS.28112024).
- Ismail H, van den Berg MA, Lamont T. 2024. Long-term observations of hourly bottom temperatures at Moheli, Comoros (September 2004 - October 2007). DFFE. doi: [10.15493/DEA.MIMS.27112024](https://doi.org/10.15493/DEA.MIMS.27112024).
- Ismail H, van den Berg MA, Lamont T. 2024. Raw temperature data for long-term observations of Bottom Temperatures at Knysna (March 1995 - July 1995). DFFE. doi: [10.15493/DEA.MIMS.50112024](https://doi.org/10.15493/DEA.MIMS.50112024).
- Ismail H, van den Berg MA, Lamont T. 2024. Raw temperature data for long-term observations of Bottom Temperatures at Knysna (July 1995 - October 1995). DFFE. doi: [10.15493/DEA.MIMS.52112024](https://doi.org/10.15493/DEA.MIMS.52112024).
- Ismail H, van den Berg MA, Lamont T. 2024. Raw temperature data for long-term observations of Bottom Temperatures at Knysna (October 1995 - April 1996). DFFE. doi: [10.15493/DEA.MIMS.54112024](https://doi.org/10.15493/DEA.MIMS.54112024).
- Ismail H, van den Berg MA, Lamont T. 2024. Raw temperature data for long-term observations of Bottom Temperatures at Knysna (April 1996 - August 1996). DFFE. doi: [10.15493/DEA.MIMS.56112024](https://doi.org/10.15493/DEA.MIMS.56112024).
- Ismail H, van den Berg MA, Lamont T. 2024. Raw temperature data for long-term observations of Bottom Temperatures at Knysna (August 1996 - November 1996). DFFE. doi: [10.15493/DEA.MIMS.58112024](https://doi.org/10.15493/DEA.MIMS.58112024).
- Ismail H, van den Berg MA, Lamont T. 2024. Raw temperature data for long-term observations of Bottom Temperatures at Knysna (November 1996 - March 1997). DFFE. doi: [10.15493/DEA.MIMS.60112024](https://doi.org/10.15493/DEA.MIMS.60112024).
- Ismail H, van den Berg MA, Lamont T. 2024. Raw temperature data for long-term observations of Bottom Temperatures at Knysna (March 1997 - July 1997). DFFE. doi: [10.15493/DEA.MIMS.62112024](https://doi.org/10.15493/DEA.MIMS.62112024).
- Ismail H, van den Berg MA, Lamont T. 2024. Raw temperature data for long-term observations of Bottom Temperatures at Knysna (July 1997 - January 1998). DFFE. doi: [10.15493/DEA.MIMS.64112024](https://doi.org/10.15493/DEA.MIMS.64112024).
- Ismail H, van den Berg MA, Lamont T. 2024. Raw temperature data for long-term observations of Bottom Temperatures at Knysna (January 1998 - July 1998). DFFE. doi: [10.15493/DEA.MIMS.66112024](https://doi.org/10.15493/DEA.MIMS.66112024).
- Ismail H, van den Berg MA, Lamont T. 2024. Raw temperature data for long-term observations of Bottom Temperatures at Knysna (July 1998 - November 1998). DFFE. doi: [10.15493/DEA.MIMS.68112024](https://doi.org/10.15493/DEA.MIMS.68112024).
- Ismail H, van den Berg MA, Lamont T. 2024. Raw temperature data for long-term observations of Bottom Temperatures at Knysna (November 1998 - March 1999). DFFE. doi: [10.15493/DEA.MIMS.70112024](https://doi.org/10.15493/DEA.MIMS.70112024).
- Ismail H, van den Berg MA, Lamont T. 2024. Raw temperature data for long-term observations of Bottom Temperatures at Knysna (March 1999 - July 1999). DFFE. doi: [10.15493/DEA.MIMS.72112024](https://doi.org/10.15493/DEA.MIMS.72112024).
- Ismail H, van den Berg MA, Lamont T. 2024. Raw temperature data for long-term observations of Bottom Temperatures at Knysna (July 1999 - November 1999). DFFE. doi: [10.15493/DEA.MIMS.74112024](https://doi.org/10.15493/DEA.MIMS.74112024).
- Ismail H, van den Berg MA, Lamont T. 2024. Raw temperature data for long-term observations of Bottom Temperatures at Knysna (November 1999 - April 2000). DFFE. doi: [10.15493/DEA.MIMS.76112024](https://doi.org/10.15493/DEA.MIMS.76112024).
- Ismail H, van den Berg MA, Lamont T. 2024. Raw temperature data for long-term observations of Bottom Temperatures at Knysna (August 2000 - November 2000). DFFE. doi: [10.15493/DEA.MIMS.78112024](https://doi.org/10.15493/DEA.MIMS.78112024).
- Ismail H, van den Berg MA, Lamont T. 2024. Raw temperature data for long-term observations of Bottom Temperatures at Knysna (November 2000 - March 2001). DFFE. doi: [10.15493/DEA.MIMS.80112024](https://doi.org/10.15493/DEA.MIMS.80112024).
- Ismail H, van den Berg MA, Lamont T. 2024. Raw temperature data for long-term observations of Bottom Temperatures at Knysna (March 2001 - July 2001). DFFE. doi: [10.15493/DEA.MIMS.82112024](https://doi.org/10.15493/DEA.MIMS.82112024).
- Ismail H, van den Berg MA, Lamont T. 2024. Raw temperature data for long-term observations of Bottom Temperatures at Knysna (July 2001 - November 2001). DFFE. doi: [10.15493/DEA.MIMS.84112024](https://doi.org/10.15493/DEA.MIMS.84112024).
- Ismail H, van den Berg MA, Lamont T. 2024. Raw temperature data for long-term observations of Bottom Temperatures at Knysna (November 2001 - June 2002). DFFE. doi: [10.15493/DEA.MIMS.86112024](https://doi.org/10.15493/DEA.MIMS.86112024).
- Ismail H, van den Berg MA, Lamont T. 2024. Raw temperature data for long-term observations of Bottom Temperatures at Knysna (June 2002 - November 2002). DFFE. doi: [10.15493/DEA.MIMS.88112024](https://doi.org/10.15493/DEA.MIMS.88112024).
- Ismail H, van den Berg MA, Lamont T. 2024. Raw temperature data for long-term observations of Bottom Temperatures at Knysna (November 2002 - November 2003). DFFE. doi: [10.15493/DEA.MIMS.90112024](https://doi.org/10.15493/DEA.MIMS.90112024).
- Ismail H, van den Berg MA, Lamont T. 2024. Raw temperature data for long-term observations of Bottom Temperatures at Knysna (November 2003 - June 2004). DFFE. doi: [10.15493/DEA.MIMS.92112024](https://doi.org/10.15493/DEA.MIMS.92112024).
- Ismail H, van den Berg MA, Lamont T. 2024. Raw temperature data for long-term observations of Bottom Temperatures at Knysna (June 2004 - June 2005). DFFE. doi: [10.15493/DEA.MIMS.94112024](https://doi.org/10.15493/DEA.MIMS.94112024).
- Ismail H, van den Berg MA, Lamont T. 2024. Raw temperature data for long-term observations of Bottom Temperatures at Knysna (June 2005 - November 2005). DFFE. doi: [10.15493/DEA.MIMS.96112024](https://doi.org/10.15493/DEA.MIMS.96112024).
- Ismail H, van den Berg MA, Lamont T. 2024. Raw temperature data for long-term observations of Bottom Temperatures at Knysna (June 2006 - November 2006). DFFE. doi: [10.15493/DEA.MIMS.98112024](https://doi.org/10.15493/DEA.MIMS.98112024).

OUTPUTS FOR 2024

- Ismail H, van den Berg MA, Lamont T. 2024. Raw temperature data for long-term observations of Bottom Temperatures at Knysna (November 2006 - June 2007). DFFE. doi: [10.15493/DEA.MIMS.18122024](https://doi.org/10.15493/DEA.MIMS.18122024).
- Ismail H, van den Berg MA, Lamont T. 2024. Raw temperature data for long-term observations of Bottom Temperatures at Knysna (June 2007 - November 2007). DFFE. doi: [10.15493/DEA.MIMS.20122024](https://doi.org/10.15493/DEA.MIMS.20122024).
- Ismail H, van den Berg MA, Lamont T. 2024. Raw temperature data for long-term observations of Bottom Temperatures at Knysna (November 2007 - July 2008). DFFE. doi: [10.15493/DEA.MIMS.22122024](https://doi.org/10.15493/DEA.MIMS.22122024).
- Ismail H, van den Berg MA, Lamont T. 2024. Raw temperature data for long-term observations of Bottom Temperatures at Knysna (July 2008 - November 2008). DFFE. doi: [10.15493/DEA.MIMS.24122024](https://doi.org/10.15493/DEA.MIMS.24122024).
- Ismail H, van den Berg MA, Lamont T. 2024. Raw temperature data for long-term observations of Bottom Temperatures at Knysna (November 2008 - November 2009). DFFE. doi: [10.15493/DEA.MIMS.26122024](https://doi.org/10.15493/DEA.MIMS.26122024).
- Ismail H, van den Berg MA, Lamont T. 2024. Raw temperature data for long-term observations of Bottom Temperatures at Knysna (November 2014 - November 2015). DFFE. doi: [10.15493/DEA.MIMS.28122024](https://doi.org/10.15493/DEA.MIMS.28122024).
- Ismail H, van den Berg MA, Lamont T. 2024. Raw temperature data for long-term observations of Bottom Temperatures at Knysna (November 2015 - September 2019). DFFE. doi: [10.15493/DEA.MIMS.30122024](https://doi.org/10.15493/DEA.MIMS.30122024).
- Ismail H, van den Berg MA, Lamont T. 2024. Raw temperature data for long-term observations of Bottom Temperatures at Knysna (September 2019 - June 2022). DFFE. doi: [10.15493/DEA.MIMS.32122024](https://doi.org/10.15493/DEA.MIMS.32122024).
- Ismail H, van den Berg MA, Lamont T. 2024. Long-term observations of hourly Bottom Temperatures at Knysna (March 1995 - July 1995). DFFE. doi: [10.15493/DEA.MIMS.49112024](https://doi.org/10.15493/DEA.MIMS.49112024).
- Ismail H, van den Berg MA, Lamont T. 2024. Long-term observations of hourly Bottom Temperatures at Knysna (July 1995 - October 1995). DFFE. doi: [10.15493/DEA.MIMS.51112024](https://doi.org/10.15493/DEA.MIMS.51112024).
- Ismail H, van den Berg MA, Lamont T. 2024. Long-term observations of hourly Bottom Temperatures at Knysna (October 1995 - April 1996). DFFE. doi: [10.15493/DEA.MIMS.53112024](https://doi.org/10.15493/DEA.MIMS.53112024).
- Ismail H, van den Berg MA, Lamont T. 2024. Long-term observations of hourly Bottom Temperatures at Knysna (April 1996 - August 1996). DFFE. doi: [10.15493/DEA.MIMS.55112024](https://doi.org/10.15493/DEA.MIMS.55112024).
- Ismail H, van den Berg MA, Lamont T. 2024. Long-term observations of hourly Bottom Temperatures at Knysna (August 1996 - November 1996). DFFE. doi: [10.15493/DEA.MIMS.57112024](https://doi.org/10.15493/DEA.MIMS.57112024).
- Ismail H, van den Berg MA, Lamont T. 2024. Long-term observations of hourly Bottom Temperatures at Knysna (November 1996 - March 1997). DFFE. doi: [10.15493/DEA.MIMS.59112024](https://doi.org/10.15493/DEA.MIMS.59112024).
- Ismail H, van den Berg MA, Lamont T. 2024. Long-term observations of hourly Bottom Temperatures at Knysna (March 1997 - July 1997). DFFE. doi: [10.15493/DEA.MIMS.61112024](https://doi.org/10.15493/DEA.MIMS.61112024).
- Ismail H, van den Berg MA, Lamont T. 2024. Long-term observations of hourly Bottom Temperatures at Knysna (July 1997 - January 1998). DFFE. doi: [10.15493/DEA.MIMS.63112024](https://doi.org/10.15493/DEA.MIMS.63112024).
- Ismail H, van den Berg MA, Lamont T. 2024. Long-term observations of hourly Bottom Temperatures at Knysna (January 1998 - July 1998). DFFE. doi: [10.15493/DEA.MIMS.65112024](https://doi.org/10.15493/DEA.MIMS.65112024).
- Ismail H, van den Berg MA, Lamont T. 2024. Long-term observations of hourly Bottom Temperatures at Knysna (July 1998 - November 1998). DFFE. doi: [10.15493/DEA.MIMS.67112024](https://doi.org/10.15493/DEA.MIMS.67112024).
- Ismail H, van den Berg MA, Lamont T. 2024. Long-term observations of hourly Bottom Temperatures at Knysna (November 1998 - March 1999). DFFE. doi: [10.15493/DEA.MIMS.69112024](https://doi.org/10.15493/DEA.MIMS.69112024).
- Ismail H, van den Berg MA, Lamont T. 2024. Long-term observations of hourly Bottom Temperatures at Knysna (March 1999 - July 1999). DFFE. doi: [10.15493/DEA.MIMS.71112024](https://doi.org/10.15493/DEA.MIMS.71112024).
- Ismail H, van den Berg MA, Lamont T. 2024. Long-term observations of hourly Bottom Temperatures at Knysna (July 1999 - November 1999). DFFE. doi: [10.15493/DEA.MIMS.73112024](https://doi.org/10.15493/DEA.MIMS.73112024).
- Ismail H, van den Berg MA, Lamont T. 2024. Long-term observations of hourly Bottom Temperatures at Knysna (November 1999 - April 2000). DFFE. doi: [10.15493/DEA.MIMS.75112024](https://doi.org/10.15493/DEA.MIMS.75112024).
- Ismail H, van den Berg MA, Lamont T. 2024. Long-term observations of hourly Bottom Temperatures at Knysna (August 2000 - November 2000). DFFE. doi: [10.15493/DEA.MIMS.77112024](https://doi.org/10.15493/DEA.MIMS.77112024).
- Ismail H, van den Berg MA, Lamont T. 2024. Long-term observations of hourly Bottom Temperatures at Knysna (November 2000 - March 2001). DFFE. doi: [10.15493/DEA.MIMS.79112024](https://doi.org/10.15493/DEA.MIMS.79112024).
- Ismail H, van den Berg MA, Lamont T. 2024. Long-term observations of hourly Bottom Temperatures at Knysna (March 2001 - July 2001). DFFE. doi: [10.15493/DEA.MIMS.81112024](https://doi.org/10.15493/DEA.MIMS.81112024).
- Ismail H, van den Berg MA, Lamont T. 2024. Long-term observations of hourly Bottom Temperatures at Knysna (July 2001 - November 2001). DFFE. doi: [10.15493/DEA.MIMS.83112024](https://doi.org/10.15493/DEA.MIMS.83112024).
- Ismail H, van den Berg MA, Lamont T. 2024. Long-term observations of hourly Bottom Temperatures at Knysna (November 2001 - June 2002). DFFE. doi: [10.15493/DEA.MIMS.85112024](https://doi.org/10.15493/DEA.MIMS.85112024).
- Ismail H, van den Berg MA, Lamont T. 2024. Long-term observations of hourly Bottom Temperatures at Knysna (June 2002 - November 2002). DFFE. doi: [10.15493/DEA.MIMS.87112024](https://doi.org/10.15493/DEA.MIMS.87112024).
- Ismail H, van den Berg MA, Lamont T. 2024. Long-term observations of hourly Bottom Temperatures at Knysna (November 2002 - November 2003). DFFE. doi: [10.15493/DEA.MIMS.89112024](https://doi.org/10.15493/DEA.MIMS.89112024).

OUTPUTS FOR 2024

- Ismail H, van den Berg MA, Lamont T. 2024. Long-term observations of hourly Bottom Temperatures at Knysna (November 2003 - June 2004). DFFE. doi: [10.15493/DEA.MIMS.9112024](https://doi.org/10.15493/DEA.MIMS.9112024).
- Ismail H, van den Berg MA, Lamont T. 2024. Long-term observations of hourly Bottom Temperatures at Knysna (June 2004 - June 2005). DFFE. doi: [10.15493/DEA.MIMS.93112024](https://doi.org/10.15493/DEA.MIMS.93112024).
- Ismail H, van den Berg MA, Lamont T. 2024. Long-term observations of hourly Bottom Temperatures at Knysna (June 2005 - November 2005). DFFE. doi: [10.15493/DEA.MIMS.95112024](https://doi.org/10.15493/DEA.MIMS.95112024).
- Ismail H, van den Berg MA, Lamont T. 2024. Long-term observations of hourly Bottom Temperatures at Knysna (June 2006 - November 2006). DFFE. doi: [10.15493/DEA.MIMS.97112024](https://doi.org/10.15493/DEA.MIMS.97112024).
- Ismail H, van den Berg MA, Lamont T. 2024. Long-term observations of hourly Bottom Temperatures at Knysna (November 2006 - June 2007). DFFE. doi: [10.15493/DEA.MIMS.99112024](https://doi.org/10.15493/DEA.MIMS.99112024).
- Ismail H, van den Berg MA, Lamont T. 2024. Long-term observations of hourly Bottom Temperatures at Knysna (June 2007 - November 2007). DFFE. doi: [10.15493/DEA.MIMS.19122024](https://doi.org/10.15493/DEA.MIMS.19122024).
- Ismail H, van den Berg MA, Lamont T. 2024. Long-term observations of hourly Bottom Temperatures at Knysna (November 2007 - July 2008). DFFE. doi: [10.15493/DEA.MIMS.21122024](https://doi.org/10.15493/DEA.MIMS.21122024).
- Ismail H, van den Berg MA, Lamont T. 2024. Long-term observations of hourly Bottom Temperatures at Knysna (July 2008 - November 2008). DFFE. doi: [10.15493/DEA.MIMS.23122024](https://doi.org/10.15493/DEA.MIMS.23122024).
- Ismail H, van den Berg MA, Lamont T. 2024. Long-term observations of hourly Bottom Temperatures at Knysna (November 2008 - November 2009). DFFE. doi: [10.15493/DEA.MIMS.25122024](https://doi.org/10.15493/DEA.MIMS.25122024).
- Ismail H, van den Berg MA, Lamont T. 2024. Long-term observations of hourly Bottom Temperatures at Knysna (November 2014 - November 2015). DFFE. doi: [10.15493/DEA.MIMS.27122024](https://doi.org/10.15493/DEA.MIMS.27122024).
- Ismail H, van den Berg MA, Lamont T. 2024. Long-term observations of hourly Bottom Temperatures at Knysna (November 2015 - September 2019). DFFE. doi: [10.15493/DEA.MIMS.29122024](https://doi.org/10.15493/DEA.MIMS.29122024).
- Ismail H, van den Berg MA, Lamont T. 2024. Long-term observations of hourly Bottom Temperatures at Knysna (September 2019 - June 2022). DFFE. doi: [10.15493/DEA.MIMS.31122024](https://doi.org/10.15493/DEA.MIMS.31122024).
- Jacobs L, Frantz F, van den Berg M, Lamont T. 2024. Processed underway Thermosalinograph (TSG) observations from the Integrated Ecosystem Programme: Southern Benguela (IEP:SB) on Algoa Voyage 242, August 2017. DFFE. doi: [10.15493/DEA.MIMS.13382023](https://doi.org/10.15493/DEA.MIMS.13382023).
- Jacobs L, Frantz F, van den Berg M, Lamont T. 2024. Raw underway Thermosalinograph (TSG) observations from the Integrated Ecosystem Programme: Southern Benguela (IEP:SB) on Algoa Voyage 244, November 2017. DFFE. doi: [10.15493/DEA.MIMS.13402023](https://doi.org/10.15493/DEA.MIMS.13402023).
- Jacobs L, Frantz F, van den Berg M, Lamont T. 2024. Raw underway Thermosalinograph (TSG) observations from the Integrated Ecosystem Programme: Southern Benguela (IEP:SB) on Algoa Voyage 244, November 2017. DFFE. doi: [10.15493/DEA.MIMS.13412023](https://doi.org/10.15493/DEA.MIMS.13412023).
- Jacobs L, Frantz F, van den Berg M, Lamont T. 2024. Processed underway Thermosalinograph (TSG) observations from the Integrated Ecosystem Programme: Southern Benguela (IEP:SB) on Algoa Voyage 246, February 2018. DFFE. doi: [10.15493/DEA.MIMS.13422023](https://doi.org/10.15493/DEA.MIMS.13422023).
- Jacobs L, Frantz F, van den Berg M, Lamont T. 2024. Raw underway Thermosalinograph (TSG) observations from the Integrated Ecosystem Programme: Southern Benguela (IEP:SB) on Algoa Voyage 246, February 2018. DFFE. doi: [10.15493/DEA.MIMS.13432023](https://doi.org/10.15493/DEA.MIMS.13432023).
- Jacobs L, Frantz F, van den Berg M, Lamont T. 2024. Processed underway Thermosalinograph (TSG) observations from the Cape Canyon Exploration Cruise on Algoa Voyage 247, March 2018. DFFE. doi: [10.15493/DEA.MIMS.13442023](https://doi.org/10.15493/DEA.MIMS.13442023).
- Jacobs L, Frantz F, van den Berg M, Lamont T. 2024. Raw underway Thermosalinograph (TSG) observations from the Cape Canyon Exploration Cruise on Algoa Voyage 247, March 2018. DFFE. doi: [10.15493/DEA.MIMS.13452023](https://doi.org/10.15493/DEA.MIMS.13452023).
- Jacobs L, Frantz F, van den Berg M, Lamont T. 2024. Processed underway Thermosalinograph (TSG) observations from the Integrated Ecosystem Programme: Southern Benguela (IEP:SB) on Algoa Voyage 248, May 2018. DFFE. doi: [10.15493/DEA.MIMS.13462023](https://doi.org/10.15493/DEA.MIMS.13462023).
- Jacobs L, Frantz F, van den Berg M, Lamont T. 2024. Raw underway Thermosalinograph (TSG) observations from the Integrated Ecosystem Programme: Southern Benguela (IEP:SB) on Algoa Voyage 248, May 2018. DFFE. doi: [10.15493/DEA.MIMS.13472023](https://doi.org/10.15493/DEA.MIMS.13472023).
- Jacobs L, van den Berg MA, Lamont T. 2024. Processed underway Thermosalinograph (TSG) observations from the South Atlantic Meridional Overturning Circulation Basin- wide Array (SAMBA) on Algoa Voyage 295, September 2023. DFFE. doi: [10.15493/DEA.MIMS.13502023](https://doi.org/10.15493/DEA.MIMS.13502023).
- Jacobs L, van den Berg MA, Lamont T. 2024. Raw underway Thermosalinograph (TSG) observations from the South Atlantic Meridional Overturning Circulation Basin- wide Array (SAMBA) on Algoa Voyage 295, September 2023. DFFE. doi: [10.15493/DEA.MIMS.13512023](https://doi.org/10.15493/DEA.MIMS.13512023).
- Jacobs L, van den Berg MA, Lamont T. 2024. Processed underway Thermosalinograph (TSG) observations from the SEAmester III and Agulhas System Climate Array (ASCA) Cruise on SA Agulhas II Voyage 033, July 2018. DFFE. doi: [10.15493/DEA.MIMS.13522023](https://doi.org/10.15493/DEA.MIMS.13522023).

OUTPUTS FOR 2024

- Jacobs L, van den Berg MA, Lamont T. 2024. Raw underway Thermosalinograph (TSG) observations from the SEAmester III and Agulhas System Climate Array (ASCA) Cruise on SA Agulhas II Voyage 033, July 2018. DFFE. doi: [10.15493/DEA.MIMS.13532023](https://doi.org/10.15493/DEA.MIMS.13532023).
- Jacobs L, van den Berg MA, Lamont T. 2024. Processed underway Thermosalinograph (TSG) observations from SA Agulhas II Voyage 034, September 2018. DFFE. doi: [10.15493/DEA.MIMS.13542023](https://doi.org/10.15493/DEA.MIMS.13542023).
- Jacobs L, van den Berg MA, Lamont T. 2024. Raw underway Thermosalinograph (TSG) observations from SA Agulhas II Voyage 034, September 2018. DFFE. doi: [10.15493/DEA.MIMS.13552023](https://doi.org/10.15493/DEA.MIMS.13552023).
- Jacobs L, van den Berg MA, Lamont T. 2024. Processed underway Thermosalinograph (TSG) observations from the Marion Island Relief Voyage on SA Agulhas II Voyage 057, April 2023. DFFE. doi: [10.15493/DEA.MIMS.13562023](https://doi.org/10.15493/DEA.MIMS.13562023).
- Jacobs L, van den Berg MA, Lamont T. 2024. Raw underway Thermosalinograph (TSG) observations from the Marion Island Relief Voyage on SA Agulhas II Voyage 057, April 2023. DFFE. doi: [10.15493/DEA.MIMS.13572023](https://doi.org/10.15493/DEA.MIMS.13572023).
- Jacobs L, van den Berg MA, Lamont T. 2024. Processed underway Thermosalinograph (TSG) observations from the SEAmester and Agulhas System Climate Array (ASCA) Cruise on SA Agulhas II Voyage 058, June 2023. DFFE. doi: [10.15493/DEA.MIMS.13582023](https://doi.org/10.15493/DEA.MIMS.13582023).
- Jacobs L, van den Berg MA, Lamont T. 2024. Raw underway Thermosalinograph (TSG) observations from the SEAmester and Agulhas System Climate Array (ASCA) Cruise on SA Agulhas II Voyage 058, June 2023. DFFE. doi: [10.15493/DEA.MIMS.13592023](https://doi.org/10.15493/DEA.MIMS.13592023).
- Jacobs L, van den Berg MA, Lamont T. 2024. Processed underway Thermosalinograph (TSG) observations from SA Agulhas II Voyage 059, September 2023. DFFE. doi: [10.15493/DEA.MIMS.13602023](https://doi.org/10.15493/DEA.MIMS.13602023).
- Jacobs L, van den Berg MA, Lamont T. 2024. Raw underway Thermosalinograph (TSG) observations from SA Agulhas II Voyage 059, September 2023. DFFE. doi: [10.15493/DEA.MIMS.13612023](https://doi.org/10.15493/DEA.MIMS.13612023).
- Jacobs L, van den Berg MA, Lamont T. 2024. Processed underway Thermosalinograph (TSG) observations from SA Agulhas II Voyage 060, November 2023. DFFE. doi: [10.15493/DEA.MIMS.13622023](https://doi.org/10.15493/DEA.MIMS.13622023).
- Jacobs L, van den Berg MA, Lamont T. 2024. Raw underway Thermosalinograph (TSG) observations from SA Agulhas II Voyage 060, November 2023. DFFE. doi: [10.15493/DEA.MIMS.13632023](https://doi.org/10.15493/DEA.MIMS.13632023).
- Lamont T. 2024. South Atlantic Meridional Overturning Circulation Basin-wide Array (SAMBA) Monitoring Line cruise on the Algoa Voyage 295, September 2023. DFFE. doi: [10.15493/DEA.MIMS.17042024](https://doi.org/10.15493/DEA.MIMS.17042024).
- Lamont T, Louw GS, van den Berg MA. 2024. Short-term observations of currents and sub-surface temperatures on the continental shelf and slope along the KwaZulu-Natal Bight, along the east coast of South Africa (project period 2009-2013). DFFE. doi: [10.15493/DEA.MIMS.78072024](https://doi.org/10.15493/DEA.MIMS.78072024).
- Lamont T, Louw GS, van den Berg MA, Perez RC, Dong S, Garcia R, Speich S, Meinen CS. 2024. Long-term observations of daily acoustic travel time along the SAMBA transect at PIES Mooring P1 (October 2021 - September 2023). DFFE. doi: [10.15493/DEA.MIMS.13822023](https://doi.org/10.15493/DEA.MIMS.13822023).
- Lamont T, Louw GS, van den Berg MA, Perez RC, Dong S, Garcia R, Speich S, Meinen CS. 2024. Long-term observations of daily acoustic travel time along the SAMBA transect at PIES Mooring P2 (October 2021 - September 2023). DFFE. doi: [10.15493/DEA.MIMS.13832023](https://doi.org/10.15493/DEA.MIMS.13832023).
- Lamont T, Louw GS, van den Berg MA, Perez RC, Dong S, Garcia R, Speich S, Meinen CS. 2024. Long-term observations of daily acoustic travel time along the SAMBA transect at PIES Mooring P3 (October 2021 - September 2023). DFFE. doi: [10.15493/DEA.MIMS.13842023](https://doi.org/10.15493/DEA.MIMS.13842023).
- Lamont T, Louw GS, van den Berg MA, Perez RC, Dong S, Garcia R, Speich S, Meinen CS. 2024. Long-term observations of daily acoustic travel time along the SAMBA transect at PIES Mooring P3a (October 2021 - September 2023). DFFE. doi: [10.15493/DEA.MIMS.13852023](https://doi.org/10.15493/DEA.MIMS.13852023).
- Lamont T, Louw GS, van den Berg MA, Perez RC, Dong S, Garcia R, Speich S, Meinen CS. 2024. Long-term observations of daily acoustic travel time along the SAMBA transect at PIES Mooring P4 (October 2021 - September 2023). DFFE. doi: [10.15493/DEA.MIMS.13862023](https://doi.org/10.15493/DEA.MIMS.13862023).
- Lamont T, Louw GS, van den Berg MA, Perez RC, Dong S, Garcia R, Speich S, Meinen CS. 2024. Long-term observations of daily acoustic travel time along the SAMBA transect at PIES Mooring P4a (September 2021 - September 2023). DFFE. doi: [10.15493/DEA.MIMS.13872023](https://doi.org/10.15493/DEA.MIMS.13872023).
- Lamont T, Louw GS, van den Berg MA, Perez RC, Dong S, Garcia R, Speich S, Meinen CS. 2024. Long-term observations of daily acoustic travel time along the SAMBA transect at PIES Mooring P5 (September 2021 - September 2023). DFFE. doi: [10.15493/DEA.MIMS.13882023](https://doi.org/10.15493/DEA.MIMS.13882023).
- Lamont T, Louw GS, van den Berg MA, Perez RC, Dong S, Garcia R, Speich S, Meinen CS. 2024. Long-term observations of daily acoustic travel time along the SAMBA transect at PIES Mooring P6 (September 2021 - September 2023). DFFE. doi: [10.15493/DEA.MIMS.13892023](https://doi.org/10.15493/DEA.MIMS.13892023).
- Lamont T, Louw GS, van den Berg MA, Perez RC, Dong S, Garcia R, Speich S, Meinen CS. 2024. Long-term observations of daily acoustic travel time along the SAMBA transect at PIES Mooring P8 (September 2021 - September 2023). DFFE. doi: [10.15493/DEA.MIMS.13902023](https://doi.org/10.15493/DEA.MIMS.13902023).
- Lamont T, Louw GS, van den Berg MA, Perez RC, Dong S, Garcia R, Speich S, Meinen CS. 2024. Raw PIES data for long-term observations of acoustic travel time (tau) and bottom pressure along the SAMBA transect at PIES P1 (October 2021 - September 2023). DFFE. doi: [10.15493/DEA.MIMS.13732023](https://doi.org/10.15493/DEA.MIMS.13732023).

OUTPUTS FOR 2024

- Lamont T, Louw GS, van den Berg MA, Perez RC, Dong S, Garcia R, Speich S, Meinen CS. 2024. Raw PIES data for long-term observations of acoustic travel time (τ) and bottom pressure along the SAMBA transect at PIES P2 (October 2021 - September 2023). DFFE. doi: [10.15493/DEA.MIMS.13742023](https://doi.org/10.15493/DEA.MIMS.13742023).
- Lamont T, Louw GS, van den Berg MA, Perez RC, Dong S, Garcia R, Speich S, Meinen CS. 2024. Raw PIES data for long-term observations of acoustic travel time (τ) and bottom pressure along the SAMBA transect at PIES P3 (October 2021 - September 2023). DFFE. doi: [10.15493/DEA.MIMS.13752023](https://doi.org/10.15493/DEA.MIMS.13752023).
- Lamont T, Louw GS, van den Berg MA, Perez RC, Dong S, Garcia R, Speich S, Meinen CS. 2024. Raw PIES data for long-term observations of acoustic travel time (τ) and bottom pressure along the SAMBA transect at PIES P3a (October 2021 - September 2023). DFFE. doi: [10.15493/DEA.MIMS.13762023](https://doi.org/10.15493/DEA.MIMS.13762023).
- Lamont T, Louw GS, van den Berg MA, Perez RC, Dong S, Garcia R, Speich S, Meinen CS. 2024. Raw PIES data for long-term observations of acoustic travel time (τ) and bottom pressure along the SAMBA transect at PIES P4 (October 2021 - September 2023). DFFE. doi: [10.15493/DEA.MIMS.13772023](https://doi.org/10.15493/DEA.MIMS.13772023).
- Lamont T, Louw GS, van den Berg MA, Perez RC, Dong S, Garcia R, Speich S, Meinen CS. 2024. Raw PIES data for long-term observations of acoustic travel time (τ) and bottom pressure along the SAMBA transect at PIES P4a (September 2021 - September 2023). DFFE. doi: [10.15493/DEA.MIMS.13782023](https://doi.org/10.15493/DEA.MIMS.13782023).
- Lamont T, Louw GS, van den Berg MA, Perez RC, Dong S, Garcia R, Speich S, Meinen CS. 2024. Raw PIES data for long-term observations of acoustic travel time (τ) and bottom pressure along the SAMBA transect at PIES P5 (September 2021 - September 2023). DFFE. doi: [10.15493/DEA.MIMS.13792023](https://doi.org/10.15493/DEA.MIMS.13792023).
- Lamont T, Louw GS, van den Berg MA, Perez RC, Dong S, Garcia R, Speich S, Meinen CS. 2024. Raw PIES data for long-term observations of acoustic travel time (τ) and bottom pressure along the SAMBA transect at PIES P6 (September 2021 - September 2023). DFFE. doi: [10.15493/DEA.MIMS.13802023](https://doi.org/10.15493/DEA.MIMS.13802023).
- Lamont T, Louw GS, van den Berg MA, Perez RC, Dong S, Garcia R, Speich S, Meinen CS. 2024. Raw PIES data for long-term observations of acoustic travel time (τ) and bottom pressure along the SAMBA transect at PIES P8 (September 2021 - September 2023). DFFE. doi: [10.15493/DEA.MIMS.13812023](https://doi.org/10.15493/DEA.MIMS.13812023).
- Lamont T, van den Berg MA. 2024. Long-term observations of daily currents on the Prince Edward Island shelf at M1 (May 2023 - April 2024). DFFE. doi: [10.15493/DEA.MIMS.14502024](https://doi.org/10.15493/DEA.MIMS.14502024).
- Lamont T, van den Berg MA. 2024. Long-term observations of hourly currents on the Prince Edward Island shelf at M1 (May 2023 - April 2024). DFFE. doi: [10.15493/DEA.MIMS.14602024](https://doi.org/10.15493/DEA.MIMS.14602024).
- Lamont T, van den Berg MA. 2024. Long-term observations of daily currents on the Prince Edward Island shelf at M2 (April 2023 - April 2024). DFFE. doi: [10.15493/DEA.MIMS.14702024](https://doi.org/10.15493/DEA.MIMS.14702024).
- Lamont T, van den Berg MA. 2024. Long-term observations of hourly currents on the Prince Edward Island shelf at M2 (April 2023 - April 2024). DFFE. doi: [10.15493/DEA.MIMS.14802024](https://doi.org/10.15493/DEA.MIMS.14802024).
- Lamont T, van den Berg MA. 2024. Long-term observations of daily bottom temperatures on the Prince Edward Island shelf at M1 (May 2023 - April 2024). DFFE. doi: [10.15493/DEA.MIMS.14902024](https://doi.org/10.15493/DEA.MIMS.14902024).
- Lamont T, van den Berg MA. 2024. Long-term observations of hourly bottom temperatures on the Prince Edward Island shelf at M1 (May 2023 - April 2024). DFFE. doi: [10.15493/DEA.MIMS.15002024](https://doi.org/10.15493/DEA.MIMS.15002024).
- Lamont T, van den Berg MA. 2024. Long-term observations of daily bottom temperatures on the Prince Edward Island shelf at M2 (April 2023 - April 2024). DFFE. doi: [10.15493/DEA.MIMS.15102024](https://doi.org/10.15493/DEA.MIMS.15102024).
- Lamont T, van den Berg MA. 2024. Long-term observations of hourly bottom temperatures on the Prince Edward Island shelf at M2 (April 2023 - April 2024). DFFE. doi: [10.15493/DEA.MIMS.15202024](https://doi.org/10.15493/DEA.MIMS.15202024).
- Lamont T, van den Berg MA. 2024. Raw ADCP Data for long-term observations of currents on the Prince Edward Island shelf at M2 (April 2023 - April 2024). DFFE. doi: [10.15493/DEA.MIMS.15402024](https://doi.org/10.15493/DEA.MIMS.15402024).
- Lamont T, van den Berg MA. 2024. Raw ADCP Data for long-term observations of currents on the Prince Edward Island shelf at M1 (May 2023 - April 2024). DFFE. doi: [10.15493/DEA.MIMS.15302024](https://doi.org/10.15493/DEA.MIMS.15302024).
- Lamont T, van den Berg MA, Ansoorge I. 2024. Raw hourly temperature, salinity, and dissolved oxygen along the SAMBA transect at SAMBA Mooring 9 (October 2020 - September 2022). SAEON. doi: [10.15493/IATL.12682023](https://doi.org/10.15493/IATL.12682023).
- Lamont T, van den Berg MA, Ansoorge I. 2024. Raw hourly temperature, salinity, and dissolved oxygen along the SAMBA transect at SAMBA Mooring 10 (October 2020 - October 2022). SAEON. doi: [10.15493/IATL.12692023](https://doi.org/10.15493/IATL.12692023).
- Lamont T, van den Berg MA, Ansoorge I. 2024. Long-term observations of hourly temperature, salinity, and dissolved oxygen along the SAMBA transect at SAMBA Mooring 9 (October 2020 - September 2022). SAEON. doi: [10.15493/IATL.12662023](https://doi.org/10.15493/IATL.12662023).
- Lamont T, van den Berg MA, Ansoorge I. 2024. Long-term observations of hourly temperature, salinity, and dissolved oxygen along the SAMBA transect at SAMBA Mooring 10 (October 2020 - October 2022). SAEON. doi: [10.15493/IATL.12672023](https://doi.org/10.15493/IATL.12672023).
- Lamont T, van den Berg MA, Louw GS. 2024. Short-term observations of currents and sub-surface temperatures on the continental shelf off Port St Johns, along the east coast of South Africa. DFFE. doi: [10.15493/DEA.MIMS.29112024](https://doi.org/10.15493/DEA.MIMS.29112024).

OUTPUTS FOR 2024

- Louw G. 2024. SEAmester and Agulhas System Climate Array (ASCA) Scientific Cruise on the SA Agulhas II Voyage 058, June 2023. DFFE. doi: [10.15493/DEA.MIMS.18042024](https://doi.org/10.15493/DEA.MIMS.18042024).
- Louw GS, van den Berg MA, Lamont T. 2024. Raw ADCP data for short-term observations of currents on the continental shelf off Natal Bight, along the east coast of South Africa at location Dbn01 (March 2009 - December 2009). DFFE. doi: [10.15493/DEA.MIMS.131072024](https://doi.org/10.15493/DEA.MIMS.131072024).
- Louw GS, van den Berg MA, Lamont T. 2024. Raw ADCP data for short-term observations of currents on the continental shelf off Natal Bight, along the east coast of South Africa at location Dbn01 (December 2009 - February 2010). DFFE. doi: [10.15493/DEA.MIMS.132072024](https://doi.org/10.15493/DEA.MIMS.132072024).
- Louw GS, van den Berg MA, Lamont T. 2024. Raw ADCP data for short-term observations of currents on the continental shelf off Natal Bight, along the east coast of South Africa at location Dbn01 (March 2010 - September 2010). DFFE. doi: [10.15493/DEA.MIMS.133072024](https://doi.org/10.15493/DEA.MIMS.133072024).
- Louw GS, van den Berg MA, Lamont T. 2024. Raw ADCP data for short-term observations of currents on the continental slope off Natal Bight, along the east coast of South Africa at location Dbn03 (April 2009 - September 2009). DFFE. doi: [10.15493/DEA.MIMS.136072024](https://doi.org/10.15493/DEA.MIMS.136072024).
- Louw GS, van den Berg MA, Lamont T. 2024. Raw ADCP data for short-term observations of currents on the continental slope off Natal Bight, along the east coast of South Africa at location Dbn03 (October 2009 - February 2010). DFFE. doi: [10.15493/DEA.MIMS.137072024](https://doi.org/10.15493/DEA.MIMS.137072024).
- Louw GS, van den Berg MA, Lamont T. 2024. Raw ADCP data for short-term observations of currents on the continental slope off Natal Bight, along the east coast of South Africa at location Dbn03 (February 2010 - September 2010). DFFE. doi: [10.15493/DEA.MIMS.138072024](https://doi.org/10.15493/DEA.MIMS.138072024).
- Louw GS, van den Berg MA, Lamont T. 2024. Raw ADCP data for short-term observations of currents on the continental shelf off Natal Bight, along the east coast of South Africa at location RiB01 (September 2009 - February 2010). DFFE. doi: [10.15493/DEA.MIMS.139072024](https://doi.org/10.15493/DEA.MIMS.139072024).
- Louw GS, van den Berg MA, Lamont T. 2024. Raw ADCP data for short-term observations of currents on the continental shelf off Natal Bight, along the east coast of South Africa at location RiB01 (February 2010 - September 2010). DFFE. doi: [10.15493/DEA.MIMS.140072024](https://doi.org/10.15493/DEA.MIMS.140072024).
- Louw GS, van den Berg MA, Lamont T. 2024. Raw ADCP data for short-term observations of currents on the continental slope off Natal Bight, along the east coast of South Africa at location RiB02 (April 2009 - September 2009). DFFE. doi: [10.15493/DEA.MIMS.141072024](https://doi.org/10.15493/DEA.MIMS.141072024).
- Louw GS, van den Berg MA, Lamont T. 2024. Raw ADCP data for short-term observations of currents on the continental slope off Natal Bight, along the east coast of South Africa at location RiB02 (September 2009 - February 2010). DFFE. doi: [10.15493/DEA.MIMS.142072024](https://doi.org/10.15493/DEA.MIMS.142072024).
- Louw GS, van den Berg MA, Lamont T. 2024. Raw ADCP data for short-term observations of currents on the continental slope off Natal Bight, along the east coast of South Africa at location RiB02 (February 2010 - September 2010). DFFE. doi: [10.15493/DEA.MIMS.143072024](https://doi.org/10.15493/DEA.MIMS.143072024).
- Louw GS, van den Berg MA, Lamont T. 2024. Raw ADCP data for short-term observations of currents on the continental shelf off Natal Bight, along the east coast of South Africa at location Sez01 (December 2009 - July 2010). DFFE. doi: [10.15493/DEA.MIMS.144072024](https://doi.org/10.15493/DEA.MIMS.144072024).
- Louw GS, van den Berg MA, Lamont T. 2024. Short-term observations of daily currents on the continental shelf off Natal Bight, along the east coast of South Africa at location Dbn01 (March 2009 - December 2009). DFFE. doi: [10.15493/DEA.MIMS.79072024](https://doi.org/10.15493/DEA.MIMS.79072024).
- Louw GS, van den Berg MA, Lamont T. 2024. Short-term observations of daily currents on the continental shelf off Natal Bight, along the east coast of South Africa at location Dbn01 (December 2009 - February 2010). DFFE. doi: [10.15493/DEA.MIMS.80072024](https://doi.org/10.15493/DEA.MIMS.80072024).
- Louw GS, van den Berg MA, Lamont T. 2024. Short-term observations of daily currents on the continental shelf off Natal Bight, along the east coast of South Africa at location Dbn01 (March 2010 - September 2010). DFFE. doi: [10.15493/DEA.MIMS.81072024](https://doi.org/10.15493/DEA.MIMS.81072024).
- Louw GS, van den Berg MA, Lamont T. 2024. Short-term observations of daily currents on the continental slope off Natal Bight, along the east coast of South Africa at location Dbn03 (April 2009 - September 2009). DFFE. doi: [10.15493/DEA.MIMS.82072024](https://doi.org/10.15493/DEA.MIMS.82072024).
- Louw GS, van den Berg MA, Lamont T. 2024. Short-term observations of daily currents on the continental slope off Natal Bight, along the east coast of South Africa at location Dbn03 (October 2009 - February 2010). DFFE. doi: [10.15493/DEA.MIMS.83072024](https://doi.org/10.15493/DEA.MIMS.83072024).
- Louw GS, van den Berg MA, Lamont T. 2024. Short-term observations of daily currents on the continental slope off Natal Bight, along the east coast of South Africa at location Dbn03 (February 2010 - September 2010). DFFE. doi: [10.15493/DEA.MIMS.84072024](https://doi.org/10.15493/DEA.MIMS.84072024).
- Louw GS, van den Berg MA, Lamont T. 2024. Short-term observations of daily currents on the continental shelf off Natal Bight, along the east coast of South Africa at location RiB01 (September 2009 - February 2010). DFFE. doi: [10.15493/DEA.MIMS.85072024](https://doi.org/10.15493/DEA.MIMS.85072024).
- Louw GS, van den Berg MA, Lamont T. 2024. Short-term observations of daily currents on the continental shelf off Natal Bight, along the east coast of South Africa at location RiB01 (February 2010 - September 2010). DFFE. doi: [10.15493/DEA.MIMS.86072024](https://doi.org/10.15493/DEA.MIMS.86072024).

OUTPUTS FOR 2024

- Louw GS, van den Berg MA, Lamont T. 2024. Short-term observations of daily currents on the continental slope off Natal Bight, along the east coast of South Africa at location RiB02 (April 2009 - September 2009). DFFE. doi: [10.15493/DEA.MIMS.87072024](https://doi.org/10.15493/DEA.MIMS.87072024).
- Louw GS, van den Berg MA, Lamont T. 2024. Short-term observations of daily currents on the continental slope off Natal Bight, along the east coast of South Africa at location RiB02 (September 2009 - February 2010). DFFE. doi: [10.15493/DEA.MIMS.88072024](https://doi.org/10.15493/DEA.MIMS.88072024).
- Louw GS, van den Berg MA, Lamont T. 2024. Short-term observations of daily currents on the continental slope off Natal Bight, along the east coast of South Africa at location RiB02 (February 2010 - September 2010). DFFE. doi: [10.15493/DEA.MIMS.89072024](https://doi.org/10.15493/DEA.MIMS.89072024).
- Louw GS, van den Berg MA, Lamont T. 2024. Short-term observations of daily currents on the continental shelf off Natal Bight, along the east coast of South Africa at location Sez01 (December 2009 - July 2010). DFFE. doi: [10.15493/DEA.MIMS.90072024](https://doi.org/10.15493/DEA.MIMS.90072024).
- Louw GS, van den Berg MA, Lamont T. 2024. Short-term observations of hourly currents on the continental shelf off Natal Bight, along the east coast of South Africa at location Dbn01 (March 2009 - December 2009). DFFE. doi: [10.15493/DEA.MIMS.91072024](https://doi.org/10.15493/DEA.MIMS.91072024).
- Louw GS, van den Berg MA, Lamont T. 2024. Short-term observations of hourly currents on the continental shelf off Natal Bight, along the east coast of South Africa at location Dbn01 (December 2009 - February 2010). DFFE. doi: [10.15493/DEA.MIMS.92072024](https://doi.org/10.15493/DEA.MIMS.92072024).
- Louw GS, van den Berg MA, Lamont T. 2024. Short-term observations of hourly currents on the continental shelf off Natal Bight, along the east coast of South Africa at location Dbn01 (March 2010 - September 2010). DFFE. doi: [10.15493/DEA.MIMS.93072024](https://doi.org/10.15493/DEA.MIMS.93072024).
- Louw GS, van den Berg MA, Lamont T. 2024. Short-term observations of hourly currents on the continental slope off Natal Bight, along the east coast of South Africa at location Dbn03 (April 2009 - September 2009). DFFE. doi: [10.15493/DEA.MIMS.94072024](https://doi.org/10.15493/DEA.MIMS.94072024).
- Louw GS, van den Berg MA, Lamont T. 2024. Short-term observations of hourly currents on the continental slope off Natal Bight, along the east coast of South Africa at location Dbn03 (October 2009 - February 2010). DFFE. doi: [10.15493/DEA.MIMS.95072024](https://doi.org/10.15493/DEA.MIMS.95072024).
- Louw GS, van den Berg MA, Lamont T. 2024. Short-term observations of hourly currents on the continental slope off Natal Bight, along the east coast of South Africa at location Dbn03 (February 2010 - September 2010). DFFE. doi: [10.15493/DEA.MIMS.96072024](https://doi.org/10.15493/DEA.MIMS.96072024).
- Louw GS, van den Berg MA, Lamont T. 2024. Short-term observations of hourly currents on the continental shelf off Natal Bight, along the east coast of South Africa at location RiB01 (September 2009 - February 2010). DFFE. doi: [10.15493/DEA.MIMS.97072024](https://doi.org/10.15493/DEA.MIMS.97072024).
- Louw GS, van den Berg MA, Lamont T. 2024. Short-term observations of hourly currents on the continental shelf off Natal Bight, along the east coast of South Africa at location RiB01 (February 2010 - September 2010). DFFE. doi: [10.15493/DEA.MIMS.98072024](https://doi.org/10.15493/DEA.MIMS.98072024).
- Louw GS, van den Berg MA, Lamont T. 2024. Short-term observations of hourly currents on the continental slope off Natal Bight, along the east coast of South Africa at location RiB02 (April 2009 - September 2009). DFFE. doi: [10.15493/DEA.MIMS.99072024](https://doi.org/10.15493/DEA.MIMS.99072024).
- Louw GS, van den Berg MA, Lamont T. 2024. Short-term observations of hourly currents on the continental slope off Natal Bight, along the east coast of South Africa at location RiB02 (September 2009 - February 2010). DFFE. doi: [10.15493/DEA.MIMS.100072024](https://doi.org/10.15493/DEA.MIMS.100072024).
- Louw GS, van den Berg MA, Lamont T. 2024. Short-term observations of hourly currents on the continental slope off Natal Bight, along the east coast of South Africa at location RiB02 (February 2010 - September 2010). DFFE. doi: [10.15493/DEA.MIMS.101072024](https://doi.org/10.15493/DEA.MIMS.101072024).
- Louw GS, van den Berg MA, Lamont T. 2024. Short-term observations of hourly currents on the continental shelf off Natal Bight, along the east coast of South Africa at location Sez01 (December 2009 - July 2010). DFFE. doi: [10.15493/DEA.MIMS.102072024](https://doi.org/10.15493/DEA.MIMS.102072024).
- Louw GS, van den Berg MA, Lamont T. 2024. Short-term observations of daily bottom temperatures on the continental shelf off Natal Bight, along the east coast of South Africa at location Dbn01 (March 2009 - December 2009). DFFE. doi: [10.15493/DEA.MIMS.103072024](https://doi.org/10.15493/DEA.MIMS.103072024).
- Louw GS, van den Berg MA, Lamont T. 2024. Short-term observations of daily bottom temperatures on the continental shelf off Natal Bight, along the east coast of South Africa at location Dbn01 (December 2009 - February 2010). DFFE. doi: [10.15493/DEA.MIMS.104072024](https://doi.org/10.15493/DEA.MIMS.104072024).
- Louw GS, van den Berg MA, Lamont T. 2024. Short-term observations of daily bottom temperatures on the continental shelf off Natal Bight, along the east coast of South Africa at location Dbn01 (March 2010 - September 2010). DFFE. doi: [10.15493/DEA.MIMS.105072024](https://doi.org/10.15493/DEA.MIMS.105072024).
- Louw GS, van den Berg MA, Lamont T. 2024. Short-term observations of daily bottom temperatures on the continental slope off Natal Bight, along the east coast of South Africa at location Dbn03 (April 2009 - September 2009). DFFE. doi: [10.15493/DEA.MIMS.106072024](https://doi.org/10.15493/DEA.MIMS.106072024).
- Louw GS, van den Berg MA, Lamont T. 2024. Short-term observations of daily bottom temperatures on the continental slope off Natal Bight, along the east coast of South Africa at location Dbn03 (October 2009 - February 2010). DFFE. doi: [10.15493/DEA.MIMS.107072024](https://doi.org/10.15493/DEA.MIMS.107072024).
- Louw GS, van den Berg MA, Lamont T. 2024. Short-term observations of daily bottom temperatures on the continental slope off Natal Bight, along the east coast of South Africa at location Dbn03 (February 2010 - September 2010). DFFE. doi: [10.15493/DEA.MIMS.108072024](https://doi.org/10.15493/DEA.MIMS.108072024).
- Louw GS, van den Berg MA, Lamont T. 2024. Short-term observations of daily bottom temperatures on the continental shelf off Natal Bight, along the east coast of South Africa at location RiB01 (September 2009 - February 2010). DFFE. doi: [10.15493/DEA.MIMS.109072024](https://doi.org/10.15493/DEA.MIMS.109072024).

OUTPUTS FOR 2024

- Louw GS, van den Berg MA, Lamont T. 2024. Short-term observations of daily bottom temperatures on the continental shelf off Natal Bight, along the east coast of South Africa at location RiB01 (February 2010 - September 2010). DFFE. doi: [10.15493/DEA.MIMS.110072024](https://doi.org/10.15493/DEA.MIMS.110072024).
- Louw GS, van den Berg MA, Lamont T. 2024. Short-term observations of daily bottom temperatures on the continental slope off Natal Bight, along the east coast of South Africa at location RiB02 (April 2009 - September 2009). DFFE. doi: [10.15493/DEA.MIMS.111072024](https://doi.org/10.15493/DEA.MIMS.111072024).
- Louw GS, van den Berg MA, Lamont T. 2024. Short-term observations of daily bottom temperatures on the continental slope off Natal Bight, along the east coast of South Africa at location RiB02 (September 2009 - February 2010). DFFE. doi: [10.15493/DEA.MIMS.112072024](https://doi.org/10.15493/DEA.MIMS.112072024).
- Louw GS, van den Berg MA, Lamont T. 2024. Short-term observations of daily bottom temperatures on the continental slope off Natal Bight, along the east coast of South Africa at location RiB02 (February 2010 - September 2010). DFFE. doi: [10.15493/DEA.MIMS.113072024](https://doi.org/10.15493/DEA.MIMS.113072024).
- Louw GS, van den Berg MA, Lamont T. 2024. Short-term observations of daily bottom temperatures on the continental shelf off Natal Bight, along the east coast of South Africa at location Sez01 (December 2009 - July 2010). DFFE. doi: [10.15493/DEA.MIMS.114072024](https://doi.org/10.15493/DEA.MIMS.114072024).
- Louw GS, van den Berg MA, Lamont T. 2024. Short-term observations of hourly bottom temperatures on the continental shelf off Natal Bight, along the east coast of South Africa at location Dbn01 (March 2009 - December 2009). DFFE. doi: [10.15493/DEA.MIMS.115072024](https://doi.org/10.15493/DEA.MIMS.115072024).
- Louw GS, van den Berg MA, Lamont T. 2024. Short-term observations of hourly bottom temperatures on the continental shelf off Natal Bight, along the east coast of South Africa at location Dbn01 (December 2009 - February 2010). DFFE. doi: [10.15493/DEA.MIMS.116072024](https://doi.org/10.15493/DEA.MIMS.116072024).
- Louw GS, van den Berg MA, Lamont T. 2024. Short-term observations of hourly bottom temperatures on the continental shelf off Natal Bight, along the east coast of South Africa at location Dbn01 (March 2010 - September 2010). DFFE. doi: [10.15493/DEA.MIMS.117072024](https://doi.org/10.15493/DEA.MIMS.117072024).
- Louw GS, van den Berg MA, Lamont T. 2024. Short-term observations of hourly bottom temperatures on the continental slope off Natal Bight, along the east coast of South Africa at location Dbn03 (April 2009 - September 2009). DFFE. doi: [10.15493/DEA.MIMS.118072024](https://doi.org/10.15493/DEA.MIMS.118072024).
- Louw GS, van den Berg MA, Lamont T. 2024. Short-term observations of hourly bottom temperatures on the continental slope off Natal Bight, along the east coast of South Africa at location Dbn03 (October 2009 - February 2010). DFFE. doi: [10.15493/DEA.MIMS.119072024](https://doi.org/10.15493/DEA.MIMS.119072024).
- Louw GS, van den Berg MA, Lamont T. 2024. Short-term observations of hourly bottom temperatures on the continental slope off Natal Bight, along the east coast of South Africa at location Dbn03 (February 2010 - September 2010). DFFE. doi: [10.15493/DEA.MIMS.120072024](https://doi.org/10.15493/DEA.MIMS.120072024).
- Louw GS, van den Berg MA, Lamont T. 2024. Short-term observations of hourly bottom temperatures on the continental shelf off Natal Bight, along the east coast of South Africa at location RiB01 (September 2009 - February 2010). DFFE. doi: [10.15493/DEA.MIMS.121072024](https://doi.org/10.15493/DEA.MIMS.121072024).
- Louw GS, van den Berg MA, Lamont T. 2024. Short-term observations of hourly bottom temperatures on the continental shelf off Natal Bight, along the east coast of South Africa at location RiB01 (February 2010 - September 2010). DFFE. doi: [10.15493/DEA.MIMS.122072024](https://doi.org/10.15493/DEA.MIMS.122072024).
- Louw GS, van den Berg MA, Lamont T. 2024. Short-term observations of hourly bottom temperatures on the continental slope off Natal Bight, along the east coast of South Africa at location RiB02 (April 2009 - September 2009). DFFE. doi: [10.15493/DEA.MIMS.123072024](https://doi.org/10.15493/DEA.MIMS.123072024).
- Louw GS, van den Berg MA, Lamont T. 2024. Short-term observations of hourly bottom temperatures on the continental slope off Natal Bight, along the east coast of South Africa at location RiB02 (September 2009 - February 2010). DFFE. doi: [10.15493/DEA.MIMS.124072024](https://doi.org/10.15493/DEA.MIMS.124072024).
- Louw GS, van den Berg MA, Lamont T. 2024. Short-term observations of hourly bottom temperatures on the continental slope off Natal Bight, along the east coast of South Africa at location RiB02 (February 2010 - September 2010). DFFE. doi: [10.15493/DEA.MIMS.125072024](https://doi.org/10.15493/DEA.MIMS.125072024).
- Louw GS, van den Berg MA, Lamont T. 2024. Short-term observations of hourly bottom temperatures on the continental shelf off Natal Bight, along the east coast of South Africa at location Sez01 (December 2009 - July 2010). DFFE. doi: [10.15493/DEA.MIMS.126072024](https://doi.org/10.15493/DEA.MIMS.126072024).
- Louw GS, van den Berg MA, Lamont T. 2024. Raw ADCP Data for short-term observations of currents on the continental shelf off Port St Johns, along the east coast of South Africa (July 2013 - December 2013). DFFE. doi: [10.15493/DEA.MIMS.38112024](https://doi.org/10.15493/DEA.MIMS.38112024).
- Louw GS, van den Berg MA, Lamont T. 2024. Raw ADCP data for short-term observations of currents on the continental shelf off Port St Johns, along the east coast of South Africa (December 2013 - September 2014). DFFE. doi: [10.15493/DEA.MIMS.39112024](https://doi.org/10.15493/DEA.MIMS.39112024).
- Louw GS, van den Berg MA, Lamont T. 2024. Short-term observations of daily currents on the continental shelf off Port St Johns, along the east coast of South Africa (July 2013 - December 2013). DFFE. doi: [10.15493/DEA.MIMS.30112024](https://doi.org/10.15493/DEA.MIMS.30112024).
- Louw GS, van den Berg MA, Lamont T. 2024. Short-term observations of hourly currents on the continental shelf off Port St Johns, along the east coast of South Africa (July 2013 - December 2013). DFFE. doi: [10.15493/DEA.MIMS.31112024](https://doi.org/10.15493/DEA.MIMS.31112024).

OUTPUTS FOR 2024

- Louw GS, van den Berg MA, Lamont T. 2024. Short-term observations of daily currents on the continental shelf off Port St Johns, along the east coast of South Africa (December 2013 - September 2014). DFFE. doi: [10.15493/DEA.MIMS.32112024](https://doi.org/10.15493/DEA.MIMS.32112024).
- Louw GS, van den Berg MA, Lamont T. 2024. Short-term observations of hourly currents on the continental shelf off Port St Johns, along the east coast of South Africa (December 2013 - September 2014). DFFE. doi: [10.15493/DEA.MIMS.33112024](https://doi.org/10.15493/DEA.MIMS.33112024).
- Louw GS, van den Berg MA, Lamont T. 2024. Short-term observations of daily bottom temperatures on the continental shelf off Port St Johns, along the east coast of South Africa (July 2013 - December 2013). DFFE. doi: [10.15493/DEA.MIMS.34112024](https://doi.org/10.15493/DEA.MIMS.34112024).
- Louw GS, van den Berg MA, Lamont T. 2024. Short-term observations of hourly bottom temperatures on the continental shelf off Port St Johns, along the east coast of South Africa (July 2013 - December 2013). DFFE. doi: [10.15493/DEA.MIMS.35112024](https://doi.org/10.15493/DEA.MIMS.35112024).
- Louw GS, van den Berg MA, Lamont T. 2024. Short-term observations of daily bottom temperatures on the continental shelf off Port St Johns, along the east coast of South Africa (December 2013 - September 2014). DFFE. doi: [10.15493/DEA.MIMS.36112024](https://doi.org/10.15493/DEA.MIMS.36112024).
- Louw GS, van den Berg MA, Lamont T. 2024. Short-term observations of hourly bottom temperatures on the continental shelf off Port St Johns, along the east coast of South Africa (December 2013 - September 2014). DFFE. doi: [10.15493/DEA.MIMS.37112024](https://doi.org/10.15493/DEA.MIMS.37112024).
- Makhetha M, Tutt G, Lamont T. 2024. Processed CTD discrete observations from the West Coast Hake Biomass on the Africana Voyage 079, January 1990. DFFE. doi: [10.15493/DEA.MIMS.11782023](https://doi.org/10.15493/DEA.MIMS.11782023).
- Makhetha M, Tutt G, Lamont T. 2024. Processed CTD discrete observations from the West Coast Hake Biomass Survey on the Africana Voyage 088, January 1991. DFFE. doi: [10.15493/DEA.MIMS.32072024](https://doi.org/10.15493/DEA.MIMS.32072024).
- Makhetha M, Tutt G, Lamont T. 2024. Processed CTD discrete observations from the Plankton Dynamics on the Africana Voyage 089, February 1991. DFFE. doi: [10.15493/DEA.MIMS.35072024](https://doi.org/10.15493/DEA.MIMS.35072024).
- Makhetha M, Tutt G, Lamont T. 2024. Processed CTD discrete observations from the Pelagic Pre-Recruit Mesopelagic Biomass Survey on the Africana Voyage 090, March 1991. DFFE. doi: [10.15493/DEA.MIMS.38072024](https://doi.org/10.15493/DEA.MIMS.38072024).
- Makhetha M, Tutt G, Lamont T. 2024. Processed CTD discrete observations from the Anchovy Recruitment Survey on the Africana Voyage 092, May 1991. DFFE. doi: [10.15493/DEA.MIMS.17072024](https://doi.org/10.15493/DEA.MIMS.17072024).
- Makhetha M, Tutt G, Lamont T. 2024. Processed CTD discrete observations from the Horse Mackerel Hydroacoustic Pilot Survey on the Africana Voyage 096, October 1991. DFFE. doi: [10.15493/DEA.MIMS.44072024](https://doi.org/10.15493/DEA.MIMS.44072024).
- Makhetha M, Tutt G, Lamont T. 2024. Processed CTD discrete observations from the Pelagic Fish Biomass Survey on the Africana Voyage 097, November 1991. DFFE. doi: [10.15493/DEA.MIMS.47072024](https://doi.org/10.15493/DEA.MIMS.47072024).
- Makhetha M, Tutt G, Lamont T. 2024. Processed CTD discrete observations from the Agulhas Bank Boundary Processes cruise on the Africana Voyage 099, January 1992. DFFE. doi: [10.15493/DEA.MIMS.50072024](https://doi.org/10.15493/DEA.MIMS.50072024).
- Makhetha M, Tutt G, Lamont T. 2024. Processed CTD discrete observations from the West Coast Hake Biomass Survey on the Africana Voyage 100, February 1992. DFFE. doi: [10.15493/DEA.MIMS.53072024](https://doi.org/10.15493/DEA.MIMS.53072024).
- Makhetha M, Tutt G, Lamont T. 2024. Processed CTD discrete observations from the Pelagic Pre-Recruit Mesopelagic Biomass Survey on the Africana Voyage 101, March 1992. DFFE. doi: [10.15493/DEA.MIMS.56072024](https://doi.org/10.15493/DEA.MIMS.56072024).
- Makhetha M, Tutt G, Lamont T. 2024. Processed CTD discrete observations from the South Coast Demersal Biomass Survey on the Africana Voyage 102, April 1992. DFFE. doi: [10.15493/DEA.MIMS.59072024](https://doi.org/10.15493/DEA.MIMS.59072024).
- Makhetha M, Tutt G, Lamont T. 2024. Processed CTD discrete observations from the Anchovy Recruitment Survey on the Africana Voyage 092, May 1991. DFFE. doi: [10.15493/DEA.MIMS.17072024](https://doi.org/10.15493/DEA.MIMS.17072024).
- Makhetha M, Tutt G, Lamont T. 2024. Processed CTD discrete observations from the South Coast Demersal Biomass Survey on the Africana Voyage 093, June 1991. DFFE. doi: [10.15493/DEA.MIMS.20072024](https://doi.org/10.15493/DEA.MIMS.20072024).
- Makhetha M, Tutt G, Lamont T. 2024. Processed CTD discrete observations from the South Coast Demersal Biomass Survey on the Africana Voyage 095, September 1991. DFFE. doi: [10.15493/DEA.MIMS.23072024](https://doi.org/10.15493/DEA.MIMS.23072024).
- Makhetha M, Tutt G, Lamont T. 2024. Processed CTD discrete observations from the South Coast Demersal Biomass Survey on the Africana Voyage 072, May 1989. DFFE. doi: [10.15493/DEA.MIMS.02112024](https://doi.org/10.15493/DEA.MIMS.02112024).
- Makhetha M, Tutt G, Lamont T. 2024. Processed CTD discrete observations from the Benguela Current Sources and Transport (BEST 1) on the Africana Voyage 105, June 1992. DFFE. doi: [10.15493/DEA.MIMS.05112024](https://doi.org/10.15493/DEA.MIMS.05112024).
- Makhetha M, Tutt G, Lamont T. 2024. Processed CTD discrete observations from the South Coast Demersal Inshore Biomass Survey on the Africana Voyage 106, September 1992. DFFE. doi: [10.15493/DEA.MIMS.08112024](https://doi.org/10.15493/DEA.MIMS.08112024).
- Makhetha M, Tutt G, Lamont T. 2024. Processed CTD discrete observations from the Horse Mackerel Hydroacoustic Survey on the Africana Voyage 107, October 1992. DFFE. doi: [10.15493/DEA.MIMS.11112024](https://doi.org/10.15493/DEA.MIMS.11112024).
- Makhetha M, Tutt G, Lamont T. 2024. Processed CTD discrete observations from the Pelagic Biomass Survey on the Africana Voyage 108, November 1992. DFFE. doi: [10.15493/DEA.MIMS.14112024](https://doi.org/10.15493/DEA.MIMS.14112024).
- Makhetha M, Tutt G, Lamont T. 2024. Processed CTD discrete observations from the West Coast Hake Biomass Survey on the Africana Voyage 109, January 1993. DFFE. doi: [10.15493/DEA.MIMS.17112024](https://doi.org/10.15493/DEA.MIMS.17112024).
- Makhetha M, Tutt G, Lamont T. 2024. Processed CTD discrete observations from the Anchovy Recruitment Survey on the Africana Voyage 103, May 1992. DFFE. doi: [10.15493/DEA.MIMS.16122024](https://doi.org/10.15493/DEA.MIMS.16122024).

OUTPUTS FOR 2024

- Sabelani Z, Ismail H, van den Berg MA, Lamont T. 2024. Raw temperature data for long-term observations of bottom temperatures at Mosterts Hoek, South Africa (January 1992 - May 1992). DFFE. doi: [10.15493/DEA.MIMS.12712023](https://doi.org/10.15493/DEA.MIMS.12712023).
- Sabelani Z, Ismail H, van den Berg MA, Lamont T. 2024. Raw temperature data for long-term observations of bottom temperatures at Mosterts Hoek, South Africa (May 1992 - August 1992). DFFE. doi: [10.15493/DEA.MIMS.12732023](https://doi.org/10.15493/DEA.MIMS.12732023).
- Sabelani Z, Ismail H, van den Berg MA, Lamont T. 2024. Raw temperature data for long-term observations of bottom temperatures at Mosterts Hoek, South Africa (August 1992 - November 1992). DFFE. doi: [10.15493/DEA.MIMS.12752023](https://doi.org/10.15493/DEA.MIMS.12752023).
- Sabelani Z, Ismail H, van den Berg MA, Lamont T. 2024. Raw temperature data for long-term observations of bottom temperatures at Mosterts Hoek, South Africa (November 1992 - January 1993). DFFE. doi: [10.15493/DEA.MIMS.12772023](https://doi.org/10.15493/DEA.MIMS.12772023).
- Sabelani Z, Ismail H, van den Berg MA, Lamont T. 2024. Raw temperature data for long-term observations of bottom temperatures at Mosterts Hoek, South Africa (January 1993 - July 1993). DFFE. doi: [10.15493/DEA.MIMS.12792023](https://doi.org/10.15493/DEA.MIMS.12792023).
- Sabelani Z, Ismail H, van den Berg MA, Lamont T. 2024. Raw temperature data for long-term observations of bottom temperatures at Mosterts Hoek, South Africa (July 1993 - November 1993). DFFE. doi: [10.15493/DEA.MIMS.12812023](https://doi.org/10.15493/DEA.MIMS.12812023).
- Sabelani Z, Ismail H, van den Berg MA, Lamont T. 2024. Raw temperatures data for long-term observations of bottom temperatures at Mosterts Hoek, South Africa (November 1993 - March 1994). DFFE. doi: [10.15493/DEA.MIMS.12832023](https://doi.org/10.15493/DEA.MIMS.12832023).
- Sabelani Z, Ismail H, van den Berg MA, Lamont T. 2024. Raw temperature data for long-term observations of bottom temperatures at Mosterts Hoek, South Africa (March 1994 - August 1994). DFFE. doi: [10.15493/DEA.MIMS.12852023](https://doi.org/10.15493/DEA.MIMS.12852023).
- Sabelani Z, Ismail H, van den Berg MA, Lamont T. 2024. Raw temperature data for long-term observations of bottom temperatures at Mosterts Hoek, South Africa (August 1994 - November 1994). DFFE. doi: [10.15493/DEA.MIMS.12872023](https://doi.org/10.15493/DEA.MIMS.12872023).
- Sabelani Z, Ismail H, van den Berg MA, Lamont T. 2024. Raw temperature data for long-term observations of bottom temperatures at Mosterts Hoek, South Africa (November 1994 - April 1995). DFFE. doi: [10.15493/DEA.MIMS.12892023](https://doi.org/10.15493/DEA.MIMS.12892023).
- Sabelani Z, Ismail H, van den Berg MA, Lamont T. 2024. Raw temperature data for long-term observations of bottom temperatures at Mosterts Hoek, South Africa (April 1995 - July 1995). DFFE. doi: [10.15493/DEA.MIMS.12912023](https://doi.org/10.15493/DEA.MIMS.12912023).
- Sabelani Z, Ismail H, van den Berg MA, Lamont T. 2024. Raw temperature data for long-term observations of bottom temperatures at Mosterts Hoek, South Africa (July 1995 - November 1995). DFFE. doi: [10.15493/DEA.MIMS.12932023](https://doi.org/10.15493/DEA.MIMS.12932023).
- Sabelani Z, Ismail H, van den Berg MA, Lamont T. 2024. Raw temperature data for long-term observations of bottom temperatures at Mosterts Hoek, South Africa (November 1995 - April 1996). DFFE. doi: [10.15493/DEA.MIMS.12952023](https://doi.org/10.15493/DEA.MIMS.12952023).
- Sabelani Z, Ismail H, van den Berg MA, Lamont T. 2024. Raw temperature data for long-term observations of bottom temperatures at Mosterts Hoek, South Africa (April 1996 - March 1997). DFFE. doi: [10.15493/DEA.MIMS.12972023](https://doi.org/10.15493/DEA.MIMS.12972023).
- Sabelani Z, Ismail H, van den Berg MA, Lamont T. 2024. Raw temperature data for long-term observations of bottom temperatures at Mosterts Hoek, South Africa (March 1997 - September 1997). DFFE. doi: [10.15493/DEA.MIMS.12992023](https://doi.org/10.15493/DEA.MIMS.12992023).
- Sabelani Z, Ismail H, van den Berg MA, Lamont T. 2024. Raw temperature data for long-term observations of bottom temperatures at Mosterts Hoek, South Africa (September 1997 - July 1998). DFFE. doi: [10.15493/DEA.MIMS.13012023](https://doi.org/10.15493/DEA.MIMS.13012023).
- Sabelani Z, Ismail H, van den Berg MA, Lamont T. 2024. Raw temperatures data for long-term observations of bottom temperatures at Mosterts Hoek, South Africa (July 1998 - October 1998). DFFE. doi: [10.15493/DEA.MIMS.13032023](https://doi.org/10.15493/DEA.MIMS.13032023).
- Sabelani Z, Ismail H, van den Berg MA, Lamont T. 2024. Raw temperature data for long-term observations of bottom temperatures at Mosterts Hoek, South Africa (October 1998 - March 1999). DFFE. doi: [10.15493/DEA.MIMS.13052023](https://doi.org/10.15493/DEA.MIMS.13052023).
- Sabelani Z, Ismail H, van den Berg MA, Lamont T. 2024. Raw temperature data for long-term observations of bottom temperatures at Mosterts Hoek, South Africa (March 1999 - July 1999). DFFE. doi: [10.15493/DEA.MIMS.13072023](https://doi.org/10.15493/DEA.MIMS.13072023).
- Sabelani Z, Ismail H, van den Berg MA, Lamont T. 2024. Raw temperature data for long-term observations of bottom temperatures at Mosterts Hoek, South Africa (July 1999 - November 1999). DFFE. doi: [10.15493/DEA.MIMS.13092023](https://doi.org/10.15493/DEA.MIMS.13092023).
- Sabelani Z, Ismail H, van den Berg MA, Lamont T. 2024. Raw temperature data for long-term observations of bottom temperatures at Mosterts Hoek, South Africa (November 1999 - April 2000). DFFE. doi: [10.15493/DEA.MIMS.13112023](https://doi.org/10.15493/DEA.MIMS.13112023).
- Sabelani Z, Ismail H, van den Berg MA, Lamont T. 2024. Raw temperature data for long-term observations of bottom temperatures at Mosterts Hoek, South Africa (April 2000 - August 2000). DFFE. doi: [10.15493/DEA.MIMS.13132023](https://doi.org/10.15493/DEA.MIMS.13132023).
- Sabelani Z, Ismail H, van den Berg MA, Lamont T. 2024. Raw temperature data for long-term observations of bottom temperatures at Mosterts Hoek, South Africa (August 2000 - November 2000). DFFE. doi: [10.15493/DEA.MIMS.13152023](https://doi.org/10.15493/DEA.MIMS.13152023).
- Sabelani Z, Ismail H, van den Berg MA, Lamont T. 2024. Raw temperature data for long-term observations of bottom temperatures at Mosterts Hoek, South Africa (November 2000 - March 2001). DFFE. doi: [10.15493/DEA.MIMS.13172023](https://doi.org/10.15493/DEA.MIMS.13172023).

OUTPUTS FOR 2024

- Sabelani Z, Ismail H, van den Berg MA, Lamont T. 2024. Raw temperature data for long-term observations of bottom temperatures at Mosterts Hoek, South Africa (March 2001 - July 2001). DFFE. doi: [10.15493/DEA.MIMS.13192023](https://doi.org/10.15493/DEA.MIMS.13192023).
- Sabelani Z, Ismail H, van den Berg MA, Lamont T. 2024. Raw temperature data for long-term observations of bottom temperatures at Mosterts Hoek, South Africa (July 2001 - October 2001). DFFE. doi: [10.15493/DEA.MIMS.13212023](https://doi.org/10.15493/DEA.MIMS.13212023).
- Sabelani Z, Ismail H, van den Berg MA, Lamont T. 2024. Raw temperature data for long-term observations of bottom temperatures at Mosterts Hoek, South Africa (October 2001 - November 2002). DFFE. doi: [10.15493/DEA.MIMS.13232023](https://doi.org/10.15493/DEA.MIMS.13232023).
- Sabelani Z, Ismail H, van den Berg MA, Lamont T. 2024. Raw temperature data for long-term observations of bottom temperatures at Mosterts Hoek, South Africa (June 2003 - June 2004). DFFE. doi: [10.15493/DEA.MIMS.13252023](https://doi.org/10.15493/DEA.MIMS.13252023).
- Sabelani Z, Ismail H, van den Berg MA, Lamont T. 2024. Raw temperature data for long-term observations of bottom temperatures at Mosterts Hoek, South Africa (June 2004 - November 2004). DFFE. doi: [10.15493/DEA.MIMS.13272023](https://doi.org/10.15493/DEA.MIMS.13272023).
- Sabelani Z, Ismail H, van den Berg MA, Lamont T. 2024. Raw temperature data for long-term observations of bottom temperatures at Mosterts Hoek, South Africa (November 2004 - November 2005). DFFE. doi: [10.15493/DEA.MIMS.13292023](https://doi.org/10.15493/DEA.MIMS.13292023).
- Sabelani Z, Ismail H, van den Berg MA, Lamont T. 2024. Raw temperatures data for long-term observations of bottom temperatures at Mosterts Hoek, South Africa (November 2005 - November 2009). DFFE. doi: [10.15493/DEA.MIMS.13312023](https://doi.org/10.15493/DEA.MIMS.13312023).
- Sabelani Z, Ismail H, van den Berg MA, Lamont T. 2024. Raw temperature data for long-term observations of bottom temperatures at Mosterts Hoek, South Africa (November 2009 - September 2019). DFFE. doi: [10.15493/DEA.MIMS.13332023](https://doi.org/10.15493/DEA.MIMS.13332023).
- Sabelani Z, Ismail H, van den Berg MA, Lamont T. 2024. Raw temperature data for long-term observations of bottom temperatures at Mosterts Hoek, South Africa (September 2019 - June 2022). DFFE. doi: [10.15493/DEA.MIMS.13352023](https://doi.org/10.15493/DEA.MIMS.13352023).
- Sabelani Z, Ismail H, van den Berg MA, Lamont T. 2024. Long-term observations of hourly bottom temperatures at Mosterts Hoek, South Africa (January 1992 - May 1992). DFFE. doi: [10.15493/DEA.MIMS.12702023](https://doi.org/10.15493/DEA.MIMS.12702023).
- Sabelani Z, Ismail H, van den Berg MA, Lamont T. 2024. Long-term observations of hourly bottom temperatures at Mosterts Hoek, South Africa (May 1992 - August 1992). DFFE. doi: [10.15493/DEA.MIMS.12722023](https://doi.org/10.15493/DEA.MIMS.12722023).
- Sabelani Z, Ismail H, van den Berg MA, Lamont T. 2024. Long-term observations of hourly bottom temperatures at Mosterts Hoek, South Africa (August 1992 - November 1992). DFFE. doi: [10.15493/DEA.MIMS.12742023](https://doi.org/10.15493/DEA.MIMS.12742023).
- Sabelani Z, Ismail H, van den Berg MA, Lamont T. 2024. Long-term observations of hourly bottom temperatures at Mosterts Hoek, South Africa (November 1992 - January 1993). DFFE. doi: [10.15493/DEA.MIMS.12762023](https://doi.org/10.15493/DEA.MIMS.12762023).
- Sabelani Z, Ismail H, van den Berg MA, Lamont T. 2024. Long-term observations of hourly bottom temperatures at Mosterts Hoek, South Africa (January 1993 - July 1993). DFFE. doi: [10.15493/DEA.MIMS.12782023](https://doi.org/10.15493/DEA.MIMS.12782023).
- Sabelani Z, Ismail H, van den Berg MA, Lamont T. 2024. Long-term observations of hourly bottom temperatures at Mosterts Hoek, South Africa (July 1993 - November 1993). DFFE. doi: [10.15493/DEA.MIMS.12802023](https://doi.org/10.15493/DEA.MIMS.12802023).
- Sabelani Z, Ismail H, van den Berg MA, Lamont T. 2024. Long-term observations of hourly bottom temperatures at Mosterts Hoek, South Africa (November 1993 - March 1994). DFFE. doi: [10.15493/DEA.MIMS.12822023](https://doi.org/10.15493/DEA.MIMS.12822023).
- Sabelani Z, Ismail H, van den Berg MA, Lamont T. 2024. Long-term observations of hourly bottom temperatures at Mosterts Hoek, South Africa (March 1994 - August 1994). DFFE. doi: [10.15493/DEA.MIMS.12842023](https://doi.org/10.15493/DEA.MIMS.12842023).
- Sabelani Z, Ismail H, van den Berg MA, Lamont T. 2024. Long-term observations of hourly bottom temperatures at Mosterts Hoek, South Africa (August 1994 - November 1994). DFFE. doi: [10.15493/DEA.MIMS.12862023](https://doi.org/10.15493/DEA.MIMS.12862023).
- Sabelani Z, Ismail H, van den Berg MA, Lamont T. 2024. Long-term observations of hourly bottom temperatures at Mosterts Hoek, South Africa (November 1994 - April 1995). DFFE. doi: [10.15493/DEA.MIMS.12882023](https://doi.org/10.15493/DEA.MIMS.12882023).
- Sabelani Z, Ismail H, van den Berg MA, Lamont T. 2024. Long-term observations of hourly bottom temperatures at Mosterts Hoek, South Africa (April 1995 - July 1995). DFFE. doi: [10.15493/DEA.MIMS.12902023](https://doi.org/10.15493/DEA.MIMS.12902023).
- Sabelani Z, Ismail H, van den Berg MA, Lamont T. 2024. Long-term observations of hourly bottom temperatures at Mosterts Hoek, South Africa (July 1995 - November 1995). DFFE. doi: [10.15493/DEA.MIMS.12922023](https://doi.org/10.15493/DEA.MIMS.12922023).
- Sabelani Z, Ismail H, van den Berg MA, Lamont T. 2024. Long-term observations of hourly bottom temperatures at Mosterts Hoek, South Africa (November 1995 - April 1996). DFFE. doi: [10.15493/DEA.MIMS.12942023](https://doi.org/10.15493/DEA.MIMS.12942023).
- Sabelani Z, Ismail H, van den Berg MA, Lamont T. 2024. Long-term observations of hourly bottom temperatures at Mosterts Hoek, South Africa (April 1996 - March 1997). DFFE. doi: [10.15493/DEA.MIMS.12962023](https://doi.org/10.15493/DEA.MIMS.12962023).
- Sabelani Z, Ismail H, van den Berg MA, Lamont T. 2024. Long-term observations of hourly bottom temperatures at Mosterts Hoek, South Africa (March 1997 - September 1997). DFFE. doi: [10.15493/DEA.MIMS.12982023](https://doi.org/10.15493/DEA.MIMS.12982023).
- Sabelani Z, Ismail H, van den Berg MA, Lamont T. 2024. Long-term observations of hourly bottom temperatures at Mosterts Hoek, South Africa (September 1997 - July 1998). DFFE. doi: [10.15493/DEA.MIMS.13002023](https://doi.org/10.15493/DEA.MIMS.13002023).

OUTPUTS FOR 2024

- Sabelani Z, Ismail H, van den Berg MA, Lamont T. 2024. Long-term observations of hourly bottom temperatures at Mosterts Hoek, South Africa (July 1998 - October 1998). DFFE. doi: [10.15493/DEA.MIMS.13022023](https://doi.org/10.15493/DEA.MIMS.13022023).
- Sabelani Z, Ismail H, van den Berg MA, Lamont T. 2024. Long-term observations of hourly bottom temperatures at Mosterts Hoek, South Africa (October 1998 - March 1999). DFFE. doi: [10.15493/DEA.MIMS.13042023](https://doi.org/10.15493/DEA.MIMS.13042023).
- Sabelani Z, Ismail H, van den Berg MA, Lamont T. 2024. Long-term observations of hourly bottom temperatures at Mosterts Hoek, South Africa (March 1999 - July 1999). DFFE. doi: [10.15493/DEA.MIMS.13062023](https://doi.org/10.15493/DEA.MIMS.13062023).
- Sabelani Z, Ismail H, van den Berg MA, Lamont T. 2024. Long-term observations of hourly bottom temperatures at Mosterts Hoek, South Africa (July 1999 - November 1999). DFFE. doi: [10.15493/DEA.MIMS.13082023](https://doi.org/10.15493/DEA.MIMS.13082023).
- Sabelani Z, Ismail H, van den Berg MA, Lamont T. 2024. Long-term observations of hourly bottom temperatures at Mosterts Hoek, South Africa (November 1999 - April 2000). DFFE. doi: [10.15493/DEA.MIMS.13102023](https://doi.org/10.15493/DEA.MIMS.13102023).
- Sabelani Z, Ismail H, van den Berg MA, Lamont T. 2024. Long-term observations of hourly bottom temperatures at Mosterts Hoek, South Africa (April 2000 - August 2000). DFFE. doi: [10.15493/DEA.MIMS.13122023](https://doi.org/10.15493/DEA.MIMS.13122023).
- Sabelani Z, Ismail H, van den Berg MA, Lamont T. 2024. Long-term observations of hourly bottom temperatures at Mosterts Hoek, South Africa (August 2000 - November 2000). DFFE. doi: [10.15493/DEA.MIMS.13142023](https://doi.org/10.15493/DEA.MIMS.13142023).
- Sabelani Z, Ismail H, van den Berg MA, Lamont T. 2024. Long-term observations of hourly bottom temperatures at Mosterts Hoek, South Africa (November 2000 - March 2001). DFFE. doi: [10.15493/DEA.MIMS.13162023](https://doi.org/10.15493/DEA.MIMS.13162023).
- Sabelani Z, Ismail H, van den Berg MA, Lamont T. 2024. Long-term observations of hourly bottom temperatures at Mosterts Hoek, South Africa (March 2001 - July 2001). DFFE. doi: [10.15493/DEA.MIMS.13182023](https://doi.org/10.15493/DEA.MIMS.13182023).
- Sabelani Z, Ismail H, van den Berg MA, Lamont T. 2024. Long-term observations of hourly bottom temperatures at Mosterts Hoek, South Africa (July 2001 - October 2001). DFFE. doi: [10.15493/DEA.MIMS.13202023](https://doi.org/10.15493/DEA.MIMS.13202023).
- Sabelani Z, Ismail H, van den Berg MA, Lamont T. 2024. Long-term observations of hourly bottom temperatures at Mosterts Hoek, South Africa (October 2001 - November 2002). DFFE. doi: [10.15493/DEA.MIMS.13222023](https://doi.org/10.15493/DEA.MIMS.13222023).
- Sabelani Z, Ismail H, van den Berg MA, Lamont T. 2024. Long-term observations of hourly bottom temperatures at Mosterts Hoek, South Africa (June 2003 - June 2004). DFFE. doi: [10.15493/DEA.MIMS.13242023](https://doi.org/10.15493/DEA.MIMS.13242023).
- Sabelani Z, Ismail H, van den Berg MA, Lamont T. 2024. Long-term observations of hourly bottom temperatures at Mosterts Hoek, South Africa (June 2004 - November 2004). DFFE. doi: [10.15493/DEA.MIMS.13262023](https://doi.org/10.15493/DEA.MIMS.13262023).
- Sabelani Z, Ismail H, van den Berg MA, Lamont T. 2024. Long-term observations of hourly bottom temperatures at Mosterts Hoek, South Africa (November 2004 - November 2005). DFFE. doi: [10.15493/DEA.MIMS.13282023](https://doi.org/10.15493/DEA.MIMS.13282023).
- Sabelani Z, Ismail H, van den Berg MA, Lamont T. 2024. Long-term observations of hourly bottom temperatures at Mosterts Hoek, South Africa (November 2005 - November 2009). DFFE. doi: [10.15493/DEA.MIMS.13302023](https://doi.org/10.15493/DEA.MIMS.13302023).
- Sabelani Z, Ismail H, van den Berg MA, Lamont T. 2024. Long-term observations of hourly bottom temperatures at Mosterts Hoek, South Africa (November 2009 - September 2019). DFFE. doi: [10.15493/DEA.MIMS.13322023](https://doi.org/10.15493/DEA.MIMS.13322023).
- Sabelani Z, Ismail H, van den Berg MA, Lamont T. 2024. Long-term observations of hourly bottom temperatures at Mosterts Hoek, South Africa (September 2019 - June 2022). DFFE. doi: [10.15493/DEA.MIMS.13342023](https://doi.org/10.15493/DEA.MIMS.13342023).
- Sabelani Z, Ismail H, van den Berg MA, Lamont T. 2024. Raw temperature data for long-term observations of bottom temperatures at Port Alfred (October 1995 - April 1996). DFFE. doi: [10.15493/DEA.MIMS.11932023](https://doi.org/10.15493/DEA.MIMS.11932023).
- Sabelani Z, Ismail H, van den Berg MA, Lamont T. 2024. Raw temperature data for long-term observations of bottom temperatures at Port Alfred (April 1996 - October 1996). DFFE. doi: [10.15493/DEA.MIMS.11952023](https://doi.org/10.15493/DEA.MIMS.11952023).
- Sabelani Z, Ismail H, van den Berg MA, Lamont T. 2024. Raw temperature data for long-term observations of bottom temperatures at Port Alfred (October 1996 - March 1997). DFFE. doi: [10.15493/DEA.MIMS.11972023](https://doi.org/10.15493/DEA.MIMS.11972023).
- Sabelani Z, Ismail H, van den Berg MA, Lamont T. 2024. Raw temperature data for long-term observations of bottom temperatures at Port Alfred (March 1997 - July 1997). DFFE. doi: [10.15493/DEA.MIMS.11992023](https://doi.org/10.15493/DEA.MIMS.11992023).
- Sabelani Z, Ismail H, van den Berg MA, Lamont T. 2024. Raw temperature data for long-term observations of bottom temperatures at Port Alfred (July 1997 - March 1998). DFFE. doi: [10.15493/DEA.MIMS.12012023](https://doi.org/10.15493/DEA.MIMS.12012023).
- Sabelani Z, Ismail H, van den Berg MA, Lamont T. 2024. Raw temperature data for long-term observations of bottom temperatures at Port Alfred (March 1998 - March 1999). DFFE. doi: [10.15493/DEA.MIMS.12032023](https://doi.org/10.15493/DEA.MIMS.12032023).
- Sabelani Z, Ismail H, van den Berg MA, Lamont T. 2024. Raw temperature data for long-term observations of bottom temperatures at Port Alfred (March 1999 - August 1999). DFFE. doi: [10.15493/DEA.MIMS.12052023](https://doi.org/10.15493/DEA.MIMS.12052023).
- Sabelani Z, Ismail H, van den Berg MA, Lamont T. 2024. Raw temperature data for long-term observations of bottom temperatures at Port Alfred (August 1999 - January 2000). DFFE. doi: [10.15493/DEA.MIMS.12072023](https://doi.org/10.15493/DEA.MIMS.12072023).
- Sabelani Z, Ismail H, van den Berg MA, Lamont T. 2024. Raw temperature data for long-term observations of bottom temperatures at Port Alfred (January 2000 - May 2000). DFFE. doi: [10.15493/DEA.MIMS.12092023](https://doi.org/10.15493/DEA.MIMS.12092023).

OUTPUTS FOR 2024

- Sabelani Z, Ismail H, van den Berg MA, Lamont T. 2024. Raw temperature data for long-term observations of bottom temperatures at Port Alfred (May 2000 - June 2000). DFFE. doi: [10.15493/DEA.MIMS.12112023](https://doi.org/10.15493/DEA.MIMS.12112023).
- Sabelani Z, Ismail H, van den Berg MA, Lamont T. 2024. Raw temperature data for long-term observations of bottom temperatures at Port Alfred (June 2000 - November 2000). DFFE. doi: [10.15493/DEA.MIMS.12132023](https://doi.org/10.15493/DEA.MIMS.12132023).
- Sabelani Z, Ismail H, van den Berg MA, Lamont T. 2024. Raw temperature data for long-term observations of bottom temperatures at Port Alfred (November 2000 - March 2001). DFFE. doi: [10.15493/DEA.MIMS.12152023](https://doi.org/10.15493/DEA.MIMS.12152023).
- Sabelani Z, Ismail H, van den Berg MA, Lamont T. 2024. Raw temperature data for long-term observations of bottom temperatures at Port Alfred (March 2001 - February 2002). DFFE. doi: [10.15493/DEA.MIMS.12172023](https://doi.org/10.15493/DEA.MIMS.12172023).
- Sabelani Z, Ismail H, van den Berg MA, Lamont T. 2024. Raw temperature data for long-term observations of bottom temperatures at Port Alfred (February 2002 - June 2002). DFFE. doi: [10.15493/DEA.MIMS.12192023](https://doi.org/10.15493/DEA.MIMS.12192023).
- Sabelani Z, Ismail H, van den Berg MA, Lamont T. 2024. Raw temperature data for long-term observations of bottom temperatures at Port Alfred (June 2002 - November 2002). DFFE. doi: [10.15493/DEA.MIMS.12212023](https://doi.org/10.15493/DEA.MIMS.12212023).
- Sabelani Z, Ismail H, van den Berg MA, Lamont T. 2024. Raw temperature data for long-term observations of bottom temperatures at Port Alfred (November 2002 - February 2003). DFFE. doi: [10.15493/DEA.MIMS.12232023](https://doi.org/10.15493/DEA.MIMS.12232023).
- Sabelani Z, Ismail H, van den Berg MA, Lamont T. 2024. Raw temperature data for long-term observations of bottom temperatures at Port Alfred (February 2003 - July 2003). DFFE. doi: [10.15493/DEA.MIMS.12252023](https://doi.org/10.15493/DEA.MIMS.12252023).
- Sabelani Z, Ismail H, van den Berg MA, Lamont T. 2024. Raw temperature data for long-term observations of bottom temperatures at Port Alfred (July 2003 - November 2003). DFFE. doi: [10.15493/DEA.MIMS.12272023](https://doi.org/10.15493/DEA.MIMS.12272023).
- Sabelani Z, Ismail H, van den Berg MA, Lamont T. 2024. Raw temperature data for long-term observations of bottom temperatures at Port Alfred (April 2004 - October 2004). DFFE. doi: [10.15493/DEA.MIMS.12292023](https://doi.org/10.15493/DEA.MIMS.12292023).
- Sabelani Z, Ismail H, van den Berg MA, Lamont T. 2024. Raw temperature data for long-term observations of bottom temperatures at Port Alfred (October 2004 - April 2005). DFFE. doi: [10.15493/DEA.MIMS.12312023](https://doi.org/10.15493/DEA.MIMS.12312023).
- Sabelani Z, Ismail H, van den Berg MA, Lamont T. 2024. Raw temperature data for long-term observations of bottom temperatures at Port Alfred (April 2005 - August 2005). DFFE. doi: [10.15493/DEA.MIMS.12332023](https://doi.org/10.15493/DEA.MIMS.12332023).
- Sabelani Z, Ismail H, van den Berg MA, Lamont T. 2024. Raw temperature data for long-term observations of bottom temperatures at Port Alfred (August 2005 - February 2006). DFFE. doi: [10.15493/DEA.MIMS.12352023](https://doi.org/10.15493/DEA.MIMS.12352023).
- Sabelani Z, Ismail H, van den Berg MA, Lamont T. 2024. Raw temperature data for long-term observations of bottom temperatures at Port Alfred (February 2006 - January 2007). DFFE. doi: [10.15493/DEA.MIMS.12372023](https://doi.org/10.15493/DEA.MIMS.12372023).
- Sabelani Z, Ismail H, van den Berg MA, Lamont T. 2024. Raw temperature data for long-term observations of bottom temperatures at Port Alfred (January 2007 - September 2007). DFFE. doi: [10.15493/DEA.MIMS.12392023](https://doi.org/10.15493/DEA.MIMS.12392023).
- Sabelani Z, Ismail H, van den Berg MA, Lamont T. 2024. Raw temperature data for long-term observations of bottom temperatures at Port Alfred (September 2007 - July 2008). DFFE. doi: [10.15493/DEA.MIMS.12412023](https://doi.org/10.15493/DEA.MIMS.12412023).
- Sabelani Z, Ismail H, van den Berg MA, Lamont T. 2024. Raw temperature data for long-term observations of bottom temperatures at Port Alfred (July 2008 - February 2009). DFFE. doi: [10.15493/DEA.MIMS.12432023](https://doi.org/10.15493/DEA.MIMS.12432023).
- Sabelani Z, Ismail H, van den Berg MA, Lamont T. 2024. Raw temperature data for long-term observations of bottom temperatures at Port Alfred (February 2009 - February 2010). DFFE. doi: [10.15493/DEA.MIMS.12452023](https://doi.org/10.15493/DEA.MIMS.12452023).
- Sabelani Z, Ismail H, van den Berg MA, Lamont T. 2024. Raw temperature data for long-term observations of bottom temperatures at Port Alfred (February 2010 - March 2011). DFFE. doi: [10.15493/DEA.MIMS.12472023](https://doi.org/10.15493/DEA.MIMS.12472023).
- Sabelani Z, Ismail H, van den Berg MA, Lamont T. 2024. Raw temperature data for long-term observations of bottom temperatures at Port Alfred (March 2011 - February 2012). DFFE. doi: [10.15493/DEA.MIMS.12492023](https://doi.org/10.15493/DEA.MIMS.12492023).
- Sabelani Z, Ismail H, van den Berg MA, Lamont T. 2024. Raw temperature data for long-term observations of bottom temperatures at Port Alfred (February 2012 - August 2012). DFFE. doi: [10.15493/DEA.MIMS.12512023](https://doi.org/10.15493/DEA.MIMS.12512023).
- Sabelani Z, Ismail H, van den Berg MA, Lamont T. 2024. Raw temperature data for long-term observations of bottom temperatures at Port Alfred (August 2012 - April 2013). DFFE. doi: [10.15493/DEA.MIMS.12532023](https://doi.org/10.15493/DEA.MIMS.12532023).
- Sabelani Z, Ismail H, van den Berg MA, Lamont T. 2024. Raw temperature data for long-term observations of bottom temperatures at Port Alfred (April 2013 - May 2014). DFFE. doi: [10.15493/DEA.MIMS.12552023](https://doi.org/10.15493/DEA.MIMS.12552023).
- Sabelani Z, Ismail H, van den Berg MA, Lamont T. 2024. Raw temperature data for long-term observations of bottom temperatures at Port Alfred (May 2014 - November 2014). DFFE. doi: [10.15493/DEA.MIMS.12572023](https://doi.org/10.15493/DEA.MIMS.12572023).
- Sabelani Z, Ismail H, van den Berg MA, Lamont T. 2024. Raw temperature data for long-term observations of bottom temperatures at Port Alfred (November 2014 - November 2015). DFFE. doi: [10.15493/DEA.MIMS.12592023](https://doi.org/10.15493/DEA.MIMS.12592023).
- Sabelani Z, Ismail H, van den Berg MA, Lamont T. 2024. Raw temperature data for long-term observations of bottom temperatures at Port Alfred (November 2015 - April 2016). DFFE. doi: [10.15493/DEA.MIMS.12612023](https://doi.org/10.15493/DEA.MIMS.12612023).
- Sabelani Z, Ismail H, van den Berg MA, Lamont T. 2024. Raw temperature data for long-term observations of bottom temperatures at Port Alfred (April 2016 - March 2017). DFFE. doi: [10.15493/DEA.MIMS.12632023](https://doi.org/10.15493/DEA.MIMS.12632023).
- Sabelani Z, Ismail H, van den Berg MA, Lamont T. 2024. Long-term observations of hourly bottom temperatures at Port Alfred (October 1995 - April 1996). DFFE. doi: [10.15493/DEA.MIMS.11922023](https://doi.org/10.15493/DEA.MIMS.11922023).

OUTPUTS FOR 2024

- Sabelani Z, Ismail H, van den Berg MA, Lamont T. 2024. Long-term observations of hourly bottom temperatures at Port Alfred (April 1996 - October 1996). DFFE. doi: [10.15493/DEA.MIMS.11942023](https://doi.org/10.15493/DEA.MIMS.11942023).
- Sabelani Z, Ismail H, van den Berg MA, Lamont T. 2024. Long-term observations of hourly bottom temperatures at Port Alfred (October 1996 - March 1997). DFFE. doi: [10.15493/DEA.MIMS.11962023](https://doi.org/10.15493/DEA.MIMS.11962023).
- Sabelani Z, Ismail H, van den Berg MA, Lamont T. 2024. Long-term observations of hourly bottom temperatures at Port Alfred (March 1997 - July 1997). DFFE. doi: [10.15493/DEA.MIMS.11982023](https://doi.org/10.15493/DEA.MIMS.11982023).
- Sabelani Z, Ismail H, van den Berg MA, Lamont T. 2024. Long-term observations of hourly bottom temperatures at Port Alfred (July 1997 - March 1998). DFFE. doi: [10.15493/DEA.MIMS.12002023](https://doi.org/10.15493/DEA.MIMS.12002023).
- Sabelani Z, Ismail H, van den Berg MA, Lamont T. 2024. Long-term observations of hourly bottom temperatures at Port Alfred (March 1998 - March 1999). DFFE. doi: [10.15493/DEA.MIMS.12022023](https://doi.org/10.15493/DEA.MIMS.12022023).
- Sabelani Z, Ismail H, van den Berg MA, Lamont T. 2024. Long-term observations of hourly bottom temperatures at Port Alfred (March 1999 - August 1999). DFFE. doi: [10.15493/DEA.MIMS.12042023](https://doi.org/10.15493/DEA.MIMS.12042023).
- Sabelani Z, Ismail H, van den Berg MA, Lamont T. 2024. Long-term observations of hourly bottom temperatures at Port Alfred (August 1999 - January 2000). DFFE. doi: [10.15493/DEA.MIMS.12062023](https://doi.org/10.15493/DEA.MIMS.12062023).
- Sabelani Z, Ismail H, van den Berg MA, Lamont T. 2024. Long-term observations of hourly bottom temperatures at Port Alfred (January 2000 - May 2000). DFFE. doi: [10.15493/DEA.MIMS.12082023](https://doi.org/10.15493/DEA.MIMS.12082023).
- Sabelani Z, Ismail H, van den Berg MA, Lamont T. 2024. Long-term observations of hourly bottom temperatures at Port Alfred (May 2000 - June 2000). DFFE. doi: [10.15493/DEA.MIMS.12102023](https://doi.org/10.15493/DEA.MIMS.12102023).
- Sabelani Z, Ismail H, van den Berg MA, Lamont T. 2024. Long-term observations of hourly bottom temperatures at Port Alfred (June 2000 - November 2000). DFFE. doi: [10.15493/DEA.MIMS.12122023](https://doi.org/10.15493/DEA.MIMS.12122023).
- Sabelani Z, Ismail H, van den Berg MA, Lamont T. 2024. Long-term observations of hourly bottom temperatures at Port Alfred (November 2000 - March 2001). DFFE. doi: [10.15493/DEA.MIMS.12142023](https://doi.org/10.15493/DEA.MIMS.12142023).
- Sabelani Z, Ismail H, van den Berg MA, Lamont T. 2024. Long-term observations of hourly bottom temperatures at Port Alfred (March 2001 - February 2002). DFFE. doi: [10.15493/DEA.MIMS.12162023](https://doi.org/10.15493/DEA.MIMS.12162023).
- Sabelani Z, Ismail H, van den Berg MA, Lamont T. 2024. Long-term observations of hourly bottom temperatures at Port Alfred (February 2002 - June 2002). DFFE. doi: [10.15493/DEA.MIMS.12182023](https://doi.org/10.15493/DEA.MIMS.12182023).
- Sabelani Z, Ismail H, van den Berg MA, Lamont T. 2024. Long-term observations of hourly bottom temperatures at Port Alfred (June 2002 - November 2002). DFFE. doi: [10.15493/DEA.MIMS.12202023](https://doi.org/10.15493/DEA.MIMS.12202023).
- Sabelani Z, Ismail H, van den Berg MA, Lamont T. 2024. Long-term observations of hourly bottom temperatures at Port Alfred (November 2002 - February 2003). DFFE. doi: [10.15493/DEA.MIMS.12222023](https://doi.org/10.15493/DEA.MIMS.12222023).
- Sabelani Z, Ismail H, van den Berg MA, Lamont T. 2024. Long-term observations of hourly bottom temperatures at Port Alfred (February 2003 - July 2003). DFFE. doi: [10.15493/DEA.MIMS.12242023](https://doi.org/10.15493/DEA.MIMS.12242023).
- Sabelani Z, Ismail H, van den Berg MA, Lamont T. 2024. Long-term observations of hourly bottom temperatures at Port Alfred (July 2003 - November 2003). DFFE. doi: [10.15493/DEA.MIMS.12262023](https://doi.org/10.15493/DEA.MIMS.12262023).
- Sabelani Z, Ismail H, van den Berg MA, Lamont T. 2024. Long-term observations of hourly bottom temperatures at Port Alfred (April 2004 - October 2004). DFFE. doi: [10.15493/DEA.MIMS.12282023](https://doi.org/10.15493/DEA.MIMS.12282023).
- Sabelani Z, Ismail H, van den Berg MA, Lamont T. 2024. Long-term observations of hourly bottom temperatures at Port Alfred (October 2004 - April 2005). DFFE. doi: [10.15493/DEA.MIMS.12302023](https://doi.org/10.15493/DEA.MIMS.12302023).
- Sabelani Z, Ismail H, van den Berg MA, Lamont T. 2024. Long-term observations of hourly bottom temperatures at Port Alfred (April 2005 - August 2005). DFFE. doi: [10.15493/DEA.MIMS.12322023](https://doi.org/10.15493/DEA.MIMS.12322023).
- Sabelani Z, Ismail H, van den Berg MA, Lamont T. 2024. Long-term observations of hourly bottom temperatures at Port Alfred (August 2005 - February 2006). DFFE. doi: [10.15493/DEA.MIMS.12342023](https://doi.org/10.15493/DEA.MIMS.12342023).
- Sabelani Z, Ismail H, van den Berg MA, Lamont T. 2024. Long-term observations of hourly bottom temperatures at Port Alfred (February 2006 - January 2007). DFFE. doi: [10.15493/DEA.MIMS.12362023](https://doi.org/10.15493/DEA.MIMS.12362023).
- Sabelani Z, Ismail H, van den Berg MA, Lamont T. 2024. Long-term observations of hourly bottom temperatures at Port Alfred (January 2007 - September 2007). DFFE. doi: [10.15493/DEA.MIMS.12382023](https://doi.org/10.15493/DEA.MIMS.12382023).
- Sabelani Z, Ismail H, van den Berg MA, Lamont T. 2024. Long-term observations of hourly bottom temperatures at Port Alfred (September 2007 - July 2008). DFFE. doi: [10.15493/DEA.MIMS.12402023](https://doi.org/10.15493/DEA.MIMS.12402023).
- Sabelani Z, Ismail H, van den Berg MA, Lamont T. 2024. Long-term observations of hourly bottom temperatures at Port Alfred (July 2008 - February 2009). DFFE. doi: [10.15493/DEA.MIMS.12422023](https://doi.org/10.15493/DEA.MIMS.12422023).
- Sabelani Z, Ismail H, van den Berg MA, Lamont T. 2024. Long-term observations of hourly bottom temperatures at Port Alfred (February 2009 - February 2010). DFFE. doi: [10.15493/DEA.MIMS.12442023](https://doi.org/10.15493/DEA.MIMS.12442023).
- Sabelani Z, Ismail H, van den Berg MA, Lamont T. 2024. Long-term observations of hourly bottom temperatures at Port Alfred (February 2010 - March 2011). DFFE. doi: [10.15493/DEA.MIMS.12462023](https://doi.org/10.15493/DEA.MIMS.12462023).
- Sabelani Z, Ismail H, van den Berg MA, Lamont T. 2024. Long-term observations of hourly bottom temperatures at Port Alfred (March 2011 - February 2012). DFFE. doi: [10.15493/DEA.MIMS.12482023](https://doi.org/10.15493/DEA.MIMS.12482023).
- Sabelani Z, Ismail H, van den Berg MA, Lamont T. 2024. Long-term observations of hourly bottom temperatures at Port Alfred (February 2012 - August 2012). DFFE. doi: [10.15493/DEA.MIMS.12502023](https://doi.org/10.15493/DEA.MIMS.12502023).
- Sabelani Z, Ismail H, van den Berg MA, Lamont T. 2024. Long-term observations of hourly bottom temperatures at Port Alfred (August 2012 - April 2013). DFFE. doi: [10.15493/DEA.MIMS.12522023](https://doi.org/10.15493/DEA.MIMS.12522023).

OUTPUTS FOR 2024

- Sabelani Z, Ismail H, van den Berg MA, Lamont T. 2024. Long-term observations of hourly bottom temperatures at Port Alfred (April 2013 - May 2014). DFFE. doi: [10.15493/DEA.MIMS.12542023](https://doi.org/10.15493/DEA.MIMS.12542023).
- Sabelani Z, Ismail H, van den Berg MA, Lamont T. 2024. Long-term observations of hourly bottom temperatures at Port Alfred (May 2014 - November 2014). DFFE. doi: [10.15493/DEA.MIMS.12562023](https://doi.org/10.15493/DEA.MIMS.12562023).
- Sabelani Z, Ismail H, van den Berg MA, Lamont T. 2024. Long-term observations of hourly bottom temperatures at Port Alfred (November 2014 - November 2015). DFFE. doi: [10.15493/DEA.MIMS.12582023](https://doi.org/10.15493/DEA.MIMS.12582023).
- Sabelani Z, Ismail H, van den Berg MA, Lamont T. 2024. Long-term observations of hourly bottom temperatures at Port Alfred (November 2015 - April 2016). DFFE. doi: [10.15493/DEA.MIMS.12602023](https://doi.org/10.15493/DEA.MIMS.12602023).
- Sabelani Z, Ismail H, van den Berg MA, Lamont T. 2024. Long-term observations of hourly bottom temperatures at Port Alfred (April 2016 - March 2017). DFFE. doi: [10.15493/DEA.MIMS.12622023](https://doi.org/10.15493/DEA.MIMS.12622023).
- Sabelani Z, Ismail H, van den Berg MA, Lamont T. 2024. Raw temperature data for long-term observations of bottom temperatures at Nosy Ve (August 2003 - September 2004). DFFE. doi: [10.15493/DEA.MIMS.63072024](https://doi.org/10.15493/DEA.MIMS.63072024).
- Sabelani Z, Ismail H, van den Berg MA, Lamont T. 2024. Raw temperature data for long-term observations of bottom temperatures at Nosy Ve (September 2004 - September 2007). DFFE. doi: [10.15493/DEA.MIMS.65072024](https://doi.org/10.15493/DEA.MIMS.65072024).
- Sabelani Z, Ismail H, van den Berg MA, Lamont T. 2024. Raw temperature data for long-term observations of bottom temperatures at Nosy Ve (September 2007 - February 2012). DFFE. doi: [10.15493/DEA.MIMS.67072024](https://doi.org/10.15493/DEA.MIMS.67072024).
- Sabelani Z, Ismail H, van den Berg MA, Lamont T. 2024. Raw temperature data for long-term observations of bottom temperatures at Nosy Ve (February 2012 - May 2013). DFFE. doi: [10.15493/DEA.MIMS.69072024](https://doi.org/10.15493/DEA.MIMS.69072024).
- Sabelani Z, Ismail H, van den Berg MA, Lamont T. 2024. Long-term observations of hourly bottom temperatures at Nosy Ve (August 2003 - September 2004). DFFE. doi: [10.15493/DEA.MIMS.62072024](https://doi.org/10.15493/DEA.MIMS.62072024).
- Sabelani Z, Ismail H, van den Berg MA, Lamont T. 2024. Long-term observations of hourly bottom temperatures at Nosy Ve (September 2004 - September 2007). DFFE. doi: [10.15493/DEA.MIMS.64072024](https://doi.org/10.15493/DEA.MIMS.64072024).
- Sabelani Z, Ismail H, van den Berg MA, Lamont T. 2024. Long-term observations of hourly bottom temperatures at Nosy Ve (September 2007 - February 2012). DFFE. doi: [10.15493/DEA.MIMS.66072024](https://doi.org/10.15493/DEA.MIMS.66072024).
- Sabelani Z, Ismail H, van den Berg MA, Lamont T. 2024. Long-term observations of hourly bottom temperatures at Nosy Ve (February 2012 - May 2013). DFFE. doi: [10.15493/DEA.MIMS.68072024](https://doi.org/10.15493/DEA.MIMS.68072024).
- Sabelani Z, Ismail H, van den Berg MA, Lamont T. 2024. Raw temperature data for long-term observations of bottom temperatures at Fort-Dauphin (May 2013 - January 2017). DFFE. doi: [10.15493/DEA.MIMS.19112024](https://doi.org/10.15493/DEA.MIMS.19112024).
- Sabelani Z, Ismail H, van den Berg MA, Lamont T. 2024. Long-term observations of hourly bottom temperatures at Fort-Dauphin (May 2013 - January 2017). DFFE. doi: [10.15493/DEA.MIMS.18112024](https://doi.org/10.15493/DEA.MIMS.18112024).
- Sabelani Z, Ismail H, van den Berg MA, Lamont T. 2024. Raw temperature data for long-term observations of bottom temperatures at Bassas da India, Mozambique Channel (August 2003 - September 2007). DFFE. doi: [10.15493/DEA.MIMS.22112024](https://doi.org/10.15493/DEA.MIMS.22112024).
- Sabelani Z, Ismail H, van den Berg MA, Lamont T. 2024. Raw temperature data for long-term observations of bottom temperatures at Bassas da India, Mozambique Channel (March 2012 - May 2013). DFFE. doi: [10.15493/DEA.MIMS.24112024](https://doi.org/10.15493/DEA.MIMS.24112024).
- Sabelani Z, Ismail H, van den Berg MA, Lamont T. 2024. Long-term observations of hourly bottom temperatures at Bassas da India, Mozambique Channel (August 2003 - September 2007). DFFE. doi: [10.15493/DEA.MIMS.21112024](https://doi.org/10.15493/DEA.MIMS.21112024).
- Sabelani Z, Ismail H, van den Berg MA, Lamont T. 2024. Long-term observations of hourly bottom temperatures at Bassas da India, Mozambique Channel (March 2012 - May 2013). DFFE. doi: [10.15493/DEA.MIMS.23112024](https://doi.org/10.15493/DEA.MIMS.23112024).
- Speich S, Lamont T, Louw GS, van den Berg MA, Meinen CS, Garcia R, Perez RC, Dong S. 2024. Long-term observations of daily acoustic travel time along the GoodHope transect at PIES Mooring GH01 (December 2014 - July 2015). DFFE. doi: [10.15493/DEA.MIMS.13642023](https://doi.org/10.15493/DEA.MIMS.13642023).
- Speich S, Lamont T, Louw GS, van den Berg MA, Meinen CS, Garcia R, Perez RC, Dong S. 2024. Long-term observations of daily acoustic travel time along the GoodHope transect at PIES Mooring GH02 (December 2014 - December 2018). DFFE. doi: [10.15493/DEA.MIMS.13682023](https://doi.org/10.15493/DEA.MIMS.13682023).
- Speich S, Lamont T, Louw GS, van den Berg MA, Meinen CS, Garcia R, Perez RC, Dong S. 2024. Long-term observations of daily acoustic travel time along the GoodHope transect at PIES Mooring GH03 (December 2014 - July 2015). DFFE. doi: [10.15493/DEA.MIMS.13652023](https://doi.org/10.15493/DEA.MIMS.13652023).
- Speich S, Lamont T, Louw GS, van den Berg MA, Meinen CS, Garcia R, Perez RC, Dong S. 2024. Long-term observations of daily acoustic travel time along the GoodHope transect at PIES Mooring GH03 (July 2015 - December 2018). DFFE. doi: [10.15493/DEA.MIMS.13692023](https://doi.org/10.15493/DEA.MIMS.13692023).
- Speich S, Lamont T, Louw GS, van den Berg MA, Meinen CS, Garcia R, Perez RC, Dong S. 2024. Long-term observations of daily acoustic travel time along the GoodHope transect at PIES Mooring GH05 (December 2014 - December 2018). DFFE. doi: [10.15493/DEA.MIMS.13702023](https://doi.org/10.15493/DEA.MIMS.13702023).
- Speich S, Lamont T, Louw GS, van den Berg MA, Meinen CS, Garcia R, Perez RC, Dong S. 2024. Long-term observations of daily acoustic travel time along the GoodHope transect at PIES Mooring GH06 (December 2014 - July 2015). DFFE. doi: [10.15493/DEA.MIMS.13662023](https://doi.org/10.15493/DEA.MIMS.13662023).

OUTPUTS FOR 2024

- Speich S, Lamont T, Louw GS, van den Berg MA, Meinen CS, Garcia R, Perez RC, Dong S. 2024. Long-term observations of daily acoustic travel time along the GoodHope transect at PIES Mooring GH06 (July 2015 – December 2018). DFFE. doi: [10.15493/DEA.MIMS.13712023](https://doi.org/10.15493/DEA.MIMS.13712023).
- Speich S, Lamont T, Louw GS, van den Berg MA, Meinen CS, Garcia R, Perez RC, Dong S. 2024. Long-term observations of daily acoustic travel time along the GoodHope transect at PIES Mooring GH07 (December 2014 – July 2015). DFFE. doi: [10.15493/DEA.MIMS.13672023](https://doi.org/10.15493/DEA.MIMS.13672023).
- Speich S, Lamont T, Louw GS, van den Berg MA, Meinen CS, Garcia R, Perez RC, Dong S. 2024. Long-term observations of daily acoustic travel time along the GoodHope transect at PIES Mooring GH07 (July 2015 – December 2018). DFFE. doi: [10.15493/DEA.MIMS.13722023](https://doi.org/10.15493/DEA.MIMS.13722023).
- Tsanwani M, Hamnca S, Monteiro PMS. 2024. Surface underway measurements of partial pressure of carbon dioxide (pCO₂), water temperature, salinity and other parameters during the R/V Algoa Benguela Air-Sea CO₂ and Heat Flux Experiment (BenFlex21) cruise (EXPOCODE 91AL20211206) in the coastal waters of South Africa, South Atlantic Ocean from 2021-12-06 to 2021-12-19 (NCEI Accession 0288036). NOAA National Centers for Environmental Information. doi: [10.25921/6Oxz-wv20](https://doi.org/10.25921/6Oxz-wv20).
- Tsanwani M, Hamnca S, Mdokwana B. 2024. Surface underway measurements of partial pressure of carbon dioxide (pCO₂), water temperature, salinity and other parameters during the R/V Algoa Southern Benguela (IEP:SB) cruise (EXPOCODE 91AL20211115) in the coastal waters of South Africa from 2021-11-15 to 2021-11-23 (NCEI Accession 0287887). NOAA National Centers for Environmental Information. doi: [10.25921/6ew7-5g23](https://doi.org/10.25921/6ew7-5g23).
- Tsanwani M, Hamnca S, Mdokwana B. 2024. Surface underway measurements of partial pressure of carbon dioxide (pCO₂), water temperature, salinity and other parameters during the R/V Algoa Southern Benguela (IEP:SB) cruises (EXPOCODEs 91AL20220810, 91AL20211121) in the coastal waters of South Africa, South Atlantic Ocean from 2022-08-10 to 2022-11-30 (NCEI Accession 0288037). National Centers for Environmental Information. doi: [10.25921/74px-tb43](https://doi.org/10.25921/74px-tb43).
- Tsanwani M, Hamnca S, Mdokwana B. 2024. Surface underway measurements of partial pressure of carbon dioxide (pCO₂), water temperature, salinity and other parameters during the R/V Algoa Southern Benguela (IEP:SB) cruise (EXPOCODE 91AL20230215) in the coastal waters of South Africa, South Atlantic Ocean from 2023-02-15 to 2023-02-23 (NCEI Accession 0288106). NOAA National Centers for Environmental Information. doi: [10.25921/9xby-5025](https://doi.org/10.25921/9xby-5025).
- Tutt G, Lamont T. 2024. Processed CTD continuous observations from the West Coast Hake Biomass on the Africana Voyage 079, January 1990. DFFE. doi: [10.15493/DEA.MIMS.11772023](https://doi.org/10.15493/DEA.MIMS.11772023).
- Tutt G, Lamont T. 2024. Raw CTD continuous observations from the West Coast Hake Biomass on the Africana Voyage 079, January 1990. DFFE. doi: [10.15493/DEA.MIMS.11792023](https://doi.org/10.15493/DEA.MIMS.11792023).
- Tutt G, Lamont T. 2024. Processed CTD continuous observations from the Anchovy Recruitment Survey on the Africana Voyage 081, May 1990. DFFE. doi: [10.15493/DEA.MIMS.09072024](https://doi.org/10.15493/DEA.MIMS.09072024).
- Tutt G, Lamont T. 2024. Processed CTD discrete observations from the Anchovy Recruitment Survey on the Africana Voyage 081, May 1990. DFFE. doi: [10.15493/DEA.MIMS.10072024](https://doi.org/10.15493/DEA.MIMS.10072024).
- Tutt G, Lamont T. 2024. Raw CTD continuous observations from the Anchovy Recruitment Survey on the Africana Voyage 081, May 1990. DFFE. doi: [10.15493/DEA.MIMS.11072024](https://doi.org/10.15493/DEA.MIMS.11072024).
- Tutt G, Lamont T. 2024. Processed CTD continuous observations from the South Coast Demersal Biomass Survey on the Africana Voyage 082, May 1990. DFFE. doi: [10.15493/DEA.MIMS.13072024](https://doi.org/10.15493/DEA.MIMS.13072024).
- Tutt G, Lamont T. 2024. Processed CTD discrete observations from the South Coast Demersal Biomass Survey on the Africana Voyage 082, May 1990. DFFE. doi: [10.15493/DEA.MIMS.14072024](https://doi.org/10.15493/DEA.MIMS.14072024).
- Tutt G, Lamont T. 2024. Processed CTD continuous observations from the West Coast Hake Biomass Survey on the Africana Voyage 084, July 1990. DFFE. doi: [10.15493/DEA.MIMS.25072024](https://doi.org/10.15493/DEA.MIMS.25072024).
- Tutt G, Lamont T. 2024. Processed CTD discrete observations from the West Coast Hake Biomass Survey on the Africana Voyage 084, July 1990. DFFE. doi: [10.15493/DEA.MIMS.26072024](https://doi.org/10.15493/DEA.MIMS.26072024).
- Tutt G, Lamont T. 2024. Processed CTD continuous observations from the West Coast Hake Biomass Survey on the Africana Voyage 088, January 1991. DFFE. doi: [10.15493/DEA.MIMS.31072024](https://doi.org/10.15493/DEA.MIMS.31072024).
- Tutt G, Lamont T. 2024. Processed CTD continuous observations from the Plankton Dynamics on the Africana Voyage 089, February 1991. DFFE. doi: [10.15493/DEA.MIMS.34072024](https://doi.org/10.15493/DEA.MIMS.34072024).
- Tutt G, Lamont T. 2024. Processed CTD continuous observations from the Pelagic Pre-Recruit Mesopelagic Biomass Survey on the Africana Voyage 090, March 1991. DFFE. doi: [10.15493/DEA.MIMS.37072024](https://doi.org/10.15493/DEA.MIMS.37072024).
- Tutt G, Lamont T. 2024. Processed CTD continuous observations from the Anchovy Recruitment Survey on the Africana Voyage 092, May 1991. DFFE. doi: [10.15493/DEA.MIMS.16072024](https://doi.org/10.15493/DEA.MIMS.16072024).
- Tutt G, Lamont T. 2024. Processed CTD continuous observations from the South Coast Demersal Biomass Survey on the Africana Voyage 093, June 1991. DFFE. doi: [10.15493/DEA.MIMS.19072024](https://doi.org/10.15493/DEA.MIMS.19072024).
- Tutt G, Lamont T. 2024. Processed CTD continuous observations from the South Coast Demersal Biomass Survey on the Africana Voyage 095, September 1991. DFFE. doi: [10.15493/DEA.MIMS.22072024](https://doi.org/10.15493/DEA.MIMS.22072024).

OUTPUTS FOR 2024

- Tutt G, Lamont T. 2024. Processed CTD continuous observations from the Horse Mackerel Hydroacoustic Pilot Survey on the Africana Voyage 096, October 1991. DFFE. doi: [10.15493/DEA.MIMS.43072024](https://doi.org/10.15493/DEA.MIMS.43072024).
- Tutt G, Lamont T. 2024. Processed CTD continuous observations from the Pelagic Fish Biomass Survey on the Africana Voyage 097, November 1991. DFFE. doi: [10.15493/DEA.MIMS.46072024](https://doi.org/10.15493/DEA.MIMS.46072024).
- Tutt G, Lamont T. 2024. Processed CTD continuous observations from the Agulhas Bank Boundary Processes cruise on the Africana Voyage 099, January 1992. DFFE. doi: [10.15493/DEA.MIMS.49072024](https://doi.org/10.15493/DEA.MIMS.49072024).
- Tutt G, Lamont T. 2024. Processed CTD continuous observations from the West Coast Hake Biomass Survey on the Africana Voyage 100, February 1992. DFFE. doi: [10.15493/DEA.MIMS.52072024](https://doi.org/10.15493/DEA.MIMS.52072024).
- Tutt G, Lamont T. 2024. Processed CTD continuous observations from the Pelagic Pre-Recruit Mesopelagic Biomass Survey on the Africana Voyage 101, March 1992. DFFE. doi: [10.15493/DEA.MIMS.55072024](https://doi.org/10.15493/DEA.MIMS.55072024).
- Tutt G, Lamont T. 2024. Processed CTD continuous observations from the South Coast Demersal Biomass Survey on the Africana Voyage 102, April 1992. DFFE. doi: [10.15493/DEA.MIMS.58072024](https://doi.org/10.15493/DEA.MIMS.58072024).
- Tutt G, Lamont T. 2024. Processed CTD continuous observations from the Benguela Current Sources and Transport (BEST 1) on the Africana Voyage 105, June 1992. DFFE. doi: [10.15493/DEA.MIMS.04112024](https://doi.org/10.15493/DEA.MIMS.04112024).
- Tutt G, Lamont T. 2024. Processed CTD continuous observations from the South Coast Demersal Inshore Biomass Survey on the Africana Voyage 106, September 1992. DFFE. doi: [10.15493/DEA.MIMS.07112024](https://doi.org/10.15493/DEA.MIMS.07112024).
- Tutt G, Lamont T. 2024. Processed CTD continuous observations from the Physical-Chemical Oceanography on the Africana Voyage 085, August 1990. DFFE. doi: [10.15493/DEA.MIMS.10122024](https://doi.org/10.15493/DEA.MIMS.10122024).
- Tutt G, Lamont T. 2024. Processed CTD discrete observations from the Physical-Chemical Oceanography on the Africana Voyage 085, August 1990. DFFE. doi: [10.15493/DEA.MIMS.12122024](https://doi.org/10.15493/DEA.MIMS.12122024).
- Tutt G, Lamont T. 2024. Processed CTD continuous observations from the South Coast Demersal Biomass Survey on the Africana Voyage 086, September 1990. DFFE. doi: [10.15493/DEA.MIMS.13122024](https://doi.org/10.15493/DEA.MIMS.13122024).
- Tutt G, Lamont T. 2024. Processed CTD discrete observations from the South Coast Demersal Biomass Survey on the Africana Voyage 086, September 1990. DFFE. doi: [10.15493/DEA.MIMS.14122024](https://doi.org/10.15493/DEA.MIMS.14122024).
- Tutt G, Lamont T. 2024. Processed CTD continuous observations from the Anchovy Recruitment Survey on the Africana Voyage 103, May 1992. DFFE. doi: [10.15493/DEA.MIMS.15122024](https://doi.org/10.15493/DEA.MIMS.15122024).
- Tutt G, Lamont T, Frantz F. 2024. Processed CTD continuous observations from the Horse Mackerel Hydroacoustic Survey on the Africana Voyage 107, October 1992. DFFE. doi: [10.15493/DEA.MIMS.10112024](https://doi.org/10.15493/DEA.MIMS.10112024).
- Tutt G, Lamont T, Frantz F. 2024. Processed CTD continuous observations from the Pelagic Biomass Survey on the Africana Voyage 108, November 1992. DFFE. doi: [10.15493/DEA.MIMS.13112024](https://doi.org/10.15493/DEA.MIMS.13112024).
- Tutt G, Lamont T, Frantz F. 2024. Processed CTD continuous observations from the West Coast Hake Biomass Survey on the Africana Voyage 109, January 1993. DFFE. doi: [10.15493/DEA.MIMS.16112024](https://doi.org/10.15493/DEA.MIMS.16112024).
- van den Berg MA. 2024. South Atlantic Meridional Overturning Circulation Basin-wide Array (SAMBA) Monitoring Line cruise on the Algoa Voyage 265, September 2019. DFFE. doi: [10.15493/DEA.MIMS.16042024](https://doi.org/10.15493/DEA.MIMS.16042024).
- van den Berg MA. 2024. Marion Island Relief Voyage on the SA Agulhas II Voyage 062, May 2024. DFFE. doi: [10.15493/DEA.MIMS.05122024](https://doi.org/10.15493/DEA.MIMS.05122024).
- van den Berg MA. 2024. Raw Expendable Bathythermograph (XBT) casts collected during the Marion Island Relief Voyage on the SA Agulhas II Voyage 062, May 2024. DFFE. doi: [10.15493/DEA.MIMS.07122024](https://doi.org/10.15493/DEA.MIMS.07122024).
- van den Berg MA. 2024. Processed Expendable Bathythermograph (XBT) casts collected during the Marion Island Relief Voyage on the SA Agulhas II Voyage 062, May 2024. DFFE. doi: [10.15493/DEA.MIMS.06122024](https://doi.org/10.15493/DEA.MIMS.06122024).
- van den Berg MA, Lamont T. 2024. Raw temperature data for short-term observations of thermistor string temperatures on the continental slope off Natal Bight, along the east coast of South Africa at location Dbn02 (March 2009 - July 2009). DFFE. doi: [10.15493/DEA.MIMS.134072024](https://doi.org/10.15493/DEA.MIMS.134072024).
- van den Berg MA, Lamont T. 2024. Raw temperature data for short-term observations of thermistor string temperatures on the continental slope off Natal Bight, along the east coast of South Africa at location Dbn02 (December 2009 - August 2010). DFFE. doi: [10.15493/DEA.MIMS.135072024](https://doi.org/10.15493/DEA.MIMS.135072024).
- van den Berg MA, Lamont T. 2024. Short-term observations of daily thermistor string temperatures on the continental slope off Natal Bight, along the east coast of South Africa at location Dbn02 (March 2009 - July 2009). DFFE. doi: [10.15493/DEA.MIMS.127072024](https://doi.org/10.15493/DEA.MIMS.127072024).
- van den Berg MA, Lamont T. 2024. Short-term observations of daily thermistor string temperatures on the continental slope off Natal Bight, along the east coast of South Africa at location Dbn02 (December 2009 - August 2010). DFFE. doi: [10.15493/DEA.MIMS.128072024](https://doi.org/10.15493/DEA.MIMS.128072024).
- van den Berg MA, Lamont T. 2024. Short-term observations of hourly thermistor string temperatures on the continental slope off Natal Bight, along the east coast of South Africa at location Dbn02 (March 2009 - July 2009). DFFE. doi: [10.15493/DEA.MIMS.129072024](https://doi.org/10.15493/DEA.MIMS.129072024).
- van den Berg MA, Lamont T. 2024. Short-term observations of hourly thermistor string temperatures on the continental slope off Natal Bight, along the east coast of South Africa at location Dbn02 (December 2009 - August 2010). DFFE. doi: [10.15493/DEA.MIMS.130072024](https://doi.org/10.15493/DEA.MIMS.130072024).

OUTPUTS FOR 2024

PUBLISHED REPORTS

- Huggett JA, Lamont T, Haupt T, Halo I, Kirkman SP. 2024. Oceans and Coasts Annual Science Report 2023. *Oceans and Coasts, DFFE, Report 23, June 2024*, ISBN: 978-0-621-51919-8, 93 pp. doi: [10.5281/zenodo.12600889](https://doi.org/10.5281/zenodo.12600889).
- Jones CD, Caccavo JA, Brooks C, Desvignes T, Dornan T, Filander Z, Finucci B, Ghigliotti L, Guerreiro PM, Halfter S, Hollyman P, Kwasniewski H, Leeger R, Maschette D, Masere C, Moreira E, Novillo M, Queirós JP, Reid WDK, Vargas-Chacoff L. 2023. Introduction to the SCAR Action group (SCARFISH). *Commission for the Conservation of Antarctic Marine Living Resources (CCAMLR) WG-FSA- IMAF-2024/74*, 12 pp.
- Koubbi P, Swadling KM, Huggett J, Makhado AB, Goberville E, Brokensha LN, Constable A, Corney I, Green D, Grilly E, Kitchener J, Ziegler P, Masere C, Mdluli N, du Preez S, Mishra RK, Moteki M, Djian V, Heures AL, Thibault D, Vilain M. 2024. Hobart 2024 workshop on WP13. The pelagic realm of the subantarctic Indian and Southern Indian Ocean. *Commission for the Conservation of Antarctic Marine Living Resources (CCAMLR) WG-EMM- 2024/07*, 25 pp.
- McQuaid K, Howell K, Muthumbi A, Adeoye O, Elegbede I, Adams L, Charuka B, Hilário A, Kadila H, Laarissa S, Mejri R, Mohamed S, Mutia D, Nyangwe A, Paterson A, Shibe S, Sink K, Talma S, Taylor U, Tuda A, and workshop participants*. 2024. Practical actions to strengthen capacity for deep-water research in Africa. A report of the African Network of Deep-water Researchers, Challenger 150 Programme, 31 pp. doi: [10.24382/gxbv-sp22](https://doi.org/10.24382/gxbv-sp22). (* including Filander Z, Samaai T).
- Somhlaba S, Geja Y, Makhado A, Filander NP, Williamson M, Maschette D. 2024. A preliminary look at bycatch data in Prince Edward and Marion Islands Sub area 58.7 and area 51 outside CCAMLR area. *Commission for the Conservation of Antarctic Marine Living Resources (CCAMLR) WG-FSA-IMAF-2024/37*, 29 pp.
- Zoleka N, Filander P, Somhlaba S, Makhado AB. 2024. First report of the Prince Edward and Marion Islands Vulnerable Marine Ecosystem by-catch data, collected in the 2009- 2023 fishing seasons. *Commission for the Conservation of Antarctic Marine Living Resources (CCAMLR) WG-FSA- IMAF-2024/45*, 15 pp.

THESES

- du Preez SA. 2024. The variability of mesozooplankton around sub-Antarctic Prince Edward Islands and the influence of the environment. BSc Honours Thesis (Oceanography), University of Cape Town, Cape Town, 76 pp.
- Kupczyk AM. 2024. An evaluation of GLORYS and BRAN ocean model outputs on the west coast of South Africa. Postgraduate Diploma Thesis (Marine Science), Cape Peninsula University of Technology, Cape Town, 41 pp.
- Nkadimeng TN. 2024. Eddy variability in the Benguela: A comparison of the northern and southern Benguela eddy fields. BSc Honours Thesis (Oceanography), University of Cape Town, Cape Town, 55 pp.
- Schäfer I. 2024. Acoustic occurrence and behaviour of Baleen whales during winter around the subantarctic Prince Edward Islands. BSc Honours Thesis (Oceanography), University of Cape Town, Cape Town, 52 pp.
- Sneddon A. 2024. Marine Heatwave characteristics in the South Atlantic and South Indian Oceans. BSc Honours Thesis (Oceanography), University of Cape Town, Cape Town, 91 pp.

UNPUBLISHED REPORTS

- Currie JC, Sink KJ, Bull LJ, Besseling NA, Adams LA, Atkinson LJ, Cedras RB, Dayaram A, Filander ZNP, Karenyi N, Porter SN, Watson RGA. 2024. Plan for the 2025 Marine Ecosystem Map. South African National Biodiversity Institute (SANBI) internal report. *South African National Biodiversity Institute, Cape Town*, 35 pp.
- Liu Q, Rogers AD, Roch C, Gordon J, Duarte CM, Robinson LF, Waller RG, Ferrier-Pagès C, Brooke S, Cerrero-Silva M, Benson K, De Carvalho Ferreira ML, Du Preez C, Banks S, Barry JP, Cordeiro RTS, Cordes E, Hennige S, Hourigan TF, Kitahara MV, Kutti T, Larsson AI, Lauretta DM, Matsumoto AK, Ross RE, Ramirez-Llodra E, Yáñez Suárez AB, Edinger E, Metaxas A, Filander ZNP, Taylor ML. 2024. Critical knowledge gaps in conservation and restoration of cold-water corals: A Roadmap for future research. *Coral Research and Development Platform (CORDAP)*, 58 pp.
- Makhado AB, Upfold L, Masotla MJ, Cebekhulu T. 2024. African Penguins continued to decline – Conservation management challenge. *DFFE Marine Top Predator Working Group Report, MTPSWG-11*, 3 pp.





**DEPARTMENT OF FORESTRY,
FISHERIES AND THE ENVIRONMENT**

Oceans & Coasts

ADDRESS

P.O. Box 52126, V&A Waterfront, Cape Town,
8002. 2 East Pier Building, East Pier Road,
Cape Town, 8001

PHONE

(+27) 21 819 2420

FAX

(+27) 21 819 2444

E-MAIL

callcentre@dfffe.gov.za

WEBSITE

www.dffe.gov.za

RP321/2025

ISBN: 978-1-83491-218-9